NOTICE

The quality of this microfiche is heavily dependent upon the quality of the original thesis submitted for microfilming. Every effort has been made to ensure the highest quality of reproduction possible.

If pages are missing, contact the university which granted the degree.

Some pages may have indistinct print especially if the original pages were typed with a poor typewriter ribbon or if the university sent us a poor photocopy.

Previously copyrighted materials (journal articles, published tests, etc.) are not filmed.

Reproduction in full or in part of this film is governed by the Canadian Copyright Act, R.S.C. 1970, c. C-30. Please read the authorization forms which accompany this thesis.

THIS DISSERTATION
HAS BEEN MICROFILMED
EXACTLY AS RECEIVED

AVIS

La qualité de cette microfiche dépend grandement de la qualité de la thèse soumise au microfilmage. Nous avons tout fait pour assurer une qualité supérieure de reproduction.

S'il manque des pages, veuillez communiquer avec l'université qui a conféré le grade.

La qualité d'impression de certaines pages peut laisser à désirer, surtout si les pages originales ont été dactylographiées à l'aide d'un ruban usé ou si l'université nous a fait parvenir une photocopie de mauvaise qualité.

Les documents qui font déjà l'objet d'un droit d'auteur (articles de revue, examens publiés, etc.) ne sont pas microfilmés.

La reproduction, même partielle, de ce microfilm est soumise à la Loi canadienne sur le droit d'auteur, SRC 1970, c. C-30. Veuillez prendre connaissance des formules d'autorisation qui accompagnent cette thèse.

LA THÈSE A ÉTÉ
MICROFILMÉE TELLE QUE
NOUS L'AVONS REÇUE

UNIVERSITÉ D'OTTAWA
UNIVERSITY OF OTTAWA

HYDROGENATION, ISOMERIZATION, ADSORPTION AND INFRARED STUDIES OF ALLENE ON SILICA SUPPORTED GROUP VIII TRANSITION METALS, COPPER AND NICKEL-COPPER ALLOY

by

Chandra Prakash Khulbe

A thesis submitted to the School of Graduate Studies
in partial fulfillment of the requirements for the
degree of Ph.D. in Chemical Engineering

UNIVERSITY OF OTTAWA
OTTAWA, CANADA, 1975

ABSTRACT

The catalytic hydrogenation of allene has been studied in a constant volume static system over silica supported group VIII transition metals, copper and copper-nickel alloy.

The order of reaction with respect to hydrogen was always one and was independent of temperature. On Pt, Pd and Ru, an inflection point occurred in the initial rate - initial hydrogen pressure plot after which the rate increased. The orders of reaction in the accelerated region were 2.0, 1.8 and 1.5 respectively. The order of reaction with respect to allene was always zero. The activation energy varied between 3.4 to 16.4 k cal/mole.

On the basis of the product analysis, these catalysts can be categorized as:

a) active for consecutive reaction (Ni,Ni-Cu,Cu), $A \rightarrow B \rightarrow C$

b) active for simultaneous reaction $A \begin{matrix} \nearrow B \\ \searrow C \end{matrix}$

Only iron and cobalt catalysts were active for the isomerization reaction. Nearly equal activity and energy of activation (11.8 and 11.2 k cal/mole) suggested that in the presence of metal the support was active for the isomerization reaction.

Two types of hydrogen adsorption were observed on these catalysts:

i) chemisorbed hydrogen which could be removed on evacuation at room temperature

ii) chemisorbed hydrogen which could not be removed by evacuation at room temperature.

For allene hydrogenation reaction, the activity pattern was fairly close to the H/M factor (total number of hydrogen atoms adsorbed on each atom of metal).

Activity Pd>Rh≥Pt>Ni>Co>Ru>Cu>Ir

H/M Pd>Pt≃Rh>Ni>Co>Ir>Ru>Cu

Infrared studies showed the presence of $CH_2{=}\overset{*}{C}{-}\overset{*}{C}H_2$ species as the initial adsorption of allene. The proposed mechanism, based on the product analysis and infrared studies, explains the kinetics of the reaction.

ACKNOWLEDGEMENT

The author wishes to express his sincere thanks to Dr. R.S. Mann for his thoughtful guidance in carrying out this work and his personal interest and assistance in the shaping of this thesis.

The author also wishes to express his thanks:

to Dr. B.C.Y. Lu for providing the facilities for this research work;

to Mr. G. Gasperetti for his technical assistance;

to Dr. B.A. Morrow for valuable discussions and his help in the interpretation of infrared spectra;

to Mrs. Ryan for typing this thesis;

to Mr. Salah Hamam and Mr. M.K. Dosi for proof-reading;

and in the last, not the least, to Mr. M. Master, Mr. A.M. Shah and Dr. K.C. Khulbe for their assistance in designing the high vacuum system and the apparatus, and constant helpful discussions, moral support and encouragement, throughout the course of this work.

TABLE OF CONTENTS

TABLE OF CONTENTS (cont'd)

TABLE OF CONTENTS (cont'd).

TABLE OF CONTENTS (cont'd)

LIST OF FIGURES

LIST OF FIGURES (cont'd)

LIST OF FIGURES (cont'd)

LIST OF FIGURES (cont'd)

LIST OF TABLES

LIST OF TABLES (cont'd)

LIST OF TABLES (cont'd)

LIST OF TABLES (cont'd)

NOMENCLATURE

A	Frequency factor, $min^{-1}gm^{-1}$
A,B	Reactants
%d	Percent-d-character
D	Dispersion (fraction of metal exposed on the surface)
E	Energy of activation, k cal/gm mole
H/M	Total number of hydrogen atoms adsorbed on each atom of metal
k	Overall reaction rate constant
K	Equilibrium constant
m	Reaction order with respect to hydrogen
M	Atomic weight of the metal
n	Reaction order with respect to allene
N	Avogadro's number
P	Pressure, mmHg
P_A	Pressure of allene, mmHg
P_M	Pressure of methylacetylene, mmHg
P_{H_2}	Initial pressure of hydrogen, mmHg
$P_{C_3H_4}$	Initial pressure of allene, mmHg
$P_{C_3H_6}$	Pressure of propylene, mmHg
$P_{C_3H_8}$	Pressure of propane, mmHg
ΔP	Pressure drop, mmHg

NOMENCLATURE (cont'd)

r_o	Initial rate, mm/min
R	Gas constant
$\overline{R}$	Initial hydrogen pressure/initial allene pressure
S	Selectivity
t	Reaction time, min.
T	Reaction temperature, °C or °K
V	Volume of adsorbed gas, cc(STP)/gm
σ	Effective molecular surface area, cm^2
$\bar{\theta}$	Surface coverage
Ni-Cu	Nickel-copper alloy

1. INTRODUCTION

In the field of heterogeneous catalysis, a fundamental understanding of the factors that affect catalytic activity and selectivity are of paramount importance. This can be approached through a knowledge of the reaction mechanism. Due to the complexity of the phenomenon at the surface of the catalyst, the correlation developed initially must be empirical. However, before such a correlation can be formulated, one needs a better method of determining specific rate constant and reaction mechanism from experimental data.

In the case of solid catalyzed gas phase reactions, the conventional approach is to measure the dependence of the reaction rate on the reactant pressures. From various postulated mechanisms, reaction rate expressions are derived in terms of the surface coverage of different species, a relationship between the surface coverage and the partial pressure of a reactant is then assumed. A comparison of the expressions of the reaction rate as a function of partial pressures derived from the postulated mechanisms is then made with the experimentally found relationship in order to ascertain the real mechanism. This method is often insufficient.

The kinetics of homogeneous catalysis have been considerably advanced in recent years by the introduction of free radicals and radical ions. Broad analogies, drawn between homogeneous acid catalyzed reactions and similar heterogeneous process at the surface of some oxide insulators containing protons, encourage the view that the same intermediate particles are active in both. Less well defined relations suggest

identical species at the surface of metals. Recent publications concerning the catalytic activity of pure metals in hydrogenation and dehydrogenation reactions and related observations on the adsorption, catalytic activity and other physical properties of the catalyst surface indicate that a definite correlation must exist between the structure of the solids and their catalytic activity. Though considerable work has been done in the last decade, the mechanism of heterogeneous catalysis is not as yet very clearly understood.

Hydrocarbons may undergo processes of dehydrogenation, isomerization and deuterium exchange on the surface of metal catalysts. In addition to that, unsaturated hydrocarbons may be hydrogenated or may undergo cis-trans isomerization or double bond migration. All these processes are considered to ensue from a state of chemisorption on the metal surface. As a consequence, techniques by which the structures of chemisorbed hydrocarbon species may be determined, have assumed great importance in elucidating mechanisms of chemical reactions occurring at surfaces.

Infrared spectroscopy has been of great help in the structural determination of molecules. Its application to the study of surface chemistry has provided one of the most direct means of observing the interactions and perturbations that occur at the surface during adsorption, and determining the structure of the adsorbed species.

Though the hydrogenation, adsorption and infrared studies of unsaturated hydrocarbons (olefins and acetylenes) over supported and unsupported metals and their alloys have been studied extensively in the past, very little has been published about the hydrogenation of allene over supported and unsupported metals.

The catalytic hydrogenation of allene aimed at more detailed and systematic investigation, especially of the kinetics of the reaction, for which purpose, use has been made of the greater control afforded by a static reaction system. The complexity of the reaction has demanded frequent full analysis of the gaseous products and the surface of the catalyst during the course of the reaction.

The objects of the present study of the catalytic hydrogenation, isomerization, adsorption and infrared studies of allene were:

1) to study the kinetics of the reaction over silica supported group VIII transition metals, copper and copper-nickel alloy and to evaluate the activation energies, frequency factors and relative activities;
2) to find whether the geometric and electronic structures of these metals are related in any way to their catalytic activities and to correlate, with the results of other investigations;
3) to compare the kinetics of allene hydrogenation with that of methylacetylene, over the same type of catalysts;
4) to study the isomerization reaction (allene-methylacetylene);
5) to obtain low pressure adsorption isotherms;
6) to calculate metal surface area, dispersion (fraction of the metal exposed on the surface) and H/M (total number of hydrogen atoms adsorbed on each atom of the metal);
7) if possible, to correlate amount adsorbed, dispersion or H/M with the catalytic activity;
8) to investigate the nature of adsorbed species of allene and, if possible, to identify the intermediate compound of the reaction;

9) to propose a possible mechanism based on the detailed product analysis and infrared studies;

10) to find the effect of different operating variables such as temperature, concentration of the reactants on the course of the reaction and the selectivity.

2. LITERATURE SURVEY

The literature on catalysis has been recently enriched by the publication of books by Sir Eric Rideal (1), Thomson and Webb (2) and Anderson (3). An enormous amount of work has been carried out on the hydrogenation of olefinic and acetylenic compounds on metals (4,5). Also, extensive work has been carried out on the infrared studies of the adsorbed state, to understand the reaction mechanism (6). The literature on the catalytic hydrogenation of unsaturated hydrocarbons is quite voluminous and is beyond the scope of this review. The first part of this Chapter deals with a brief review of the published literature on the experimental work done on the hydrocarbons of the acetylenic series (acetylene, methylacetylene and ethylacetylene). The second part deals with the hydrogenation of allene. The third part deals with the hydrogenation of olefins and diolefins. The fourth part summarizes the results of the isomerization of acetylenes and allenes. The fifth part deals with the hydrogen adsorption and metal surface area measurements. The last part deals with the adsorption and infrared studies of unsaturated hydrocarbons.

2.1 LITERATURE RELATED TO ACETYLENE SERIES

In the hydrogenation of acetylene over reduced nickel powder, Sabatier and Senderens (7) observed the formation of higher hydrocarbons in addition to ethane and ethylene. Later investigators (8-12) reported varying yields of these products. Sheridan (13) reported the reaction to be a first order with respect to hydrogen and negative and zero order with respect to acetylene over platinum and nickel, respectively. While de Pauw and Jungers (14), using hydrogen in excess, reported a negative

(-0.5) order with respect to acetylene and first order with respect to hydrogen, Bond (15) reported a two rate expression for nickel-pumice catalyst. Subsequently, Bond and Mann (16) confirmed the earlier findings of Bond (15).

Tamaru (17) reported the hydrogenation of acetylene over palladium catalyst to be taking place in two steps. Bond et al (18) studied the hydrogenation of acetylene over alumina supported palladium catalyst and observed that the selectivity $\left[S=P_{C_2H_4}/(P_{C_2H_4}+P_{C_2H_6})\right]$ could be increased to more than 96% by using hydrogen/acetylene ratios greater than two. Bond and Mann (19) investigated this reaction over supported and unsupported nickel and cobalt, and observed that the activity for pure nickel was maximum. Sheridan and Reid (20) also studied the reaction of acetylene with hydrogen over pumice supported rhodium, ruthenium, iridium and osmium catalysts. They found that the reaction orders were similar to those observed for nickel pumice catalysts and that iridium showed a poor selectivity.

Bond and Sheridan (21) studied the hydrogenation of methylacetylene over pumice supported nickel, palladium and platinum catalysts. For hydrogen/methylacetylene ratios of 0.4 to 6.0, they found that in the case of nickel catalyst the order of reaction at 91°C was the same as that for acetylene hydrogenation at about 60°C. Mann and Naik (22) and Mann and Khulbe (23) studied this reaction over supported and unsupported group VIII transition metals, copper and nickel-copper alloy powders. They observed that the order of reaction with respect to hydrogen was always about one and the order with respect to methylacetylene was zero and temperature independent except for nickel, cobalt and platinum powders, where it was slightly negative. For copper and some of the alloys,

the order with respect to methylacetylene was +0.5. The apparent activation energy varied between 6.2 to 21.2 k cal/mole.

Meyer and Burwell (24) studied the gas phase reaction between deuterium and ethylacetylene over a palladium-alumina (Pd=0.3%) catalyst and reported that the deuteneted products were 1-butene (99.1%), cis and trans-2-butene (each 0.2%) and n-butane (0.5%) only. Isomerization and further addition of deuterium to 1-butene occurred only after the alkyne was completely removed. Mann and Khulbe (25) have reported the hydrogenation of ethylacetylene over supported and unsupported metals. In the case of iron powder, detailed study could not be made due to the slow deactivation of the catalyst.

2.2 LITERATURE RELATED TO ALLENE HYDROGENATION

Though an enormous amount of work has been done on the hydrogenation of olefinic and acetylenic compounds over the transition metals, very little work has been done on the hydrogenation of allenic compounds due partly to the complexity of the reaction. The double bond system C=C=C is a highly strained one. It resembles the acetylenic system in that the addition to the first C=C bond is more exothermic than a like addition to the C=C which remains after the opening of the first (26). Hence, associative chemisorption of allene is expected to be stronger than that of propylene, just as acetylene is more strongly adsorbed on metals than ethylene (13). Therefore, the hydrogenation of allene is expected to yield propylene relatively free from propane until most of the allene has been consumed. Such selective hydrogenation would not normally be expected in diolefins in which the double bonds are more widely separated as a result of the first addition being faster than the

second and not of selective adsorption of diolefins.

Bond and Sheridan (21) have studied the hydrogenation of allene over pumice supported nickel, palladium and platinum catalysts. The orders of reaction were one and zero with respect to hydrogen and allene respectively. The observed activation energies were 12.9, 12.3 and 17.1 k cal/mole for nickel, palladium and platinum, respectively.

The selectivity observed in the first stage of the reaction has been reported for most of alumina supported group VIII metals (27,28).

Mann and To (29) studied the catalytic hydrogenation of allene over pumice supported group VIII metal catalysts. The orders of reaction were one or slightly higher and zero with respect to hydrogen and allene respectively and the activation energy varied between 3.0 and 17.4 k cal/mole. The catalytic activities of the metals were in the following sequence:

Pt>Pd>Rh>Ir>Ni>Co>Fe>Ru>Os

While selectivity was found to decrease with increasing initial hydrogen pressure, it increased with increasing temperature for pumice supported nickel catalysts.

Mann and Tiu (30) observed the reaction to be first order with respect to hydrogen and zero order with respect to allene over nickel, iron and cobalt catalysts. Recently, Mann and Shah (31) studied this reaction over unsupported nickel-copper alloys and palladium, platinum, iridium, rhodium, ruthenium and osmium catalysts. The orders of reaction with respect to hydrogen and allene were always one and zero, respectively. The energy of activation varied between 5.61 to 11.77 k cal/mole for the nickel-copper alloy system. The activation energy for platinum, iridium, palladium and rhodium were 17.7, 9.1, 6.4 and 17.4

k cal/mole, respectively. The catalytic activity of the unsupported metals were in the following sequence:

Pd>Ir>Rh>Pt>Ru,Os

While selectivity was highest with palladium and rhodium, it was least with iridium.

2.3 LITERATURE RELATED TO DIOLEFINS

The hydrogenation of 1,3-butadiene has been studied in the gas phase as well as in the liquid phase over the metal catalysts of the eighth group (24,27,28,32). In the case of gas phase hydrogenation, the orders of reaction with respect to hydrogen were mostly one except for palladium and platinum catalysts, for which the orders were 1.7 and 1.3, respectively. The orders with respect to 1,3-butadiene were mostly zero, with a trend to be slightly negative for nickel, palladium and platinum. Phillipson et al (32) observed that the hydrogenation of 1,3-butadiene to butene was very selective. Two types of catalyst behaviour were obtained: type A in which the yield of 1-butene was high and the trans-cis ratio in the 2-butene was low (about 1-2) and type B in which the yield of 1-butene was low and trans-cis ratio was high (about 4-11). Iron, copper, cobalt and nickel catalysts reduced below 350°C showed type A behaviour whereas cobalt and nickel reduced above 400°C showed type B behaviour.

The palladium catalyzed hydrogenation of 1,2-butadiene at room temperature has been studied both in the gas phase using a flow system (24) and in the liquid phase using a solvent (33). The product distribution for the gas and liquid phase reaction showed that the solvent had substantially no effect upon the reaction mechanism.

2.4 LITERATURE RELATED TO ACETYLENE-ALLENE ISOMERIZATION

While the isomerization (double bond migration) of olefins, diolefins and substituted diolefins (34-42) have been studied extensively, very little has been reported about the acetylene-allene isomerization.

On treatment of acetylenic compounds with a base, hydrogen from a propargylic methylene group migrates to the triple bond carbon atom, thus giving allenic compounds or on further migration, a mixture of acetylenic compounds including allene derivatives. The alkoxide-catalyzed rearrangement of ethylacetylene to dimethylacetylene was described as a prototropic rearrangement with methylallene as an intermediate (42). The postulation of an allenic intermediate in this process was supported by the rearrangement of isopropylacetylene to 3-methylbuta-1,2-diene catalyzed by KOH-ETOH at 170°C, the subsequent formation of 2-alkyne being impossible in this case. The fact that t-butylacetylene was unchanged under comparable conditions also provides confirmation of this postulation (43). In his review, Iwai (44) has summarized acetylene-allene isomerization.

Chang and Kokes (45) have studied the isomerization of methylacetylene over zinc oxide. The kinetics of the first half of allene isomerization to methylacetylene could be represented fairly well by first order. The infrared studies show a similarity between the adsorbed state of allene and methylacetylene indicating the same adsorbed species for both the compounds.

2.5 ADSORPTION

While studying the adsorption of hydrogen on zinc oxide, Kokes and Dent (46) observed two types of adsorbed hydrogen at room temperature: Type I - chemisorbed hydrogen which could be removed on evacuation at room temperature; Type II - chemisorbed hydrogen which could not be removed even after several hours of evacuation at room temperature. In the hydrogenation of ethylene on ZnO using deuterium as a tracer, they also observed that hydrogen chemisorbed reversibly (Type I) on a limited number of sites with the formation of ZnOH and ZnH and reacted with ethylene to form ethane. Non-removable chemisorbed hydrogen (Type II) played a passive role at room temperature. It did neither participate as a reactant nor contribute to infrared bands. Type I and Type II adsorption isotherms for hydrogen were also observed by Sholten and Montfoort (47) on zinc oxide and by Komers, Amenomiya and Cvetanovic (48) on silica supported platinum at 25°C. By using the temperature programmed desorption (TPD) technique, Tsuchiya et al (49) observed four different states of chemisorbed hydrogen on platinum black, at -100, -20, 90 and 300°C. These various states were referred to as α, β, γ and δ respectively. The structure for various adsorbed hydrogen species has been classified as follows:

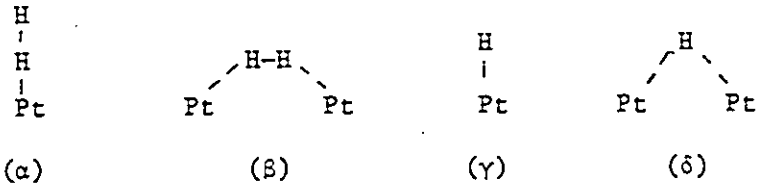

(α) (β) (γ) (δ)

The results of TPD of hydrogen from platinum films, studied by Stephan et al (50), revealed the existence of three different adsorption states:

1) a very weakly bounded γ state (at 120 °K) and

2) two more strongly bounded states β_1 (200 °K) and β_2 (330 °K).

Recently, Dixon, Barth, Kokes and Gryder (51) studied the hydrogen adsorption isotherms at 295 and 77°K on wet and dry catalyst samples. They obtained five kinds of hydrogen adsorption isotherms on alumina supported platinum.

Type I. Reversibly bounded (infrared inactive) mostly on the support at 77°K.

Type II. Irreversibly bounded at 77°K (infrared inactive) on the catalyst previously unexposed to hydrogen.

Type III. Reversibly bounded at room temperature with an infrared absorption band at 2060 cm^{-1}.

Type IV. Adsorbed at 77°K on samples containing Type V hydrogen with an infrared band at 2120 cm^{-1}.

Type V. Adsorbed at 295°K but not at 77°K (necessary for the adsorption of Type IV).

They have associated Types II, III, IV and V to γ, β, α and δ states observed by Tsuchiya, Amenomia and Cvetanovic (49) on platinum black. Toya (52) considered the hydrogen platinum system theoretically and predicted the existence of two types of adsorbed hydrogen atoms on the surface, r and s type, corresponding to weak and strong adsorption proposed by Eischenes and Pliskin (53). Using microcalorimetric (54) and infrared techniques (55), Primet et al showed that at room temperature two forms of adsorbed hydrogen could be observed on a platinum-alumina catalyst.

Clewley, Lynch and Flanagan (56), while studying the chemisorption of hydrogen on oxygenated platinum black, obtained adsorption isotherms at pressures below 50mm. This type of chemisorption was tentatively assigned to additional weak chemisorption which usually occurs following the completion of strongly held monolayers. Dala Betta (57) observed that while silica and alumina supported ruthenium catalyst evacuated at temperatures of 500, 400 and 300°C for 2 hrs. gave identical uptakes of hydrogen, the one evacuated at 200°C for 2 hrs. showed an uptake which was smaller by 7%. It is suggested that the evacuation at 400°C for two hours is sufficient to remove the adsorbed hydrogen.

Brooks and Christopher (58) estimated metal surface area of nickel powder and nickel supported on different zeolites by obtaining hydrogen desorption isotherms at 250°C. The irreversible hydrogen retention at 100 mm hydrogen pressure was attributed to chemisorption on nickel surface. Nickel catalyst areas estimated from hydrogen chemisorption and nickel crystallite size determined by x-ray diffraction line broadening were in good agreement. Vannice, Benson and Boudart (59) studied gravimetrically and volumetrically the adsorption of hydrogen and oxygen as well as the reaction of hydrogen with adsorbed oxygen on platinum black. The amount of hydrogen adsorbed on a reduced and evacuated surface was the same as it was on a pre-oxidized surface. The ratio of adsorbed hydrogen and oxygen atoms to surface platinum atoms was close to unity at room temperature and a pressure of 50 torr. Dalla Betta (57) studied the hydrogen adsorption isotherms on unsupported and silica supported ruthenium catalysts. At pressures of about 120 torr and 21°C, the adsorption on ruthenium metal was consistent with a surface stoichiometry of Ru_s-H. A good agreement was obtained between particle size

distribution observed by electron-microscopy and particle size calculated from hydrogen adsorption. Sinfelt and Yates (60) obatined hydrogen adsorption isotherms at room temperature for low pressures (up to 20 torr) by expanding a known amount of hydrogen gas in the adsorption chamber. The volume of gas adsorbed was calculated employing ideal behaviour. Hydrogen uptake was estimated at zero pressure. The H/M and O/M (total number of gas atoms adsorbed on each atom of metal) ratio on silica supported ruthenium, rhodium, iridium, palladium, platinum, cobalt, nickel, osmium and iron were nearly equal in each case.

2.6 INFRARED STUDIES

In the past decade, infrared spectroscopy has been extensively applied to the study of the surface species formed during the adsorption of hydrocarbons and during their interaction with hydrogen on supported metal catalysts (6,61).

The spectrum of adsorbed hydrogen on platinum supported on γ alumina consisted of two bands at 2105 and 2055 cm^{-1} (53). On repeating the experiments with deuterium, bands appeared at 1512 and 1480 cm^{-1}, corresponding to the two bands observed for adsorbed hydrogen. The structure favoured by Piliskin and Eischens for the two types of adsorbed hydrogen atoms was:

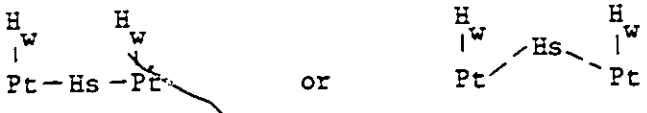

where H_w and H_s refer to weakly and strongly adsorbed hydrogen atoms respectively.

The infrared spectra of ethylene on nickel supported on Cab-O-Sil (63) showed that the adsorption could be associative or dissociative

depending on experimental conditions. Associative chemisorption of ethylene was obtained at 35°C when a pre-adsorbed layer of hydrogen had been left on the nickel surface. When ethylene was chemisorbed on bare nickel surface, dissociative chemisorption was obtained. The infrared spectrum of ethylene on various metals was studied by Little, Sheppard and Yates (62). However, they were not able to obtain a spectrum of initially adsorbed species on nickel.

The adsorption of ethylene on bare platinum-silica catalysts (63-68) at room temperature leads to spectra in which associatively bonded structures were predominant. Bonds ascribed to dissociatively adsorbed species were also observed. On the admission of hydrogen to the ethylene precovered surface, ethane was observed in the gas phase, and the intensity of the spectrum increased. This had been interpreted as indicating the formation of surface carbides in the initial adsorption. On increasing the temperature to 95°C, bands corresponding to surface n-butyl groups were observed together with the appearance of butane in the gas phase. It was suggested that the C_4 species were the result of random polymerization of dissociatively adsorbed ethylenic residue.

The spectra of ethylene adsorbed on nickel (66-68) showed close similarities to those observed with platinum silica. Adsorption of ethylene on 'bare' palladium-silica produced only weak bands (6). These bands indicated the presence of species with double bond character, together with surface methyl and methylene groups. Infrared studies of this reaction have also been made on rhodium (69) and zinc oxide (70,71).

On silica supported nickel, palladium and platinum (72), adsorption of acetylene on the 'bare' surface gave rise to bands ascribed to

olefinic species and surface alkyl groups (=CH-, CH_2 and $-CH_3$). Addition of hydrogen resulted in an intensification of the spectra and the appearance of new bands corresponding to surface alkyl groups of average structure $CH_3(CH_2)_n-$ where $n \geq 4$ for platinum and $n=3$ for nickel. The spectra of acetylene with metals on different supports (73,74) were very similar to those obtained with silica supported metals.

Sheppard (75) studied the chemisorption of propylene and methylacetylene on silica supported platinum. Propylene was considered to be adsorbed by a dissociative mechanism rather than the associative mechanism. Methylacetylene produced weak absorption bands, which suggested the occurrence of some olefinic and some saturated groups. Kokes et al (45,70,71) studied the adsorption of propylene, allene and methylacetylene on zinc oxide. They assigned the spectra to a π alkyl and propargyl species.

The results of all these studies are often used to deduce mechanism of catalytic reaction although there are no special investigations directed to the study of the relationship between surface compounds spectroscopically observed and intermediates of certain heterogeneous catalytic reactions. Thus, the spectroscopic data have not been, so far, successfully used for elucidating the reaction mechanism of catalytic process on supported metals. Recently, Palazov et al (76) have tried to use infrared spectroscopic data to investigate the mechanism of some catalytic reactions of the hydrocarbons on metals by investigating the behaviour of surface compounds spectroscopically observed under carefully selected experimental conditions. They have suggested that the C-C bond rupture in the hydrogenolysis of paraffins was the rate controlling step.

3. EXPERIMENTAL RESULTS

3.1 Apparatus

3.1.1 Kinetics and Analysis

The experiments were performed in a constant volume static conventional high vacuum system. The schematic diagram of the apparatus is given in Fig. 1.

The apparatus essentially consisted of five sections.

1) Hydrogen Section

This section consisted of a hydrogen cylinder supplied by Linde Company, connected to a Deoxo purifier supplied by Engelhard Industries Inc., which in turn was connected to a cylindrical tube (glass thimble) containing palladium asbestos catalyst which was surrounded by an electric furnace. The glass thimble was connected to a 3-litre hydrogen reservoir via a liquid N_2 trap.

2) Allene Section

This section consisted of an allene cylinder, supplied by Matheson Company of Canada Ltd., connected to two fractionating bulbs which in turn were connected to two hydrocarbon reservoirs.

3) Reactor Section

This section consisted of a pyrex cylindrical reactor (capacity about 50 $m\ell$ connected through pyrex tubes and stopcocks to the hydrogen and hydrocarbon section. The reactor was connected to a mercury manometer which facilitated the measurement of the change of pressure with time. The reactor was surrounded by a furnace which was heated by nichrome wires wrapped on the outside of lower section of a ceramic tube. The

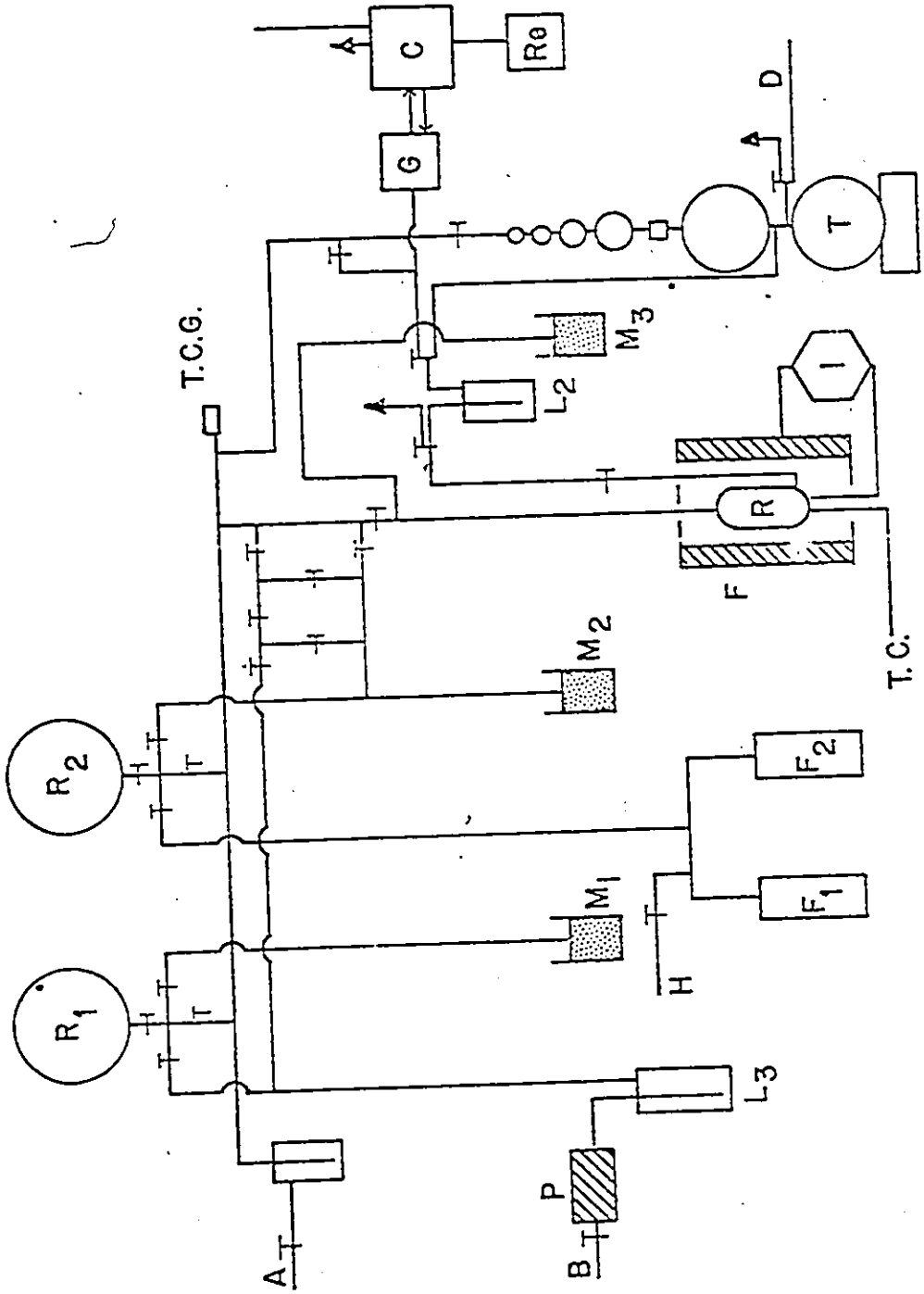

Fig. 1. Schematic diagram of the experimental apparatus

Figure 1

A —	= To high vacuum system
B	= Hydrogen supply
C	= Gas chromatograph
D	= Vacuum pump
F	= Furnace
F_1,F_2	= Fractionation bulbs
G	= Glass sampling loop
H	= Allene supply
I	= Temperature controller
L_1,L_2,L_3	= Liquid N_2 traps
M_1,M_2,M_3	= Manometers
R	= Reactor
R_1,R_2	= Reservoirs
R_e	= Recorder
T	= Toepler pump
T.C.	= Thermocouple
TCG	= Thermocouple gauge

reactor temperature was controlled by a temperature controller, coupled with variac and actuated by an iron-constantan thermocouple placed inside the furnace near the wall of the reactor. A Honeywell Pyr-O-Vane temperature controller was used to control the temperature of the furnace surrounding the reactor during the reduction of the catalyst. A Fisher proportional temperature controller was used to control the reactor temperature while performing the experiments. The temperature of the catalyst lying in the bottom of the reactor was measured by placing the iron-constantan thermocouple at the bottom of the reactor. The thermocouple in turn was connected to a Honeywell potentiometer.

4) Product Anslysis Section

This section consisted of a trap connected to the reactor and also connected through a 3-way valve to the Toepler pump, supplied by Eck and Krebs Inc., and the gas sampling valve. The Toepler pump was connected to an oil pump. The hydrocarbons were analyzed by means of a Hewlett Packard Research Gas Chromatograph employing 16'x1/4" column at 35°C packed with 30% dimethylsulpholane on acid washed 20-60 mesh chromosorb P. Helium was used as the carrier gas (25 cc/min).

5) High Vacuum System

The main high vacuum system consisted of a Duoseal vacuum pump, an oil diffusion pump and two liquid nitrogen traps (before and after the oil diffusion pump) connected to the entire system in series. The vacuum was measured by a N.R.C. Thermocouple gauge.

3.1.2 Adsorption and Infrared

The hydrogen, hydrocarbon and high vacuum sections were essentially the same as they were for kinetics. Vacuum was measured by means of an

ion gauge supplied by Ion Equipment Corporation, California. The reactor consisted of a cylindrical tube (5"xl" dia.) of stainless steel (volume = 65.0253 cc). The vacuum tightness between the body of the cell and the salt windows (CaF_2) was realized with Viton-O-rings positioned with a metal flange as shown in Fig. 2. The cell was connected to the system with glass metal joints and stopcocks lubricated by Apezone M grease. The cell was heated externally by nichrome wires wrapped around the cell using Alundum cement as an electrical insulator. To protect O-rings and salt crystals from elevated temperatures, the ends of the cell were cooled by water jackets. The temperature of the catalyst was measurec by using a chromel-alumel thermocouple placed inside the cell near the pellet protector. Adsorption section (Fig. 2z) consisted of a doser of known volume (Appendix E). Pressures were measured by means of a 90P3 MKS Baratron Pressure meter, with a sensitivity of $5x10^{-4}$torr. Reference side of the pressure head was connected to a high vacuum system. The adsorption and infrared studies were made on the same catalyst sample in the form of a pellet (=1" dia.) pressed at 4000 pounds. A Perkin Elmer 421 dual grating spectrophotometer was used to record the infrared spectra of the surface of the catalyst. The die (Fig. 2y) was made of FNS steel, machined in proper form and hardened at high temperatures. The surface of the die was polished to a fine mirror.

3.2 THE PURIFICATION OF THE REACTANTS

3.2.1 Hydrogen

The hydrogen gas from the cylinder was purified by passing it slowly (20cc/min) through a Deoxo purifier, silica gel and a reactor (glass thimble) containing 10% palladium asbestos catalyst at 250°C. The palladium asbestos catalyst converted the traces of oxygen into

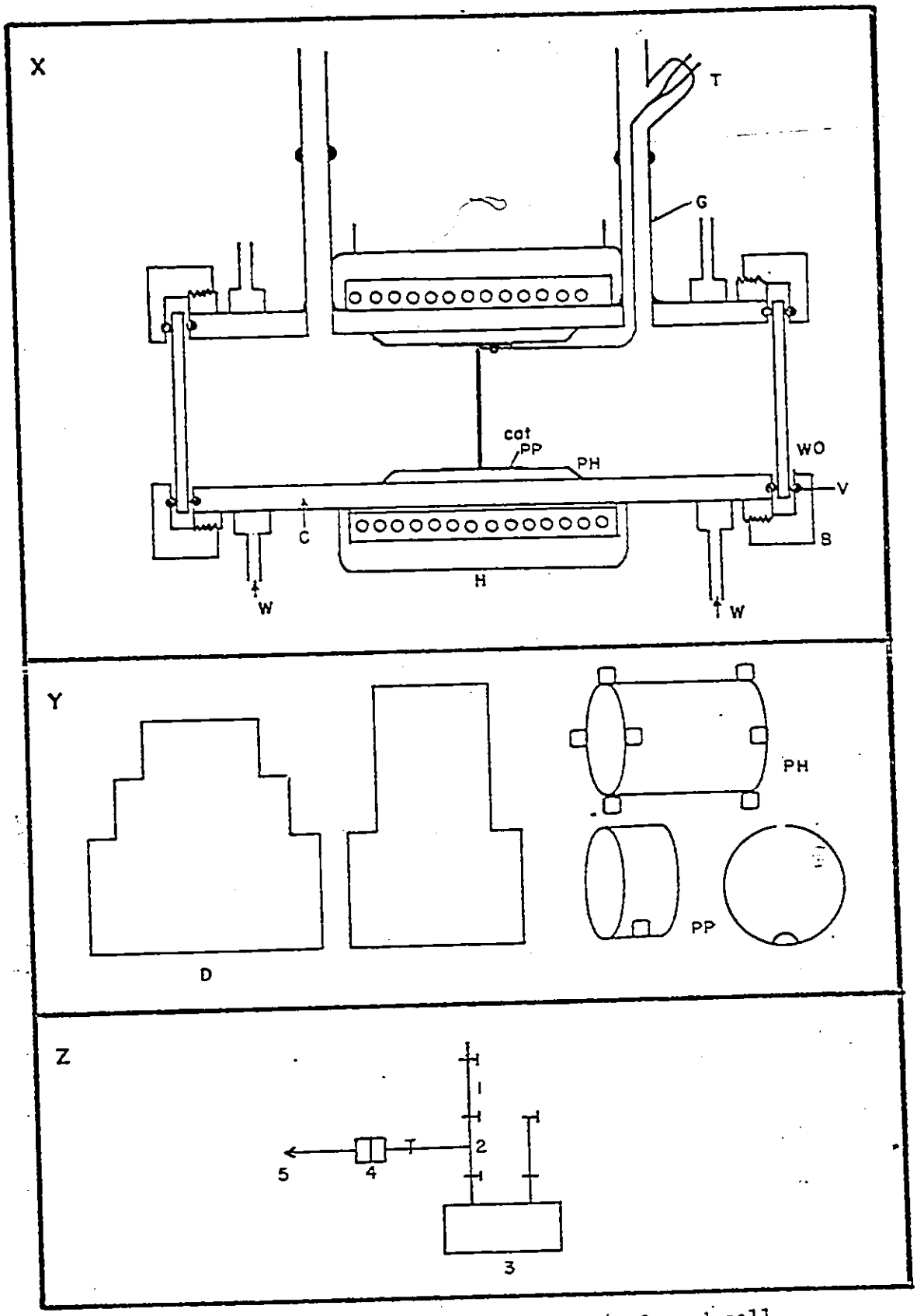

Fig. 2. Diagram of adsorption section and infrared cell.

Figure 2

T	= Thermocouple
G	= Glass metal joint
Cat	= Catalyst
PP	= Pellet protector
PH	= Pellet holder
WO	= CaF_2 window
V	= Viton-O-ring
B	= Metal flange
H	= Heater
W	= Water jacket
C	= Cell body
D	= FNS steel die
1	= Hg calibrated loop
2	= Doser of known volume
3	= Cell
4	= Pressure head
5	= Reference side of pressure head

water vapour. The hydrogen gas was then dried by passing it through a liquid nitrogen trap which removed the water vapour and the condensible impurities. The purified hydrogen gas was subsequently stored in a 3-litre hydrogen reservoir previously evacuated.

3.2.2 Allene

Chemically pure allene from the cylinder was introduced into one of the fractionating bulbs previously evacuated and allene was condensed using liquid nitrogen. The uncondensed gases were pumped off. The condensed allene was gently heated and the middle fraction was recondensed in the second bulb by means of dry ice after pumping off the head and tail fractions. The second bulb was then gently heated and the middle fraction containing dry allene was analyzed by gas chromatograph for the presence of impurities. The distillation process was repeated until the analysis showed no detectable impurities. Dry allene was stored in a previously evacuated reservoir.

3.3 PREPARATION OF THE CATALYSTS

Metal catalysts containing 5% metal were prepared using Fisher Scientific Co. certified $Ni(NO_3)_2$, $6H_2O$; $Co(NO_3)_2$, $6H_2O$; $Fe(NO_3)_2$, $9H_2O$ and $Cu(NO_3)_2$, H_2O. These contained less than 0.05% metals as impurity. Pd, Pt, Rh, Ru, Ir and Os were prepared from $Pd(NO_3)_2$, $PtCl_2$, $RhCl_3$, $RuCl_3$, $Ir(NH_4)Cl_6$ and OsO_4 respectively. These were supplied by K&K Laboratories (New York, U.S.A. and had research grade purity (% impurities not defined)). Silica (EH-5) was supplied by Cabot Corporation, Boston. It was heated at 650°C for about 12 hrs. prior to its use. 0.5 gm of the desired compound was dissolved in about 100 ccs. of acetone or water. This solution was added to the required amount of silica powder. The slurry thus obtained was stirred and dried at room temperature. The impregnated catalyst was then crushed into fine powder.

3.4 REDUCTION OF THE CATALYST

The reaction vessel containing the catalyst was sealed and evacuated until a high vacuum (10^{-4}torr for kinetics and 10^{-6}torr for adsorption and infrared studies) was obtained. A stream of hydrogen (80 cc/min) was passed through the reactor and the temperature raised slowly to 400°C in about 12 hrs. and then maintained constant for 24 hrs. The stream of hydrogen was stopped and the reaction vessel was allowed to cool to room temperature in about 200 mm Hg of hydrogen.

3.5 EXPERIMENTAL PROCEDURE

3.5.1 Kinetics

The catalyst was aged by hydrogenating allene over the catalyst for sufficient time at room temperature until the catalyst attained constant activity. The reactor temperature was adjusted to required value by means of a Fisher Proportional Temperature Controller. The reactor was evacuated and a hard vacuum obtained. The required amount of allene was introduced into the reactor. Soon after the admission of the required amount of the second reactant (hydrogen) into the reactor, the change of pressure with time was measured by the mercury manometer connected to the reaction vessel. In order to make the second and subsequent runs, the reactor was again evacuated for several minutes and the procedure repeated. The runs were made at random to nullify the effect of any change in the activity of the catalyst. For a particular temperature, a number of runs were taken by changing the hydrogen pressure while keeping the allene pressure constant at 50 mmHg. These runs gave the order of

reaction with respect to hydrogen. Similar procedure was followed to obtain the order of reaction with respect to allene by keeping the hydrogen pressure fixed at 50 mm Hg and varying allene pressure. The change of temperature during the reaction was within 0.1°C.

Runs were taken at several temperatures. After completing the runs at a particular temperature, the catalyst was kept in about 200 mm Hg of hydrogen before starting the next series.

3.5.2 Analysis of the Products

A series of runs were carried out with each catalyst except for iron and osmium. Hydrocarbons were analyzed by the gas chromatograph using helium as the carrier gas. Hydrogen was measured with the help of the Toepler pump by transferring it to a series of bulbs calibrated at different pressures.

After the pressure had fallen to the desired extent, the reactor was connected to the glass trap kept in liquid nitrogen. The non-condensable hydrogen was transferred to the bulbs. The glass trap was disconnected from the reactor and the Toepler pump and the condensed products transferred to the sampling glass loop maintained at room temperature. A definite volume (5 ml) was injected into the chromatograph and the product composition determined. The product distribution was obtained for different temperatures, pressure drops and initial reactant pressures.

3.5.3 Isomerization

The catalyst was reduced after studying the kinetics and evacuated for four hours at 450°C and then cooled to room temperature under vacuum.

The catalyst was aged by introducing allene (50 mm). The reactor was connected to the liquid nitrogen trap after 30 minutes. Allowing sufficient time for condensation, the trap was disconnected and the gases were analyzed as described in Section 3.5.2. When a constant activity (same distribution) was obtained, the desired temperature was maintained with the help of temperature controller. Definite amount of allene (50 mmHg) was introduced in the reactor and the gas was analyzed after a certain time. The same amount of gas was introduced again and the analysis was made at different time intervals. Runs were made for different allene pressures, to obtain the order of reaction with respect to initial allene pressure, and at several temperatures.

3.5.4 Adsorption

About 100 mg of the catalyst was pressed at a pressure of 4000 pounds. A good pellet was selected for the adsorption and infrared studies. The pellet was placed in the sample cell and another pellet of pure silica (equivalent weight of silica present in the catalyst pellet) was placed in the reference cell. Both cells were sealed by placing the calcium fluoride windows at the ends. The system was evacuated until a high vacuum (10^{-6} torr) was obtained and the catalyst was reduced by the method described in Section 3.4. Silica was treated similar to the catalyst. After reduction, the catalyst was degassed for 4 hrs. at 450°C and cooled to room temperature under vacuum. The cell was disconnected from the doser and the evacuation system by closing the stopcocks. Hydrogen was introduced in the doser and the pressure measured by means of the pressure meter. Hydrogen from the doser was expanded

into the cell by opening the valve between the doser and the cell. After waiting for sufficient time, the equilibrium pressure was measured and the cell was again disconnected from the doser. The hydrogen pressure in the doser was increased. The adsorption process was repeated again for several times to obtain a low pressure adsorption isotherm. The cell was evacuated for 4 hrs. at room temperature and adsorption isotherms on hydrogen exposed surface were measured. After reducing the catalyst, adsorption isotherms of allene and propylene on bare catalyst surfaces were measured.

3.5.5 Infrared Studies

In the initial stages of the investigation, reduced platinum catalyst, when degassed for more than 1/2 hr. at 400°C yielded a sharp band at 2060 cm^{-1} at pressures of 10^{-6} torr. On introducing propylene into the cell, the band shifted to a lower frequency. Addition of deuterium had no effect on the intensity of the 2060 cm^{-1} band. The absorption band at 2060 cm^{-1} was probably due to CO or some carbonyl compounds originating from an unidentified source. Hydrogen gas was analyzed for the presence of CO and the system checked for small leaks. These measures could not identify the source of contamination as hydrogen was free of CO and no leak in the system could be detected. A fine shining film (mirror) deposited on the window when the temperature of the cell was increased to more than 700°C. Apparently, the contaminating material was evaporating under vacuum and at high temperatures from the cell body (stainless steel). After evacuating the cell for weeks at 700°C, no film deposition on the window was observed. With a reduced platinum-silica catalyst,

the cell was evacuated again for 8 hrs. at 400°C. The infrared spectra showed no absorption band at 2060 cm^{-1}. To reduce the chances of any possible contamination due to prolonged heating at higher temperatures about 100 mm of dry helium was introduced in the cell every hour for a few minutes. The cell was cooled to 200°C in the presence of helium and then evacuated for 30 minutes at 200°C before cooling to room temperature under vacuum.

Following the adsorption isotherms, sample and reference cells were connected and the catalyst was reduced and evacuated for 4 hrs. at 400°C, cooled to room temperature under vacuum. An infrared spectrum of the bare surface was taken between 4000 and 1300 cm^{-1}. Hydrogen at different pressures was introduced and spectra recorded. The cell was evacuated and the spectrum was recorded again. Similar steps were repeated for allene and propylene. After initial adsorption and evacuation, small doses of hydrogen were introduced in the cell and spectra recorded for all the doses of hydrogen or at different time intervals. The instrument (infrared spectrophotometer) setting was kept same for all infrared studies and the details of the setting are given in Appendix D.

4. INTERPRETATION OF THE DATA

The kinetics of allene hydrogenation and isomerization were studied with the purpose of determining the following parameters.

4.1 Shape of Pressure-Time Curves

Bond (15), while studying the acetylene hydrogenation over pumice supported nickel catalyst, found that the shape of the pressure-time curves depended on:

a) the initial hydrogen to acetylene ratio

b) the pretreatment of the catalyst

c) the order of admission of the reactants.

The observed pressure-time curves were classifed as follows.

Type I. Zero order reaction, the rate being constant up to a pressure fall about equal to the initial acetylene pressure.

Type IIA. A "borken" curve, consisting of two linear portions of different rates.

Type IIB. A "broken" curve, consisting of a curved portion (order greater than zero) followed by a linear portion (zero order).

Type IIC. Same as Type IIA, but the break occurring after a greater percentage of reaction.

Type III. First order in hydrogen, such curves were observed when acetylene was admitted first and the initial H_2/C_2H_2 ratio was less than two.

4.2 INITIAL RATE EXPRESSION AND THE ORDERS OF THE REACTION

While studying the hydrogenation of ethylene over a supported catalyst, Schuit and Reijen (77) used a "Power Law" rate expression for correlating their data for a general bimolecular reaction:

$$aA + bB \longrightarrow (A_aB_b)^* \longrightarrow \text{Products} \qquad (4.1)$$

The "Power Law" rate expression for the rate of reaction may be written as:

$$r_o = k(P_A)^m(P_B)^n \qquad (4.2)$$

where

r_o = the rate of reaction

k = the rate constant

m,n = the orders of reaction with respect to A and B, respectively

P_A, P_B = the pressures of A and B, respectively.

The "Power Law" rate expression was used to correlate the kinetic data of the present study of allene hydrogenation and to express the initial rate of the reaction in the following form.

Taking the natural logarithm of both sides of Equation (4.2):

$$\log r_o = \log k + n \log P_{H_2} + m \log P_{C_3H_4} \qquad (4.3)$$

Several experiments were conducted to determine m and n by the initial rate method. In all cases, allene was admitted first to the reactor.

4.3 THE ACTIVATION ENERGY

It is well known that the specific rate constant k is a function of the temperature. It was Arrhenius (78) who folowing Van't Hoff arrived at an expression relating the specific rate constant with the temperature namely:

$$k = A \exp\left(-\frac{E}{RT}\right) \tag{4.4}$$

where

k = the specific rate constant at T °K

A = frequency factor

E = apparent activation energy for the reaction

R = universal gas constant

A and E are assumed constants for a given reaction.

Taking the natural logarithm on both sides of Equation (4.4):

$$\log k = \log A - \frac{E}{2.303RT} \tag{4.5}$$

By determining the specific rate constants at various temperatures and plotting $\ell n\, k$ or $\log k$ against the reciprocal of the absolute temperature, a straight line relationship has been observed for various reactions. The gradient of the line is (-E/RT) or (-E/2.303R) from which the activation energy can be computed. The frequency factor can be determined from the intercept or using Equation (4.5).

4.4 PRODUCT DISTRIBUTION AND SELECTIVITY

The hydrogenation of allene usually takes place according to the following sequence:

$$\text{Allene} \xrightarrow{H_2} \text{Propylene} \xrightarrow{H_2} \text{Propane} \qquad (4.6)$$

Several products, besides propylene and propane, could form during the reaction depending on the nature of the catalyst. However, in the present study over cobalt catalyst, only methylacetylene was detected in addition to the normally formed propylene and propane.

Selectivity is defined as:

$$S = \frac{P_{propylene}}{P_{propylene}+P_{propane}+P_{methylacetylene}} \qquad (4.7)$$

where

$P_{propylene}$ = pressure of propylene, mm Hg

$P_{propane}$ = pressure of propane, mm Hg

$P_{methylacetylene}$ = pressure of methylacetylene, mm Hg.

4.5 ADSORPTION

Low pressure adsorption isotherms of hydrogen, allene and propylene were measured with the purpose of determining:

1) amounts of gases adsorbed at room temperature
2) to calculate metal surface area
3) to calculate dispersion or H/M ratio
4) if possible, to correlate these parameters with the catalytic activity.

1) Adsorption Isotherms

The adsorption isotherms were measured volumetrically. In a pre-calibrated doser, a particular gas was introduced at a known pressure. The doser was connected to the reactor. After waiting for sufficient time (for adsorption), equilibrium pressure was measured. The doser was disconnected from the reactor and the same process was repeated several times. All the adsorption studies were made at room temperature (25±1°C).

Suppose V_1, V_2, P_n, P_{nc} and P'_n represent the volume of the doser, volume of the reactor, pressure of the gas in the doser before expansion, calculated pressure of the gas after expansion or before adsorption and pressure of the gas after adsorption (equilibrium pressure) for nth dose, respectively.

Assuming ideal gas behaviour at room temperature:

$$P_1V_1 = P_2V_2 \tag{4.8}$$

For the first dose:

$$P_1V_1 = P_{1c}(V_1+V_2) \tag{4.9}$$

or

$$P_{1c} = \frac{V_1}{V_1+V_2} P_1 = V_T P_1 \tag{4.10}$$

where

$$V_T = \frac{V_1}{V_1+V_2}$$

The amount of gas adsorbed at (V_1+V_2) and (25°C) $= P_{1c}-P'_1$

$$= V_T P_1 - P'_1 \tag{4.11}$$

For the second dose, the pressure of the gas to be expanded:

$$= P_2 - P'_1$$

$$(P_2-P_1')V_1 = P_{2c}(V_1+V_2)$$

or

$$P_{2c} = V_T(P_2-P_1') \tag{4.12}$$

Actual calcualted pressure before adsorption = $P_{2c}+P'$.

$$\text{Amount adsorbed } (V_T,T) = P_{2c} + P_1' - P_2' \quad \text{mm Hg}$$

$$= V_T(P_2-P_1') - P_2' \quad \text{mm Hg} \tag{4.13}$$

The total amount of gas adsorbed after the second dose

$$= V_T(P_2-P_1') - P_2' + V_TP_1 - P_1' \tag{4.14}$$

For the nth dose, the pressure of the gas to be expanded

$$= V_T(P_n-P'_{n-1}) \tag{4.15}$$

and

$$P_{nc} = V_T(P_n-P'_{n-1}) \tag{4.16}$$

The actual calculated pressure = $P_{nc} + P'_{n-1}$.

The amount adsorbed for the nth dose

$$= P_{nc} + P'_{n-1} - P'_n$$

$$= V_T(P_n-P'_{n-1}) + P'_{n-1} - P'_n \tag{4.17}$$

The amount of gas adsorbed after the nth dose

$$= V_T \sum_{n=1}^{n} (P_n-P'_{n-1}) + \sum_{n=1}^{n} P'_{n-1} - \sum_{n=1}^{n} P'_n \tag{4.18}$$

The amount adsorbed in terms of pressure at total volume (V_1+V_2) and temperature T(25°) can be converted to volume adsorbed (cc STP)/gm employing the following relationship:

$$\frac{P_1V_1}{T_1} = \frac{P_2V_2}{T_2} \qquad (4.19)$$

The volume adsorbed at P'_n

$$= \frac{273}{293} \cdot \frac{\text{amount adsorbed}}{760} \cdot \frac{V_1+V_2}{\text{cat.wt.}} \qquad (4.20)$$

Using Equations (4.18) and (4.20), volumes adsorbed at equilibrium pressure P'_n were calculated to get the adsorption isotherms in the pressure range (0-20 mm).

4.6 CALCULATION OF METAL SURFACE AREA AND DISPERSION

The total surface area is of primary importance for many catalysts, notably for various oxides. Supported metal catalysts, however, have distinct different characteristics in that the principal reactive sites are considered to be on the surface of the metal phase which may be distributed in a discontinuous fashion, partially covering the oxide support. Although nitrogen surface area measurements are adequate to measure the total surface area, more specialized techniques are normally required to measure the metal surface area of the supported metals.

The technique (to measure the metal surface area) falls into two principal categories: those which determine the effective metal particle size distribution from which the metal surface area can be calculated (light microscopy, electron microscopy and x-ray diffraction line broadening) and those which determine the metal surface area directly (chemisorption of a gas which occurs with a high degree of specificity on metal surfaces but not on oxide surfaces).

The chemisorption techniques have a very definite advantage over the particle size techniques since the metal surface is measured directly

by adsorption from the gas phase of an adsorbed molecule which, in many instances, closely resembles in size, shape and chemical reactivity to the molecule of interest. Chemisorption techniques essentially require that such gas adsorption conditions be selected under which physical adsorption does not occur as a variable and intermediate component on the metal phase. In addition, correction must be made for any adsorption component of the given gas on the oxide support. These difficulties can be overcome by obtaining the adsorption isotherms at very low pressures and estimating the gas uptake at zero pressure.

The gas chemisorption data can be used to estimate the metal surface area, dispersion D defined as the fraction of the total number of metal atoms which are at the surface of the metal particles, and H/M defined as number of hydrogen atoms adsorbed per metal atom, by making certain assumptions and employing the following relationships.

$$\text{Surface metal per gm of catalyst} = \frac{2VM}{2.24\times10^{4}} \text{ gm} \qquad (4.21)$$

$$\text{Metal surface area} = \frac{2\,VN\sigma}{(2.24\times10^{4})\times10^{4}} \text{ m}^2/\text{gm} \qquad (4.22)$$

$$D = \frac{\text{total number of metal atoms on the surface}}{\text{total number of metal atoms in the catalyst}}$$

$$= \frac{\text{total number of hydrogen atoms adsorbed}}{\text{total number of metal atoms in the catalyst}}$$

$$= \frac{H}{M} = \frac{2VM}{2.24\times10^{4} \times \text{wt. of metal present in the catalyst}} \qquad (4.23)$$

where

V = volume (STP) of the gas adsorbed per gm

M = atomic weight of the metal

N = Avogadro's number

σ = effective molecular coverage area as cm^2 per adsorbed molecule (12×10^{-16} per molecule of hydrogen and 6×10^{-16} per atom of hydrogen)

2.24×10^4 = molecular volume in cm^3 at STP of an ideal gas.

Assumptions:

1) hydrogen is adsorbed dissociatively
2) each atom of hydrogen is adsorbed on single metal atom-exposed on the surface of the catalyst
3) total hydrogen uptake at zero pressure accounts for the monolayer coverage of the catalyst surface.

4.7 INFRARED STUDIES

The interpretation of the spectra of chemisorbed species must be carried out by reference to the spectra of model compounds of known structure (53). Many spectra of hydrocarbons have been analyzed in detail (79) and conclusions particularly with respect to intensities have been reviewed by Wexler (80). The usual assignments of the adsorbed bands in the infrared spectra are given in Table 4.1.

Sheppard and Ward (72) have discussed some of the criteria for using the assignments for the qualitative interpretation of the spectra of chemisorbed molecules and have concluded that such assignments are generally valid except possibly for the functional group which is attached directly to the metal which may be shifted to a somewhat lower frequency. The spectra of chemisorbed species appear to fall somewhere between those of the hydrocarbons and the metal alkyl compounds.

TABLE 4.1
Infrared frequency for hydrocarbon grouping.

GROUP	FREQUENCY (cm^{-1})	ASSIGNMENTS
C≡CH	3300–3250	νCH
$C{=}CH_2$	3080±10 ~2980	νCH_2 (as) νCH_2 (s)
–C=CH–	3025±10	νCH
CH_3–C	2955±5 2870±5 1462±5 1380	νCH_3(as) νCH_3 (s) δCH_3 (as) δCH_3 (s)
	2927±5 2855±5 ~1467	νCH_2 (as) νCH_2 (s) δCH_2
	2890±10	νCH

5. RESULTS

5.1 Kinetics

The experimental results for the kinetic study are given in Appendix B.

The pressure time curves observed were of Type III (Fig. 3a) for all the catalysts except for Pt where Type I and Type II (Fig. 3b) were observed. The shape of the curve was independent of initial hydrogen to allene ratio.

The orders of hydrogenation reaction were mostly one and zero with respect to hydrogen and allene respectively and independent of the temperature. Hence, the initial rate of reaction for the hydrogenation of allene over the series of the catalysts studied may be expressed as:

$$r_o = k' P_{H_2} (P_{C_3H_4})^{0.0} \qquad (5.1)$$

5.1.1 Reaction Over Nickel Catalyst

The experimental data obtained for the hydrogenation of allene over nickel catalyst (0.02158 gm) are given in Appendix B, Table B-1.

In the beginning, the rate of reaction over fresh catalyst was very fast even at room temperature but it decreased with each successive run. The catalyst was stabilized only after about 100 runs. The reaction had a measurable rate at 70°C. Type III pressure-time curve (Fig. 3a) similar to those obtained by Bond (15) for acetylene hydrogenation over nickel pumice and Mann and Khulbe (81) for 2-butyne hydrogenation over nickel powder were observed.

The dependence of initial rates on the initial hydrogen and allene pressures at different temperatures is shown in Figs. 4, 5 and 6. The

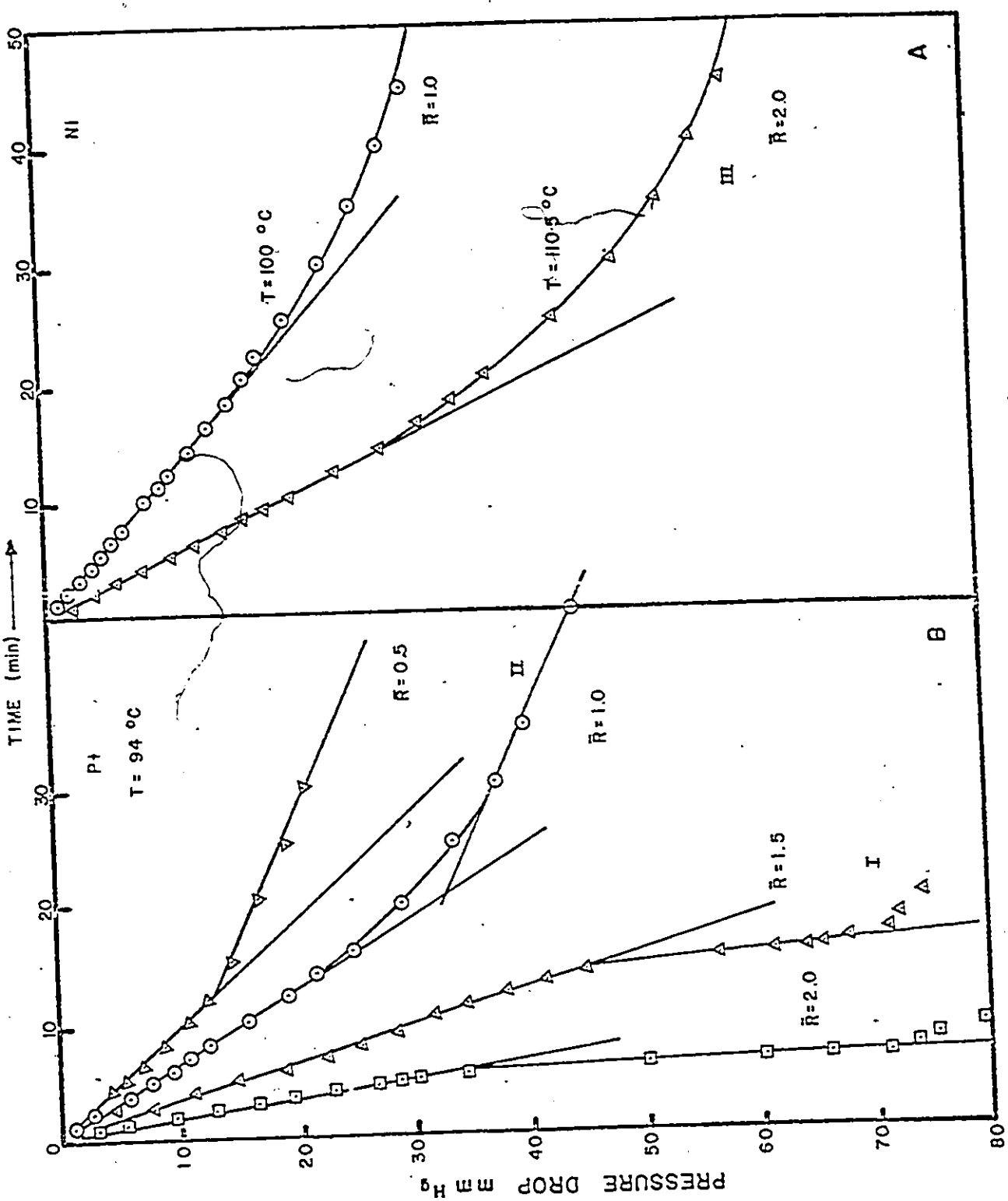

Fig. 3. Pressure-time curves.

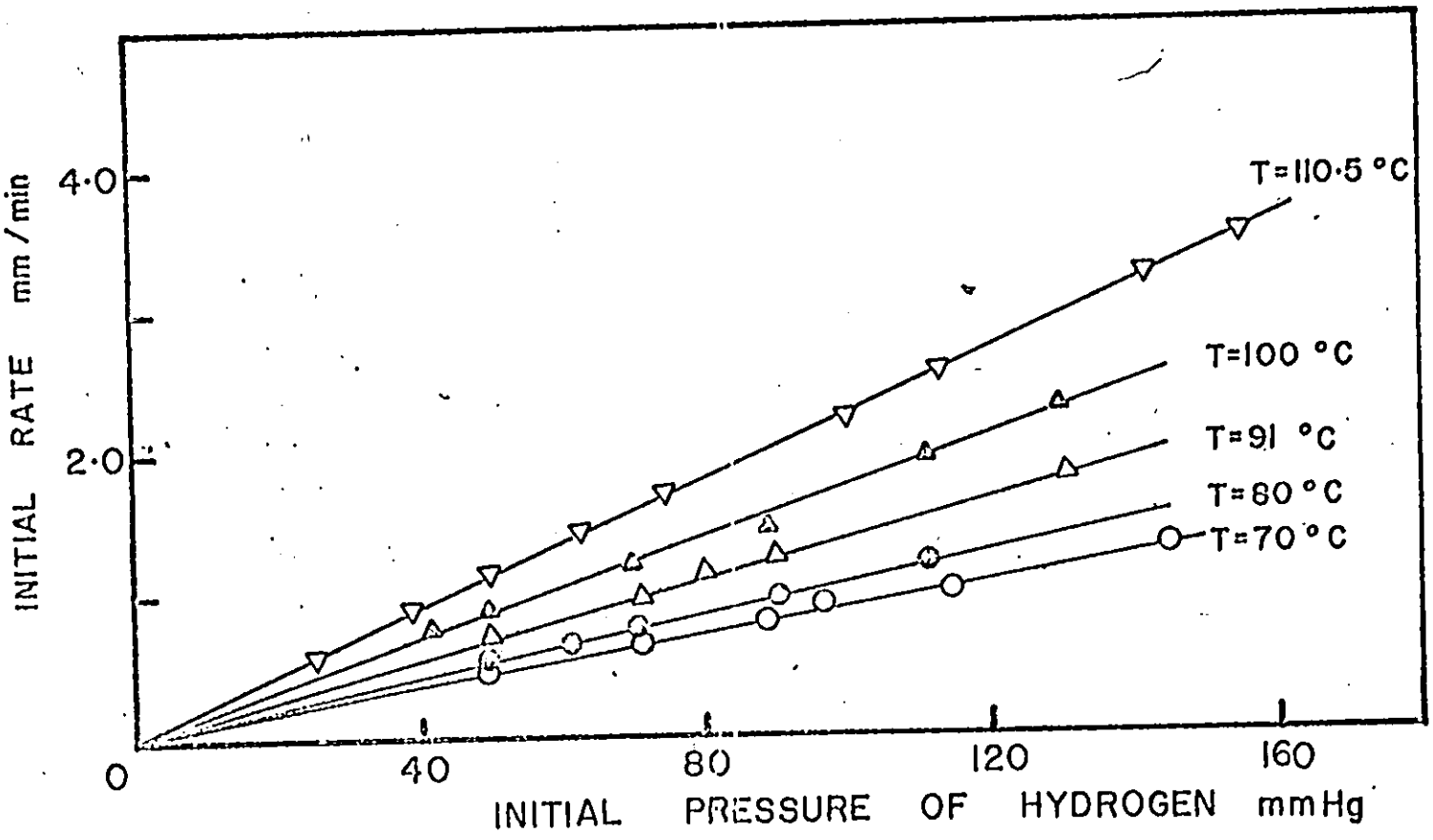

Fig. 4. Dependence of initial rate on initial hydrogen pressure (Ni catalyst).

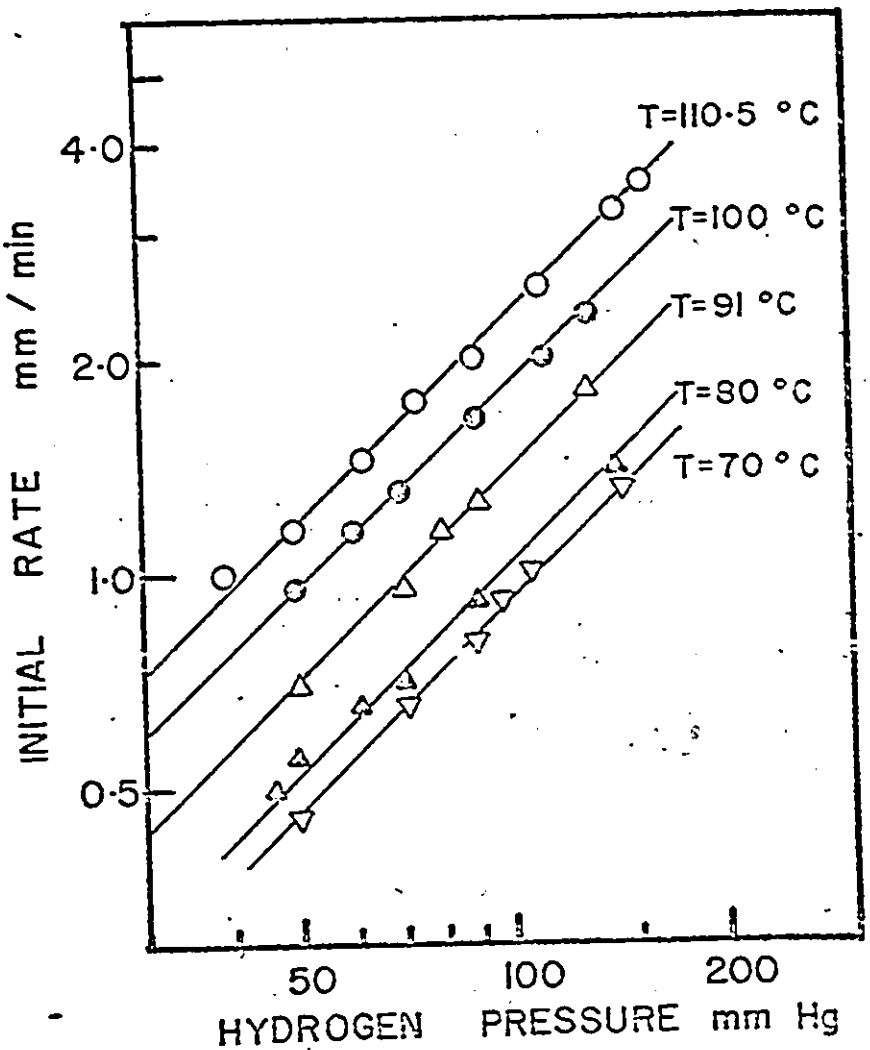

Fig. 5. Dependence of initial rate on initial hydrogen pressure (Ni catalyst).

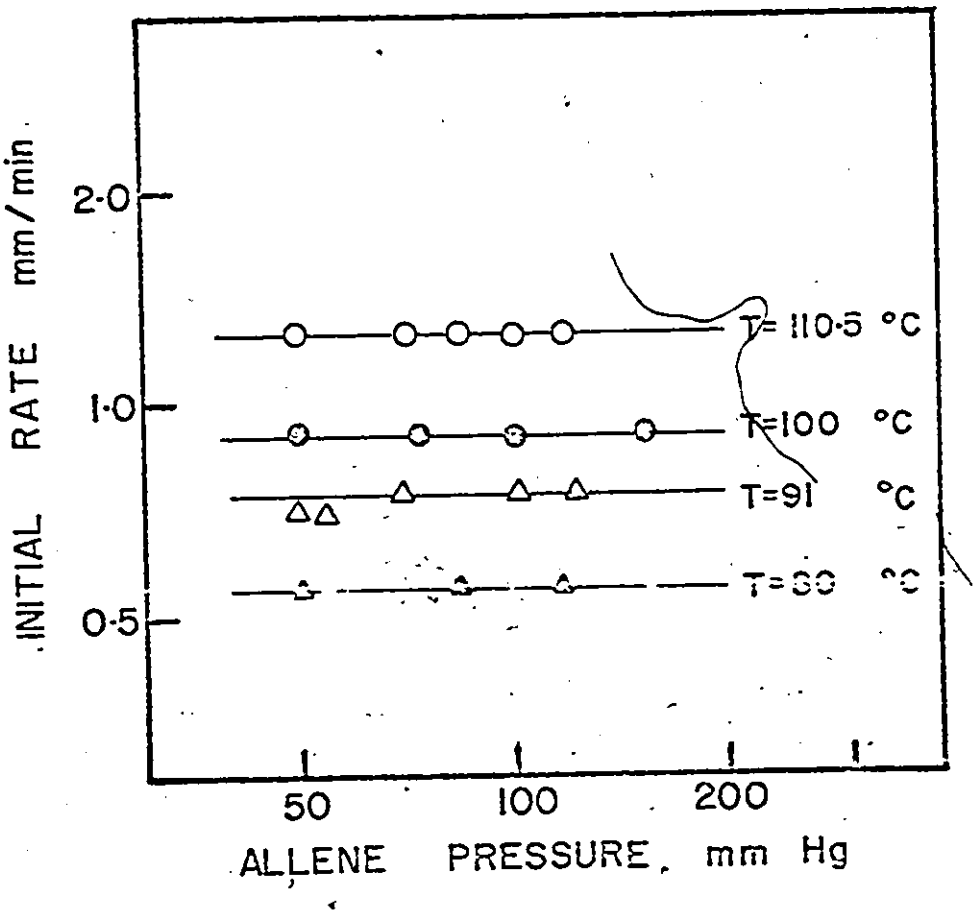

Fig. 6. Dependence of initial rate on initial allene pressure (Ni catalyst).

order of reaction with respect to hydrogen was always one and temperature independent. The order of reaction with respect to allene was always zero. The results are consistent with most of the investigations for the allene hydrogenation (21,30,31).

The influence of the temperature on the specific rate is shown in the Arrhenius plot (Fig. 7) from which the activation energy and the frequency factor were calculated to be 10.8 k cal/mole and $1.75 \times 10^6 min^{-1}/gm$, respectively.

Similar results were obtained with other catalysts and are given in Table 5.1.

TABLE 5.1
Results of allene hydrogenation on different catalysts.

CATALYST	TEMP. RANGE °C	TYPE OF PRESSURE-TIME CURVES	ORDER OF REACTION H_2	Allene	E k cal/mole
Ni	70-110	III	1.0	0.0	10.81
Cu-Ni	97-142	III	1.0	0.0	5.63
Cu	98-145	III	1.0	0.0	7.94
Rh	20-50	III	1.0	0.0	7.73
Co	50-80	III	1.0	0.0	8.64
Ir	193-260	III	1.0	0.0	8.89

5.1.2 Reaction Over Platinum Catalyst

The experimental data obtained for the hydrogenation of allene on platinum catalysts are given in Appendix B, Table B-4.

The catalyst was stabilized at 74.5°C and the reaction was studied between 74.5 and 150°C. Figs. 8 and 9 show the dependence of initial rate on initial hydrogen pressures. An inflection point was obtained at temperatures over 84°C. Similar results were obtained by Bond (15) and

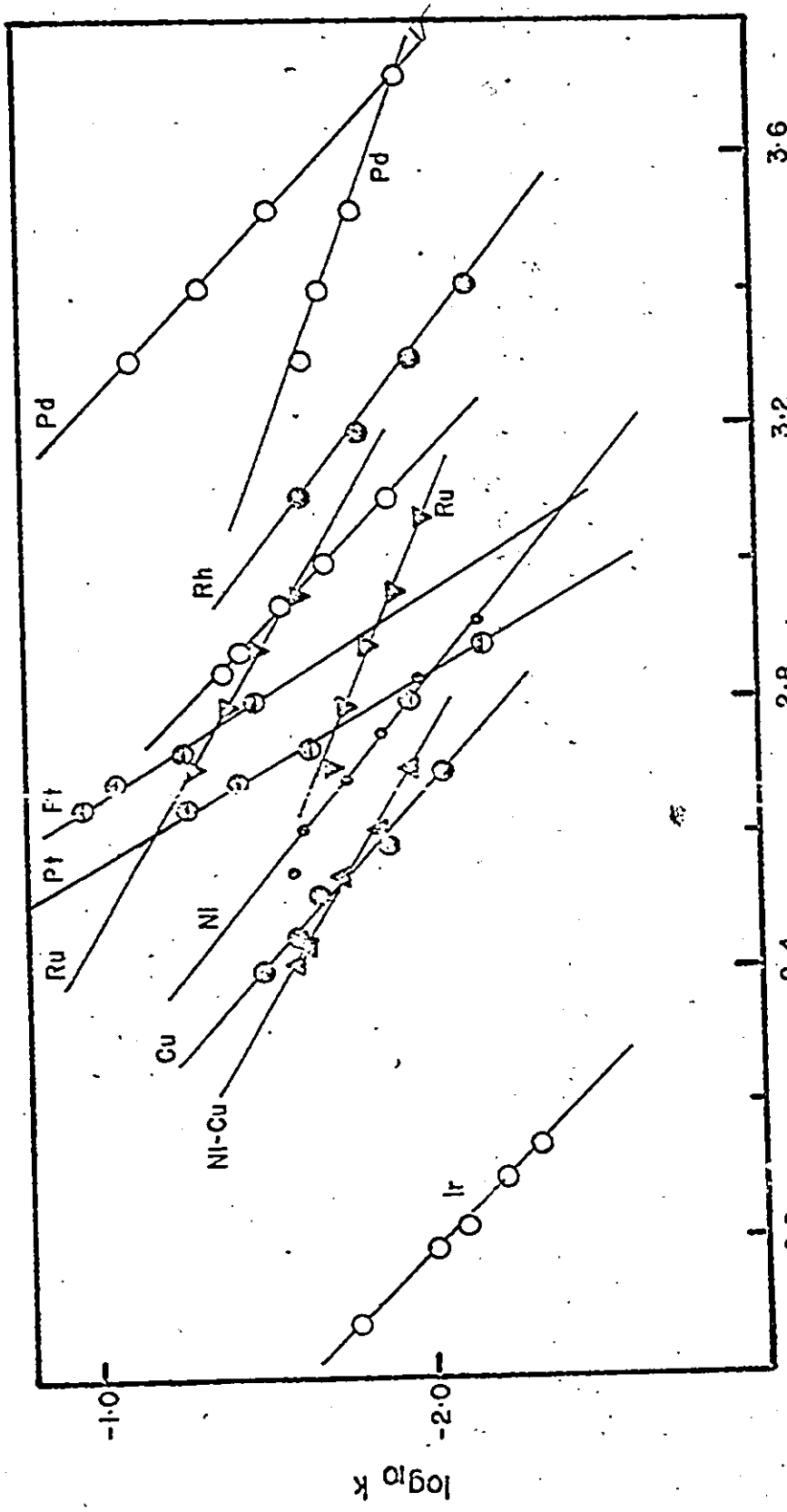

Fig. 7. Plots of $\log_{10}$ k against the reciprocal of absolute temperature.

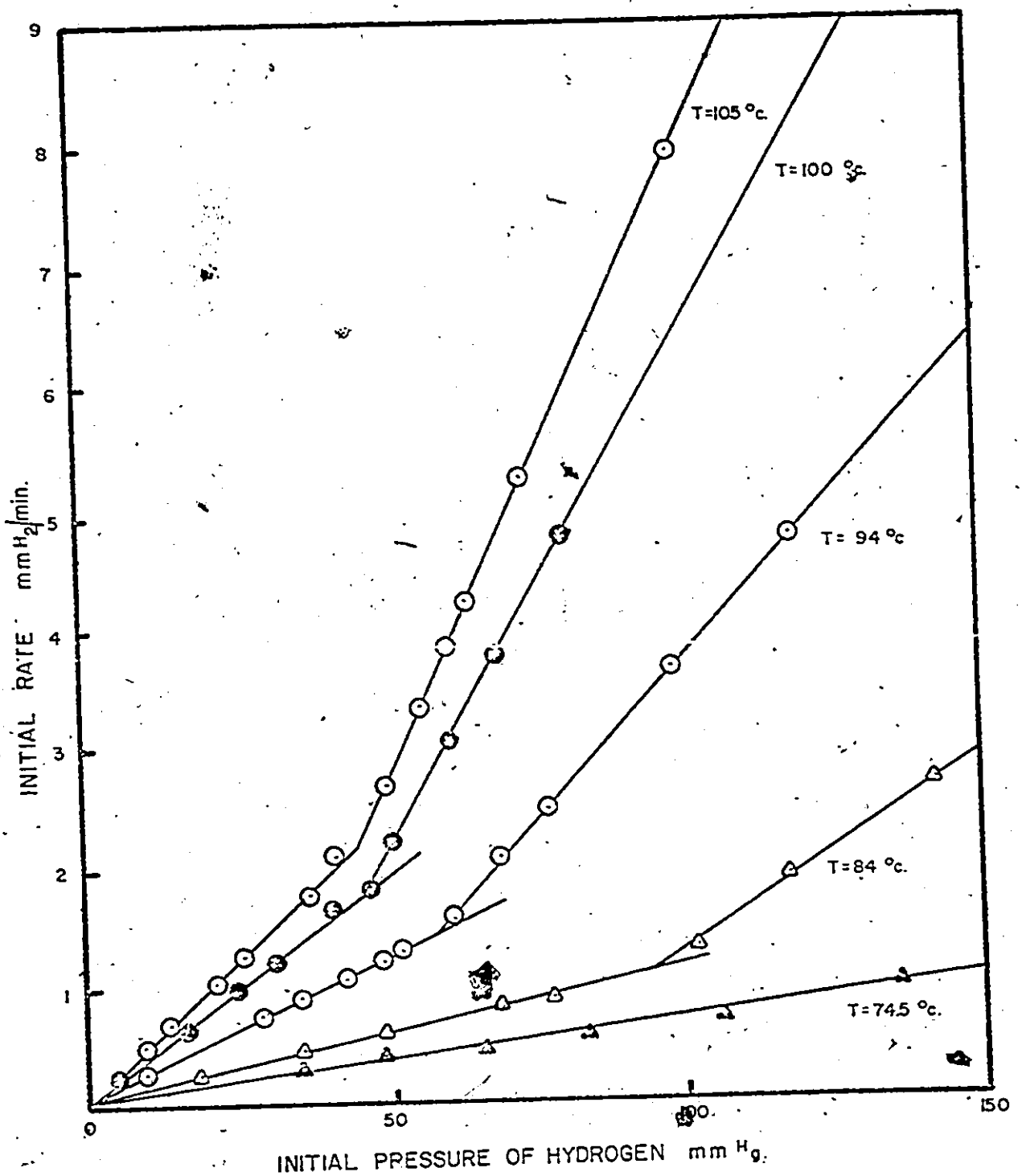

Fig. 8. Dependence of initial rate on initial hydrogen pressure (Pt catalyst).

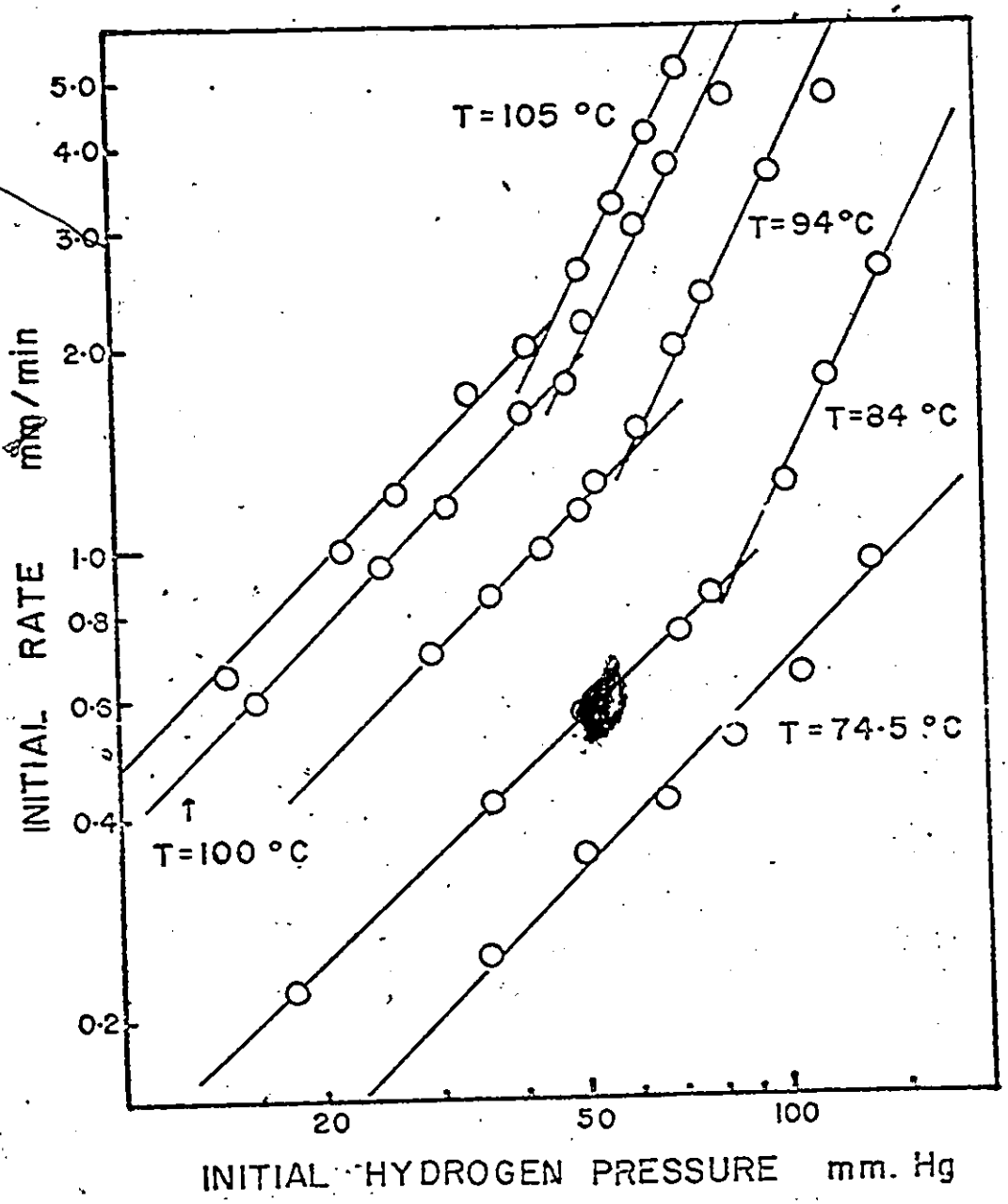

Fig. 9. Dependence of initial rate on initial pressure of hydrogen (Pt catalyst).

Bond and Mann (16) while studying the hydrogenation of acetylene on Ni-pumice, and nickel powders. They attributed these results to a complex rate equation:

$$-\frac{dP}{dt} = k_A P_{H_2} + k_B (P_{H_2} - P^o_{H_2}) \qquad (5.2)$$

where k_A and k_B are the rate constants in the first and second stages of the reaction and $P^o_{H_2}$ is the inflection point (mm H_2). This ($P^o_{H_2}$) was nearly equal to $2P_{C_2H_2}$. However, in the present case, $P^o_{H_2}/P_{allene}$ decreased with temperature. Assuming an existence of two different rate expressions, one before and the other after the inflection point, the order with respect to hydrogen was one and two, respectively. This kinetic behaviour is discussed in the next Chapter. Fig. 10 shows the dependence of initial rate on initial allene pressures. The calculated apparent activation energy was 16.4 k cal/gm mole.

Palladium and ruthenium catalysts showed similar kinetic behaviour. The results obtained with Pt, Pd and Ru are tabulated below, where m and m'

TABLE 5.2
Kinetic results obtained with Pt, Pd and Ru.

CATALYST	TEMP. RANGE °C	TYPE OF PRESSURE-TIME CURVES	m	n	m'	E_A	E_B
						k cal/gm mole	
Pt	75–115	I and II	1.0	0.0	2.0	16.4	16.4
Pd	0–40	III	1.0	0.0	1.8	8.0	3.4
Ru	55–100	III	1.0	0.0	1.5	5.64	4.0

are the orders of reaction with respect to hydrogen, n is the order of reaction with respect to allene. E_A and E_B are the calculated apparent energy of activation before and after the inflection point.

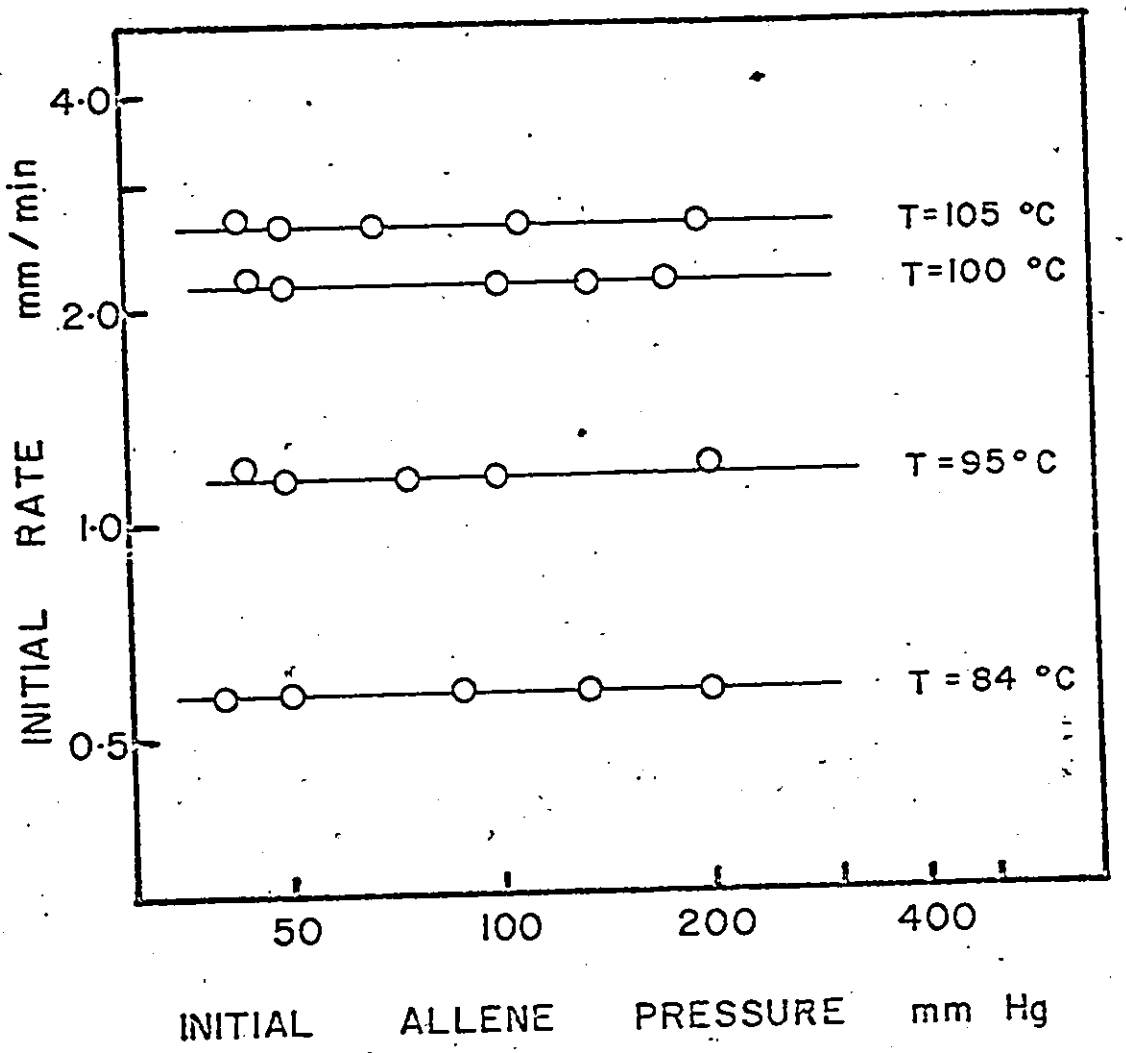

Fig. 10. Dependence of initial rate on initial pressure of allene (Pt catalyst).

5.2 SELECTIVITY

The reaction products were analyzed for different reactant ratios ($\bar{R}$) at various pressure falls and at several temperatures. Experimental results are given in Appendix B. Special attention was paid to the manner in which the observed yield of propylene depended on the operating variables. Selectivity has been defined as expressed by Equation (4.7).

5.2.1 Nickel Catalyst

1) Course of Reaction. The course of reaction was followed by analyzing the products of the reaction after various pressure falls for hydrogen allene ratios of 1 and 2. The distribution of the products and the selectivity during the course of reaction are shown in Figs. 11a and 11b.

2) Dependence of Selectivity on the Initial Pressure of Hydrogen.

The dependence of selectivity upon hydrogen pressure was studied at different temperatures (91 to 120°C) keeping allene pressure at 50 mm and varying the hydrogen pressure between 40 and 160 mm. The products were analyzed at 20 mm pressure fall in all cases. The selectivity was independent of the initial hydrogen pressure up to 100 mm and then decreased slightly (Fig. 12b). The decrease in the selectivity increased with increasing temperatures.

3) Dependence of the Selectivity on the Initial Allene Pressure.

The dependence of the selectivity upon allene pressures was studied at 120°C keeping hydrogen pressure constant at 50 mm while varying allene pressure between 40 and 90 mm and analyzing the products at 20 mm pressure fall. The selectivity was independent of allene pressures (Fig. 12a).

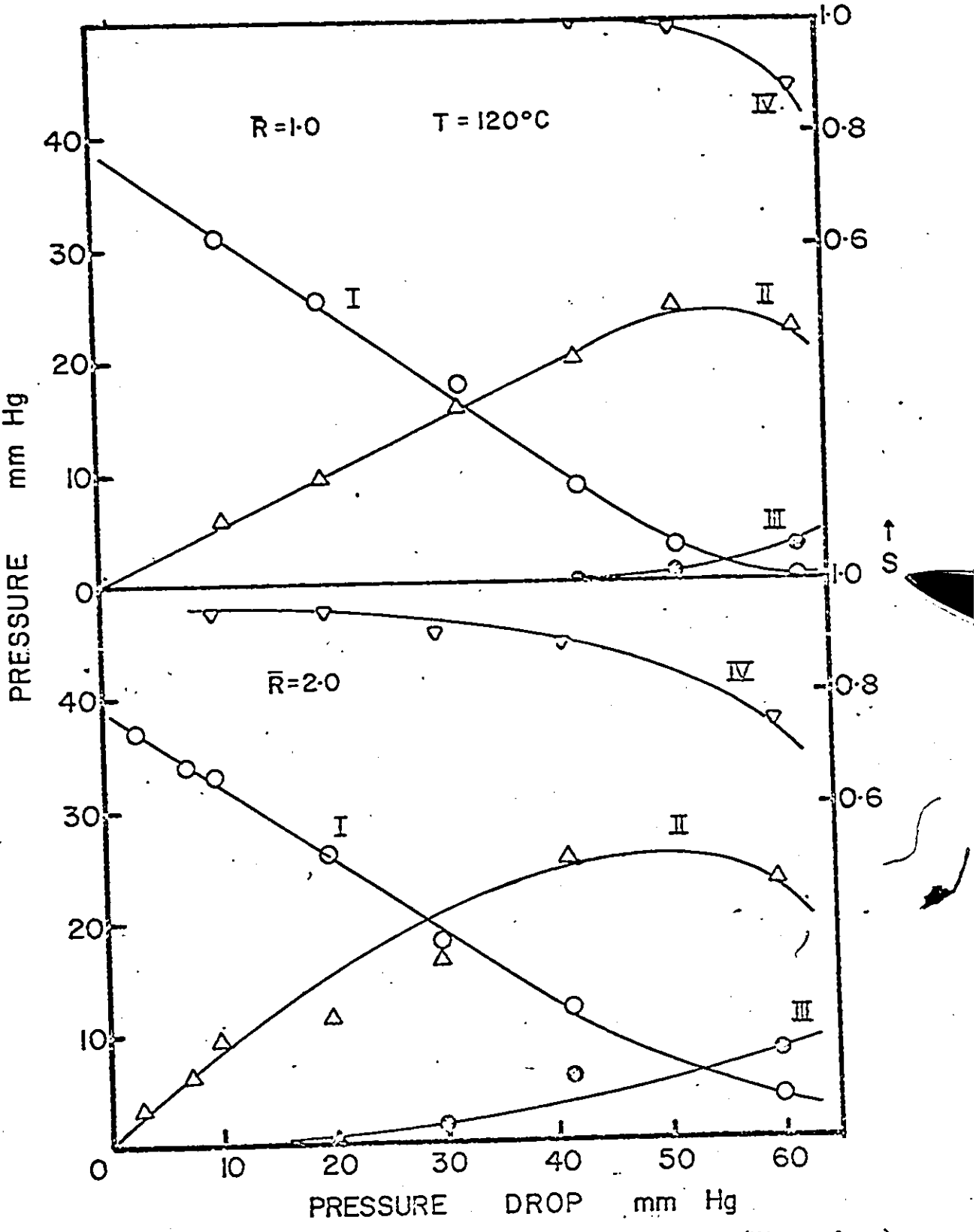

Fig. 11. Product distribution during the course of reaction (Ni-catalyst). I = allene, II = propylene, III = propane, IV = selectivity.

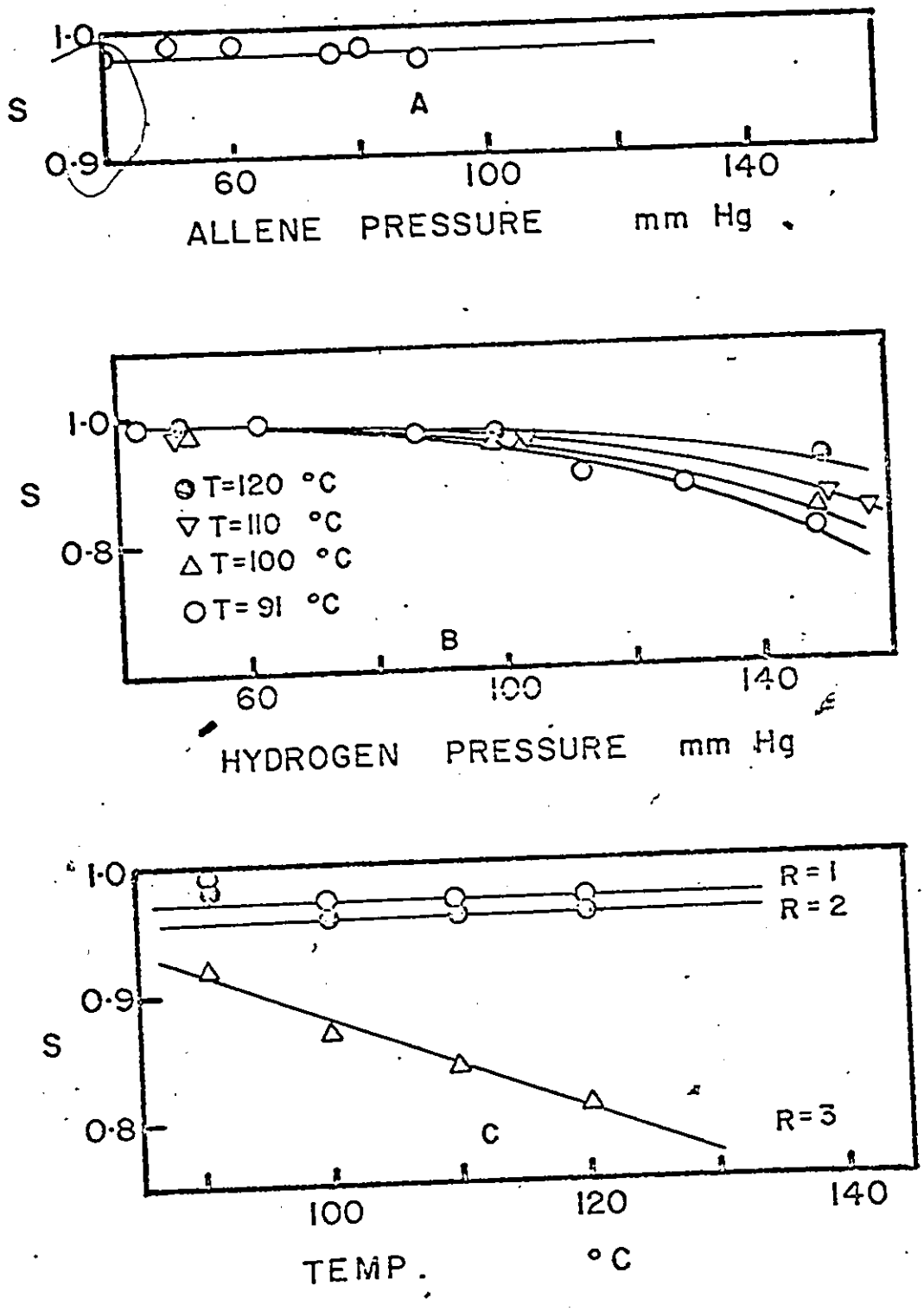

Fig. 12. Dependence of selectivity (Ni catalyst).

4) Dependence of the Selectivity on the Temperature. The temperature dependence of the selectivity was studied at hydrogen-allene ratio of 1, 2 and 3 ($P_{C_3H_4}$=50 mm) between 91 and 120°C. The products were analyzed for a 20 mm pressure-fall. No significant change in the selectivity with the temperature was observed for reactant ratios of 1 and 2. For a reactant ratio of 3, the selectivity decreased linearly with the temperature (Fig. 12c).

5.2.2 Nickel-Copper Alloy (95% Ni and 5% Cu)

Fig. 13 shows the distribution of products, reactants and selectivity during the course of reaction for reactant ratios of 1, 2 and 3 ($P_{C_3H_4}$=50 mm) at 142°C. The initial product of the reaction was propylene. Small amounts of propane were obtained at higher pressure falls due to further hydrogenation of propylene. The selectivity was independent of allene pressure but decreased sharply with increasing hydrogen pressures. Fig. 14a shows the dependence of the selectivity with initial hydrogen pressures at various temperatures. Fig. 14 b shows the dependence of the selectivity on temperature for reactant ratios of 1, 2 and 3. The selectivity increased with increasing temperatures for reactant ratios of 2 and 3.

5.2.3 Copper Catalyst

The only product from the hydrogenation of allene on copper was propylene and the selectivity was independent of the variables studied. Fig. 15 shows the results of the product analysis for $\bar{R}$=1 and 2 at 145°C.

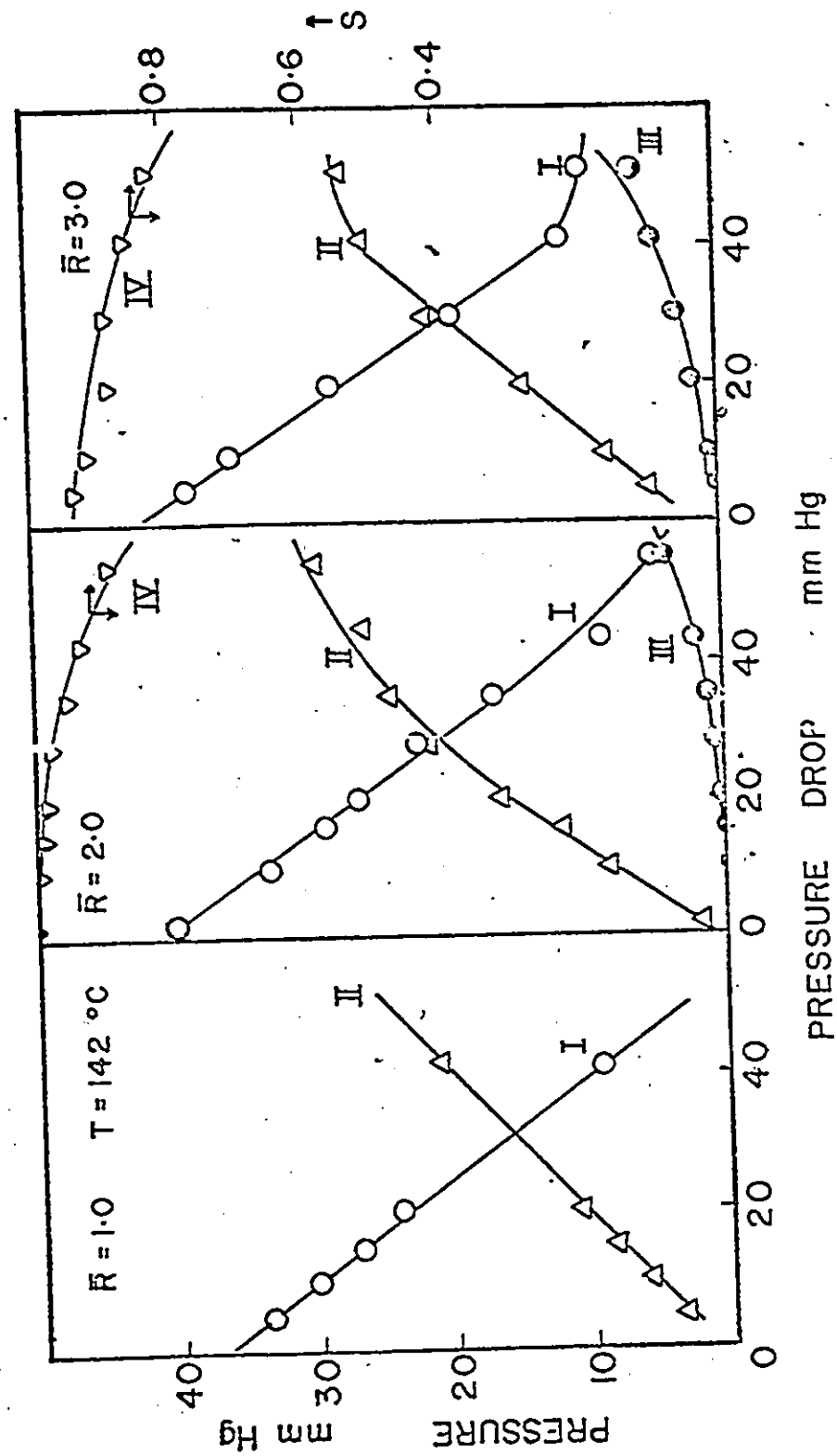

Fig. 13. Product distribution during the course of reaction (Ni-Cu catalyst). I = allene, II = propylene, III = propane, IV = selectivity.

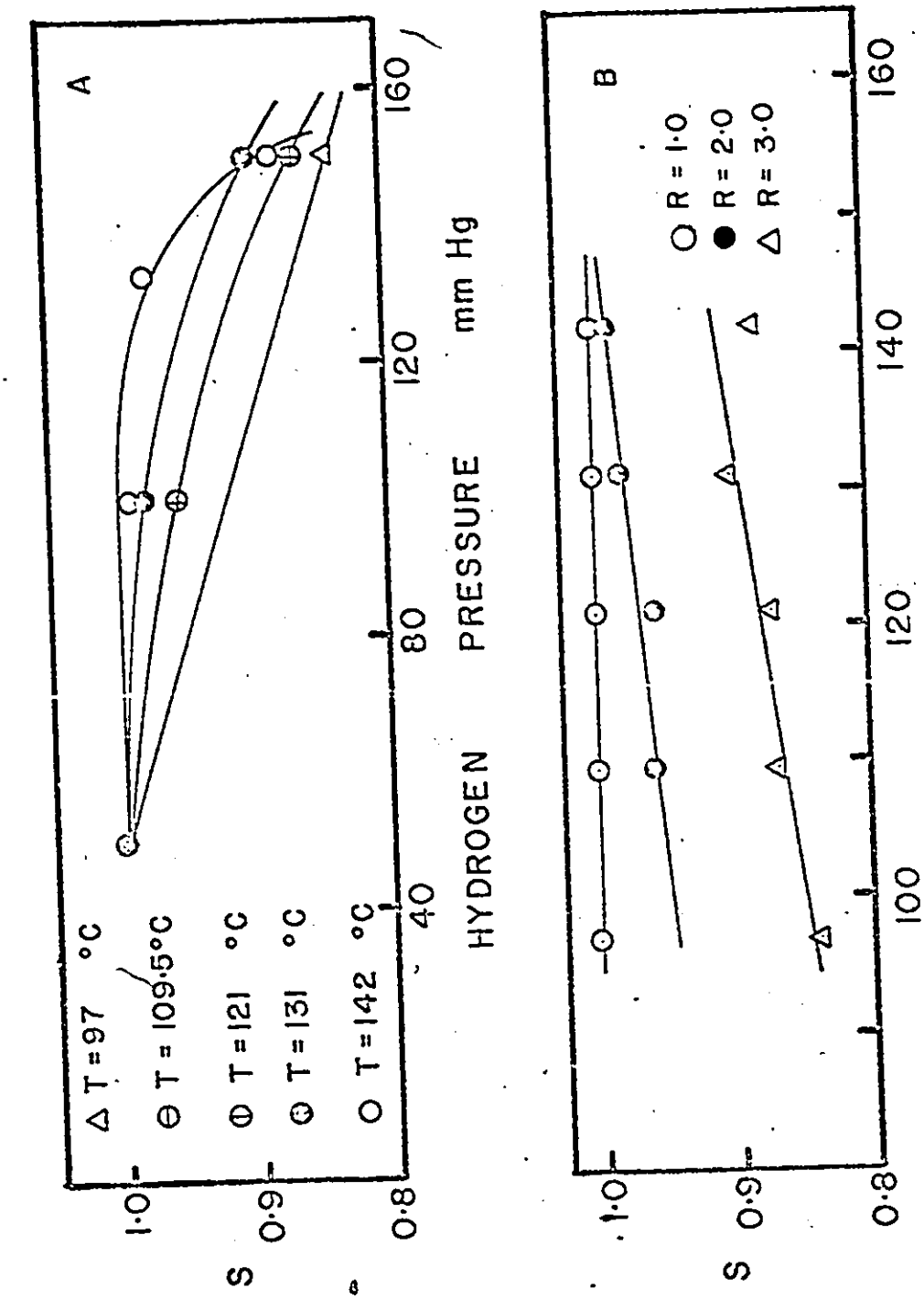

Fig. 14. Dependence of selectivity (Ni-Cu catalyst).

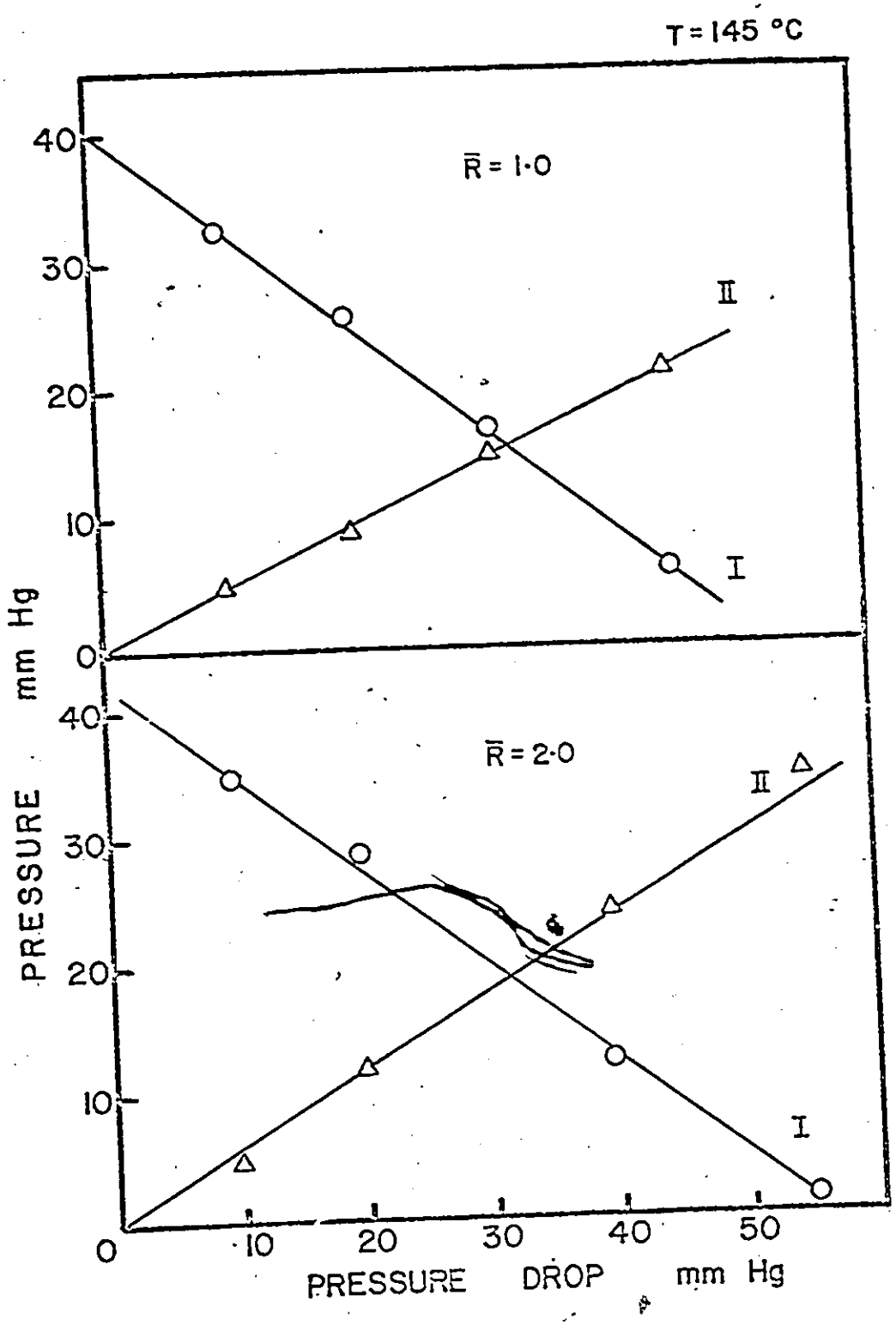

Fig. 15. Product distribution during the course of reaction (Cu catalyst). I = allene, II = propylene.

5.2.4 Platinum Catalyst

Fig. 16 shows the product distribution and the selectivity during the course of the reaction at 100°C for reactant ratios of 0.5, 1, 1.5 and 2.0. The figure shows that the initial products of the reaction were both propylene and propane. The formation of propane increased with increasing hydrogen pressures. Fig. 17 shows the variation of the selectivity on initial hydrogen pressure at different temperatures. The selectivity increased slightly with increasing temperatures, but for reactant ratios of 1.5 and 2 at temperatures of 100 and 105°C, a sudden drop in the selectivity was observed (Fig. 18a).

5.2.5 Palladium Catalyst

The initial products for the hydrogenation of allene over 5% palladium at 40°C were propane and propylene for reactant ratios of 1 and 2.15 ($P_{C_3H_4}$=50 mm). The selectivity was nearly constant for a reactant ratio of 1 and decreased slightly during the course of reaction for a reactant ratio of 2.15 (Fig. 19). The selectivity increased slightly with increasing allene pressures (Fig. 20a) and decreased with increasing hydrogen pressures (Fig. 20b) at all temperatures.

5.2.6 Ruthenium Catalyst

Fig. 21 shows the distribution of the products during the course of the reaction for R=1, 1.5 and 2 at 100°C. The yields of propylene and propane were nearly the same for all ratios. The selectivity was nearly independent of all the operating variables (Fig. 22).

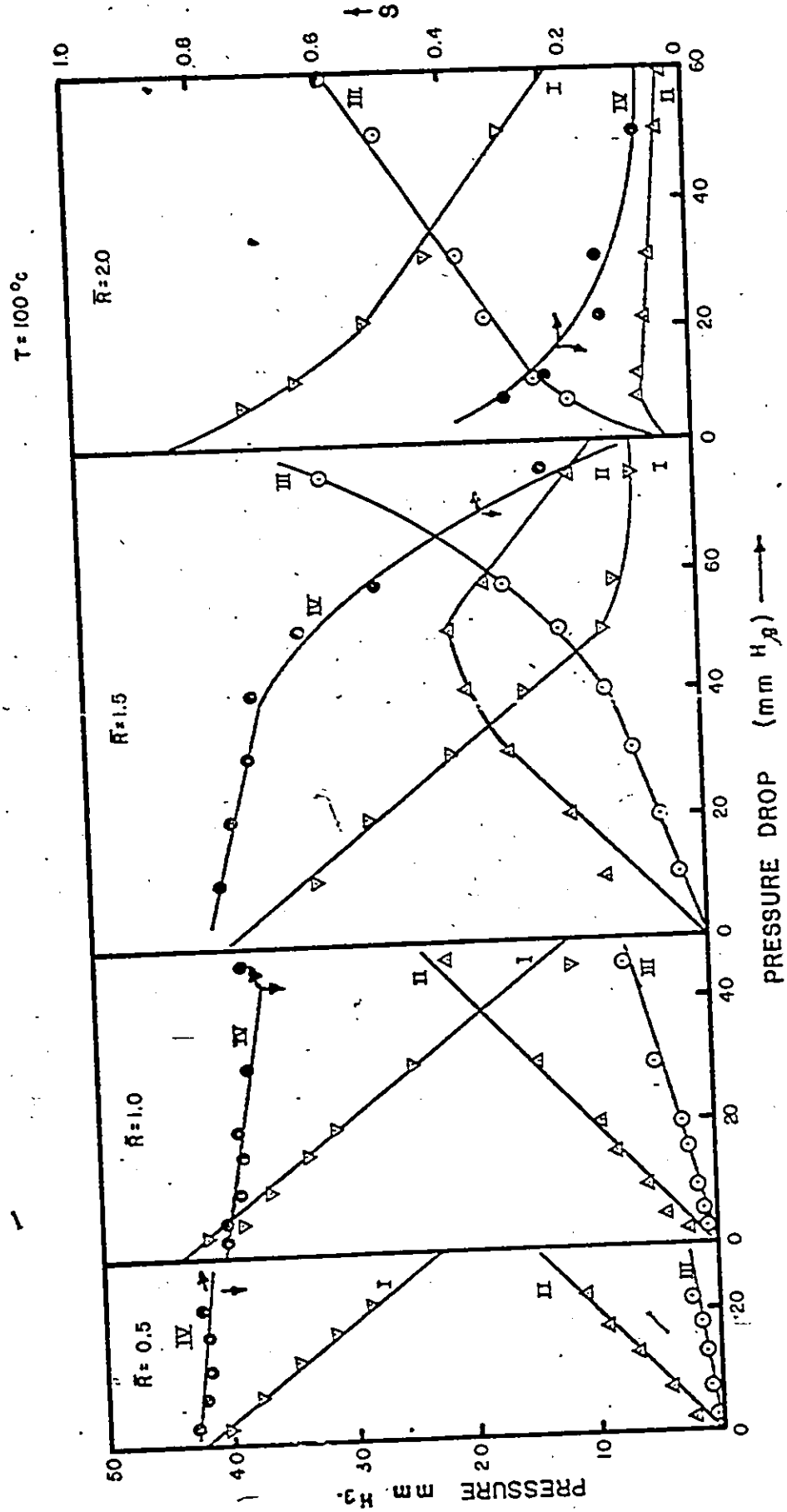

Fig. 16. Product distribution during the course of reaction (Pt catalyst).
I = allene, II = propylene, III = propane, IV = selectivity.

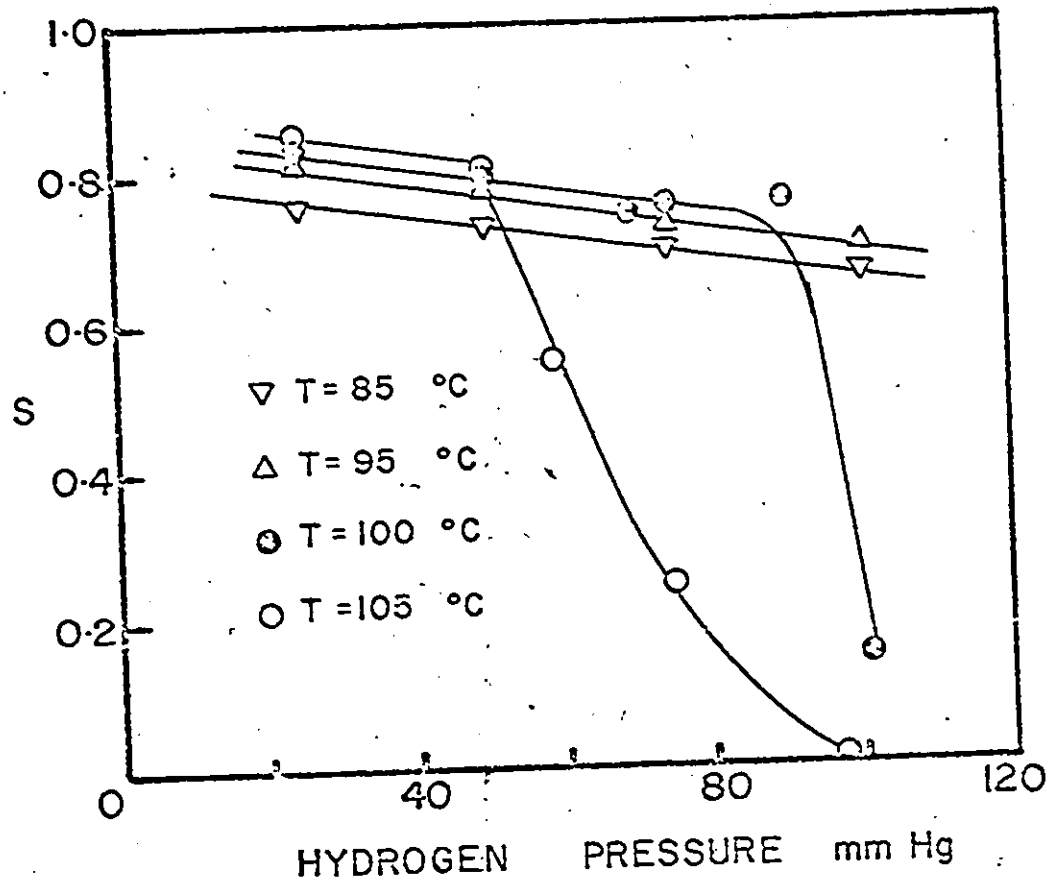

Fig. 17. Dependence of selectivity on initial pressure of hydrogen (Pt catalyst).

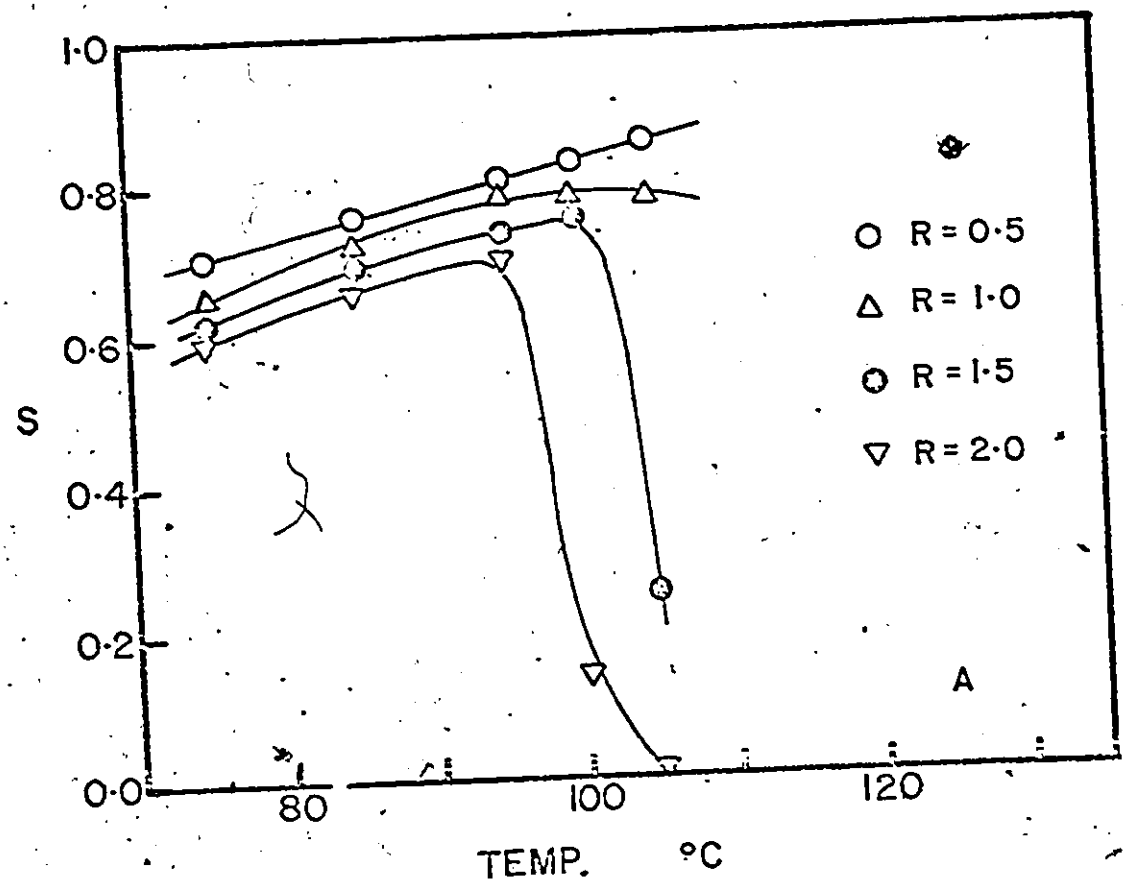

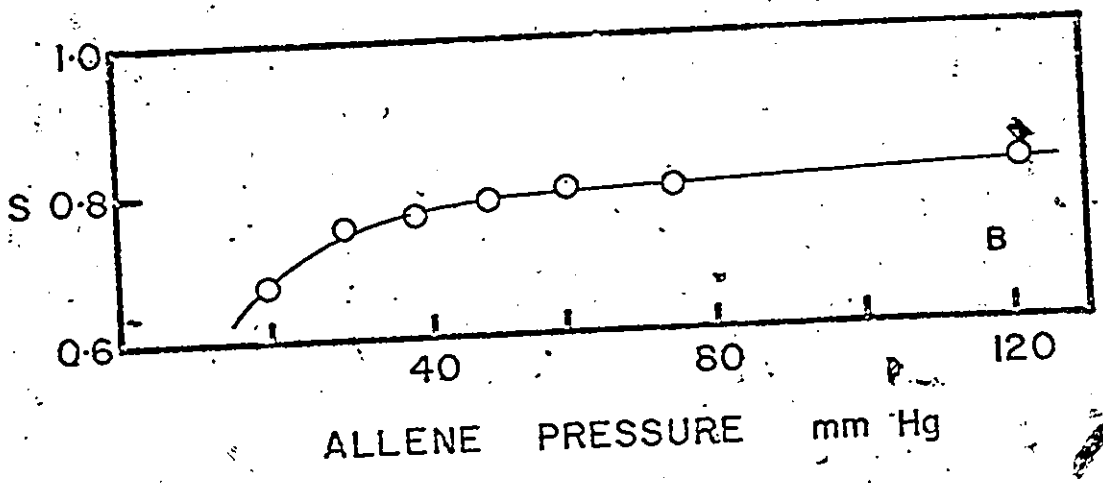

Fig. 18. Dependence of selectivity (Pt catalyst).

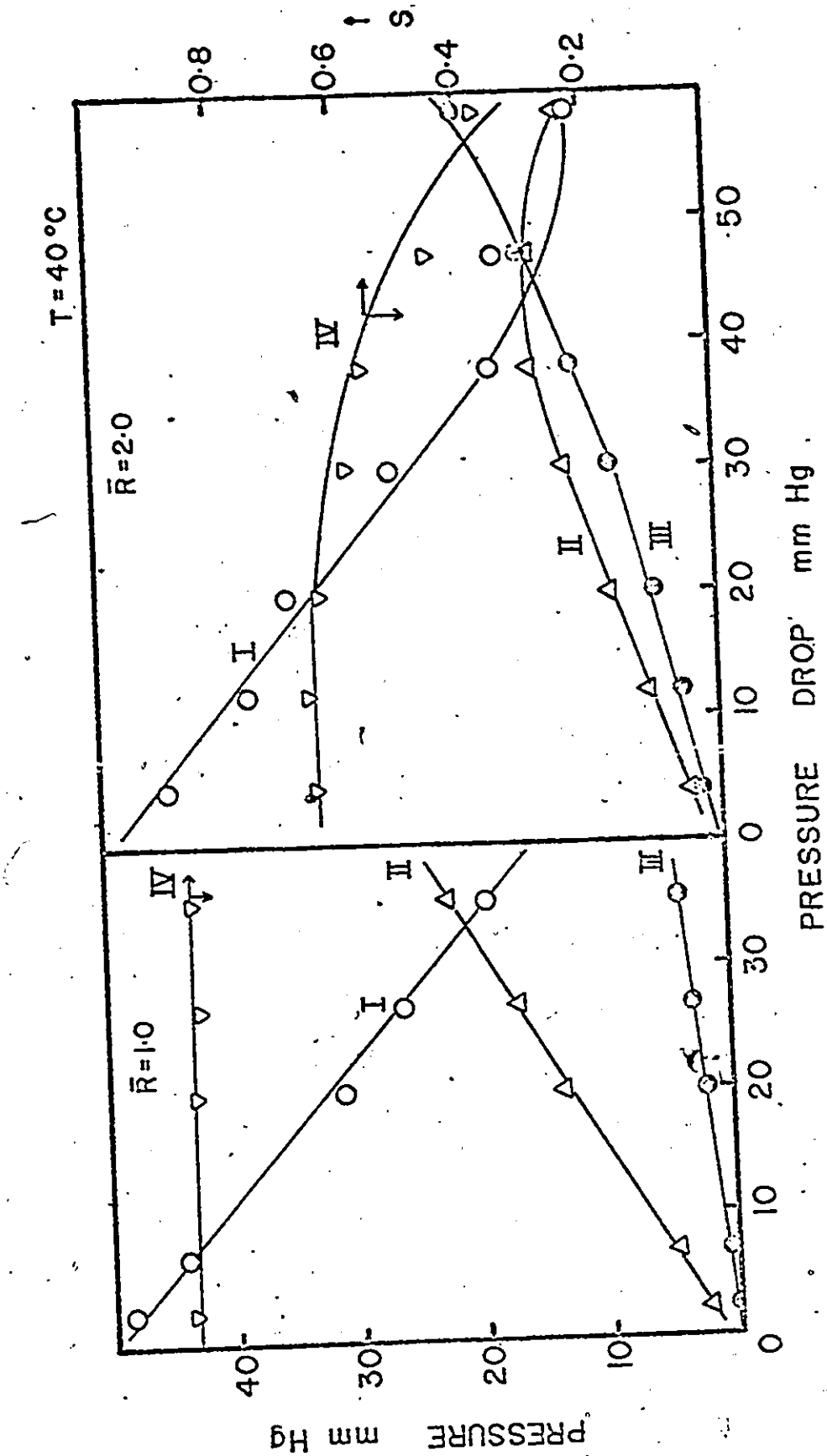

Fig. 19. Product distribution during the course of reaction (Pd catalyst).
I = allene, II = propylene, III = propane, IV = selectivity.

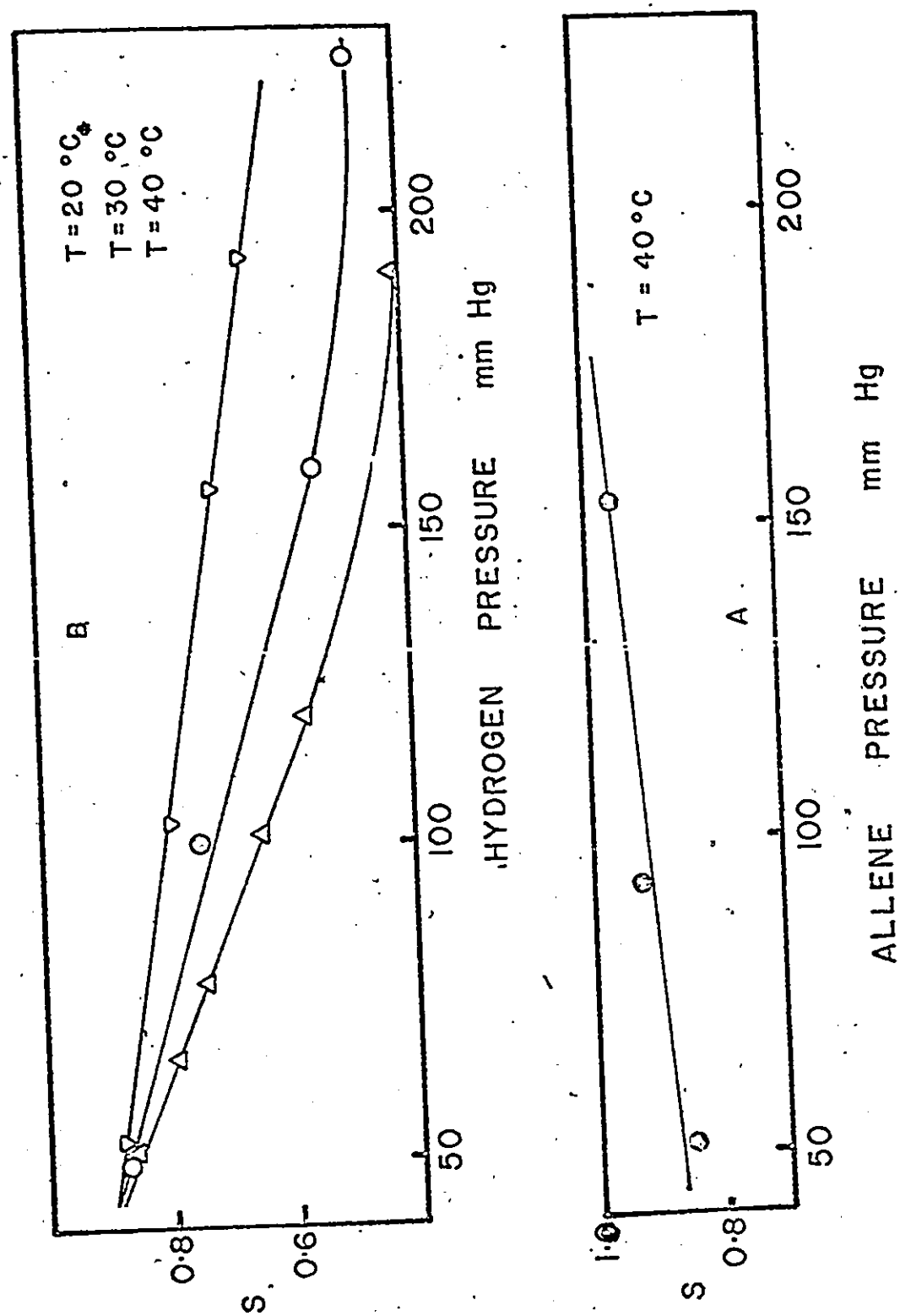

Fig. 20. Dependence of selectivity (Pd catalyst).

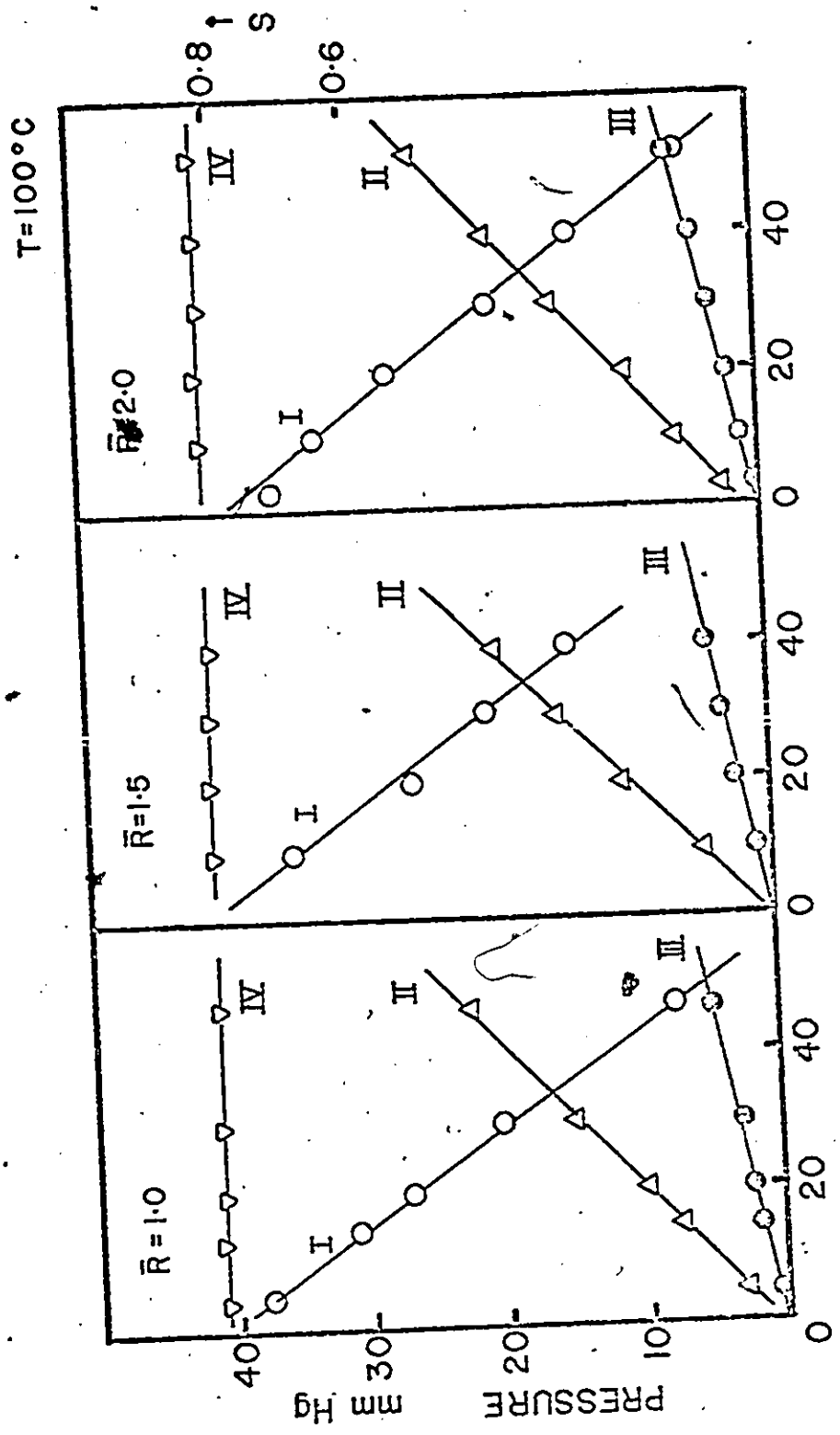

Fig. 21. Product distribution during the course of reaction (Ru-catalyst).
I = allene, II = propylene, III = propane, IV = selectivity.

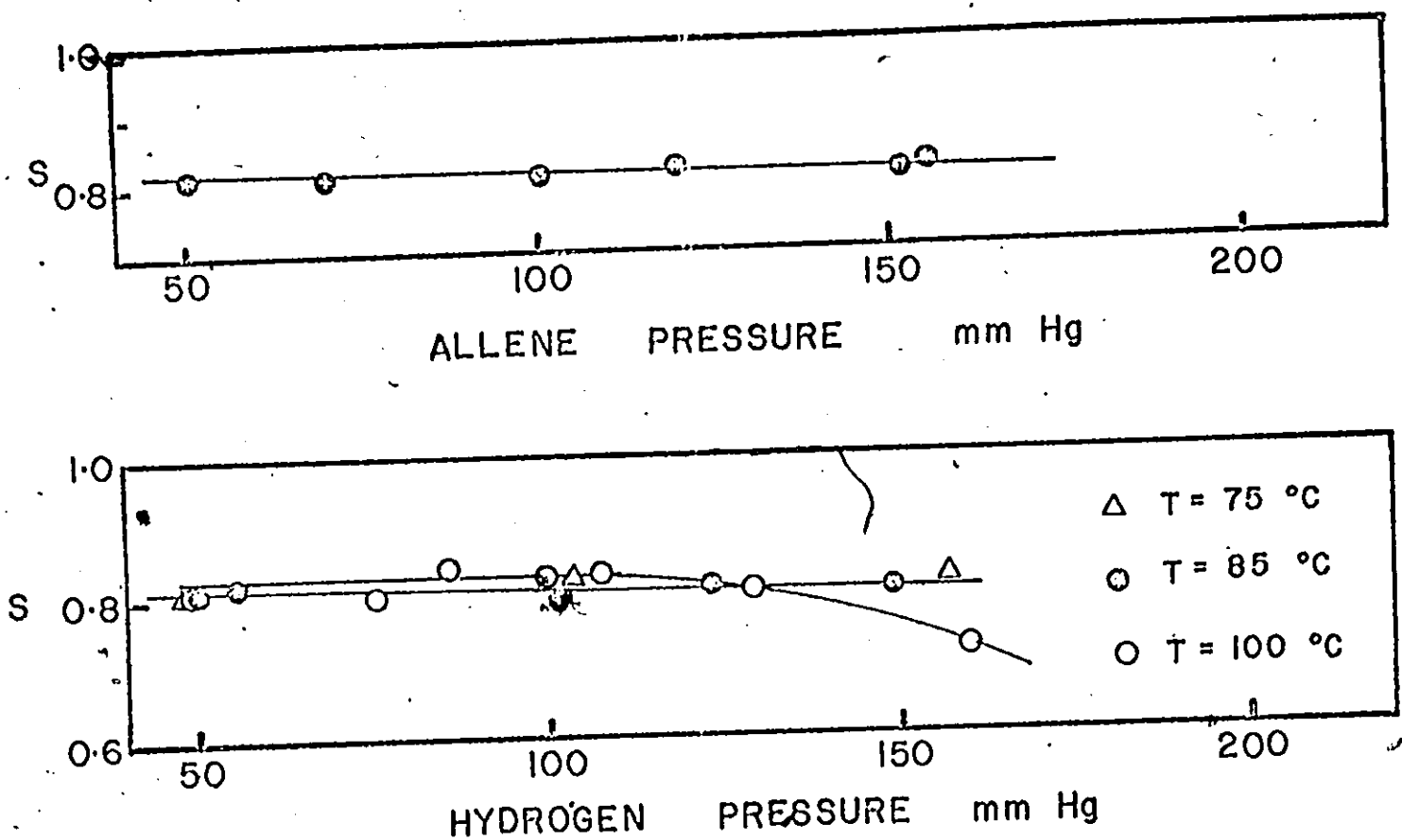

Fig. 22. Dependence of selectivity (Ru catalyst).

5.2.7 Iridium Catalyst

The distribution of products was studied at 260°C for reactant ratios of 4, 5 and 6 ($P_{C_3H_4}$=50 mm). For reactant ratios of 6, formation of propylene decreased after a pressure drop of 50 mm (Fig. 23c) due to the further hydrogenation of propylene. The selectivity was nearly independent of initial reactant pressures and temperatures (Fig. 24).

5.2.8 Rhodium Catalyst

Fig. 25 shows the distribution of the products for reactant ratios of 1 and 2 at 50°C. The selectivity was nearly independent of pressure fall, reactant ratios, initial reactant pressures and temperatures (Fig. 26).

5.2.9 Cobalt Catalyst

Fig. 27 shows the distribution of products and selectivity during the course of reaction at 80°C. The selectivity was nearly equal for all the ratios. At higher allene pressures, small amounts of methylacetylene were obtained due to which the selectivity decreased (Fig. 28a) but it was constant with increasing hydrogen pressures ~~or~~ temperatures (Fig. 28b).

5.2.10 Osmium and Iron Catalysts

Due to the continuous deactivating nature of the catalysts, the product analysis was not studied in detail. However, products for a few runs were analyzed: propylene and propane were formed during the reaction over both the catalysts.

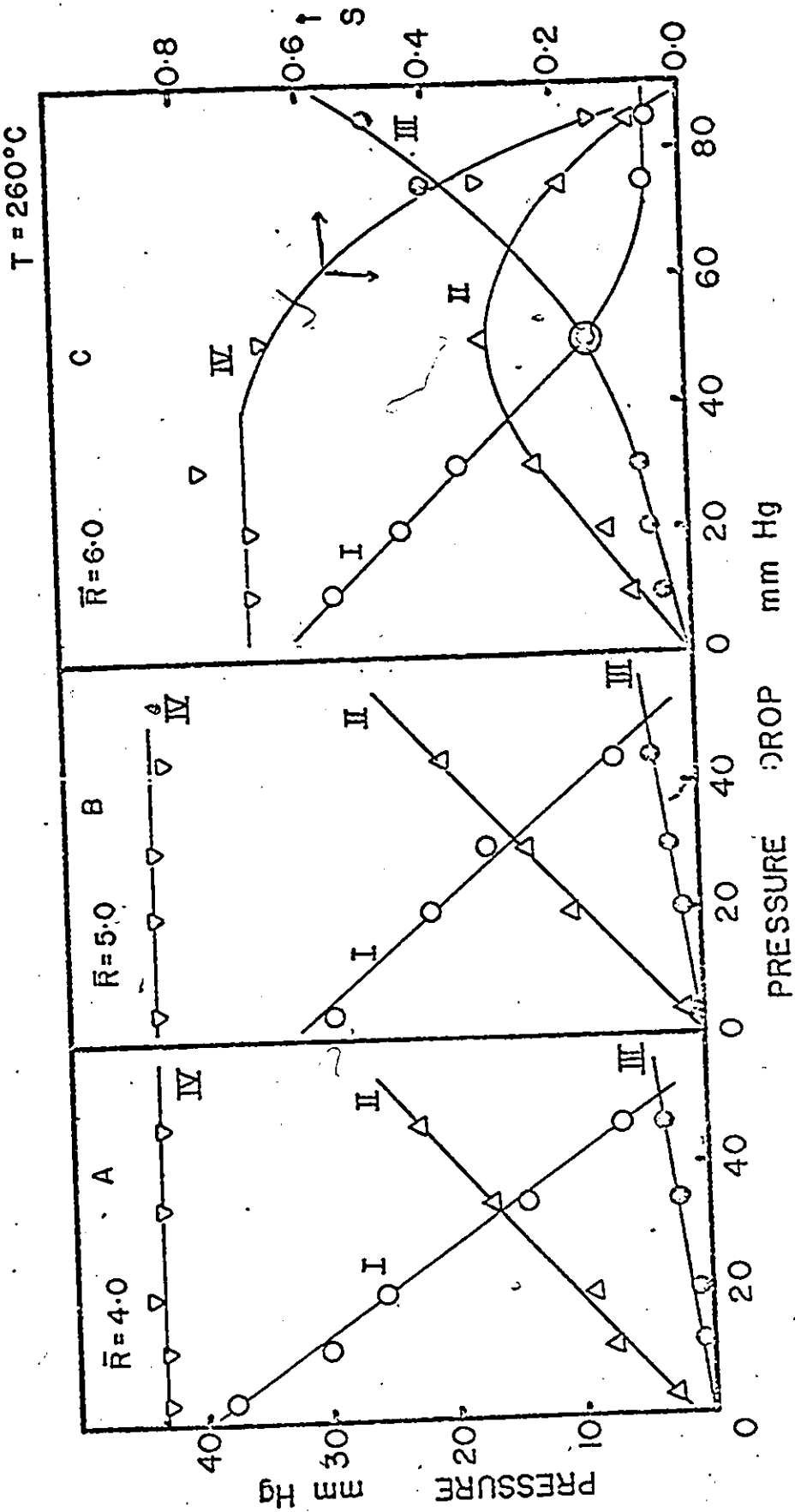

Fig. 23. Product distribution during the course of reaction (Ir catalyst).
I = allene, II = propylene, III = propane, IV = selectivity.

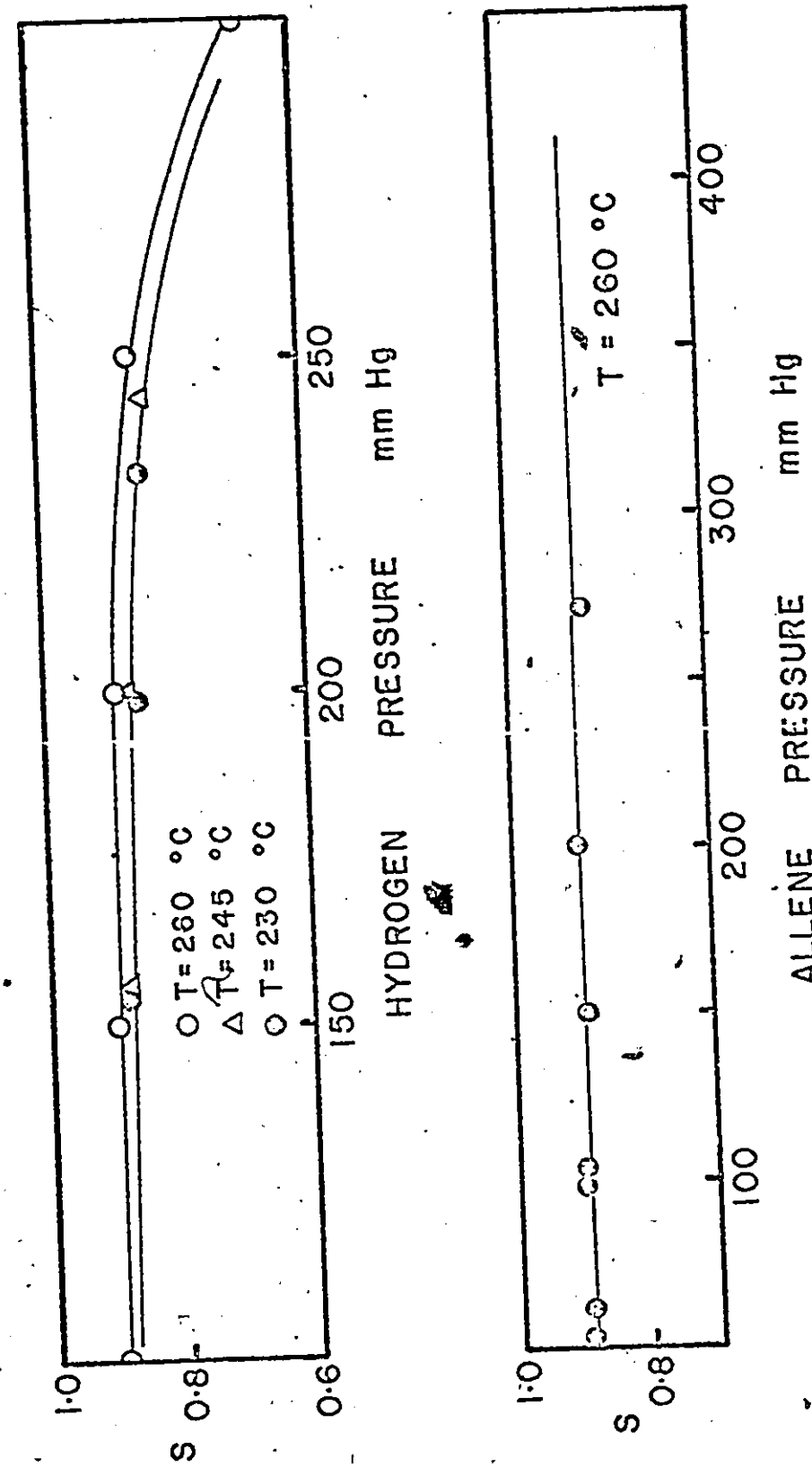

Fig. 24. Dependence of selectivity (Ir catalyst).

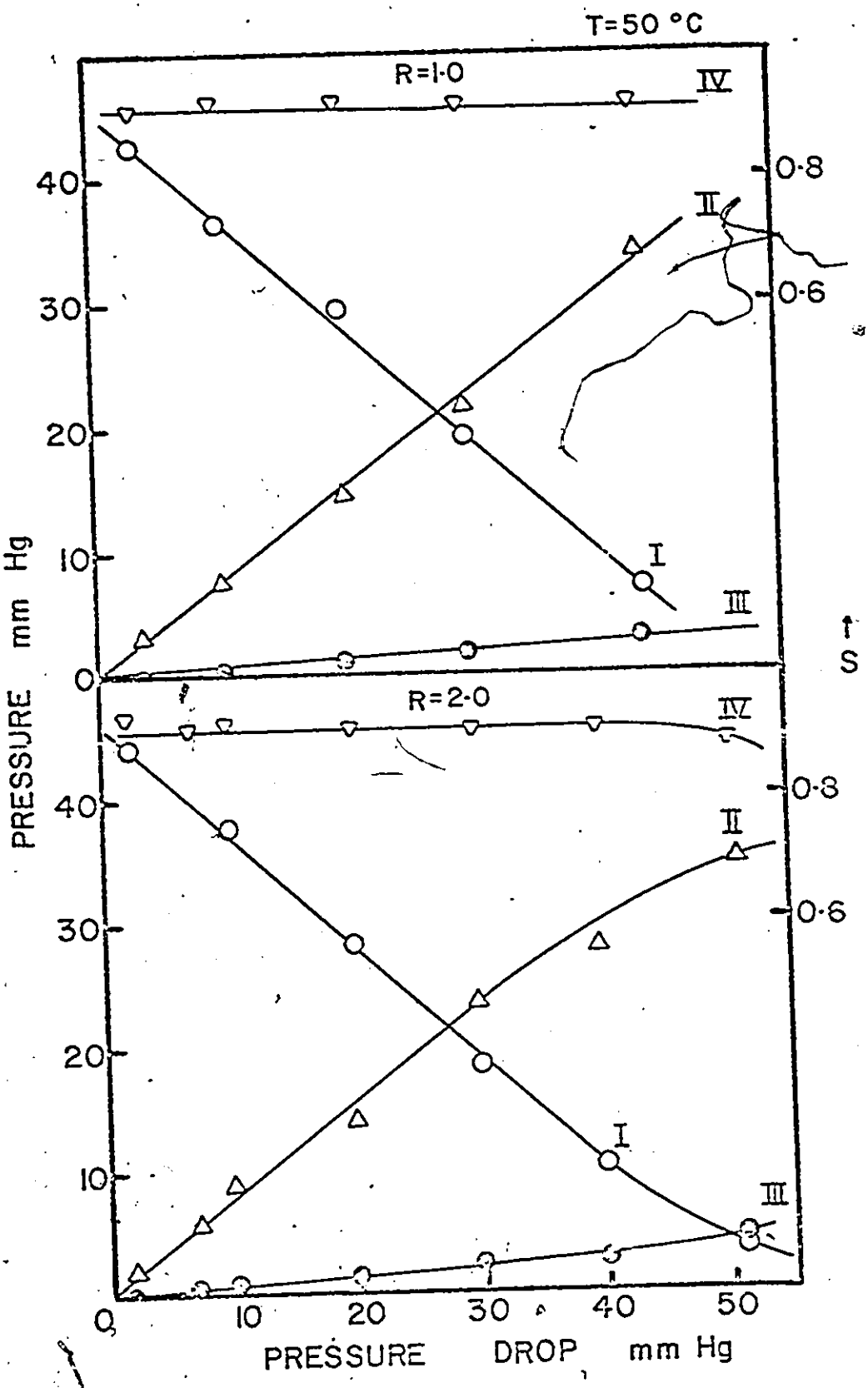

Fig. 25. Product distribution during the course of reaction (Rh catalyst). I = allene, II = propylene, III = propane, IV = selectivity.

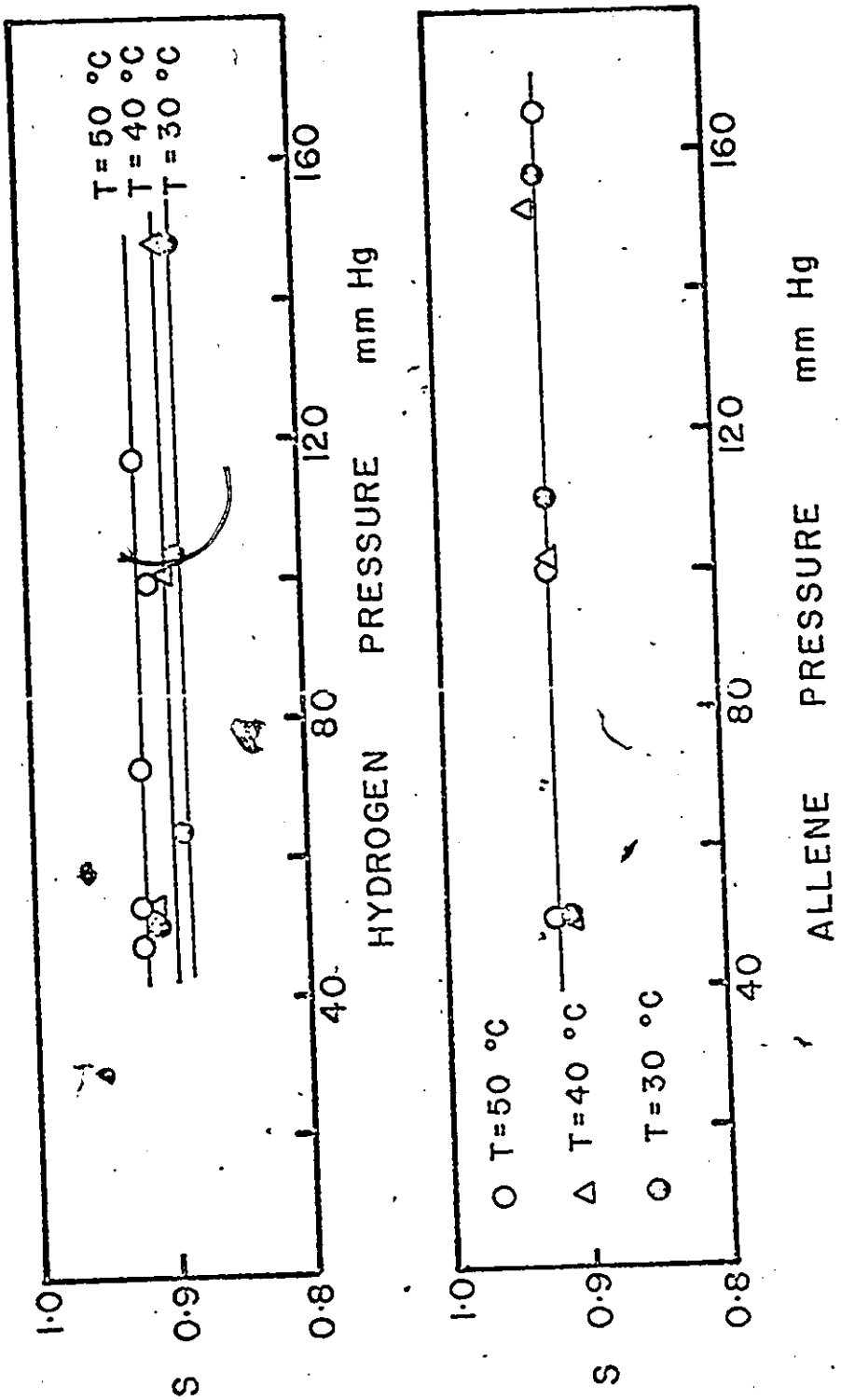

Fig. 26. Dependence of selectivity (Rh catalyst).

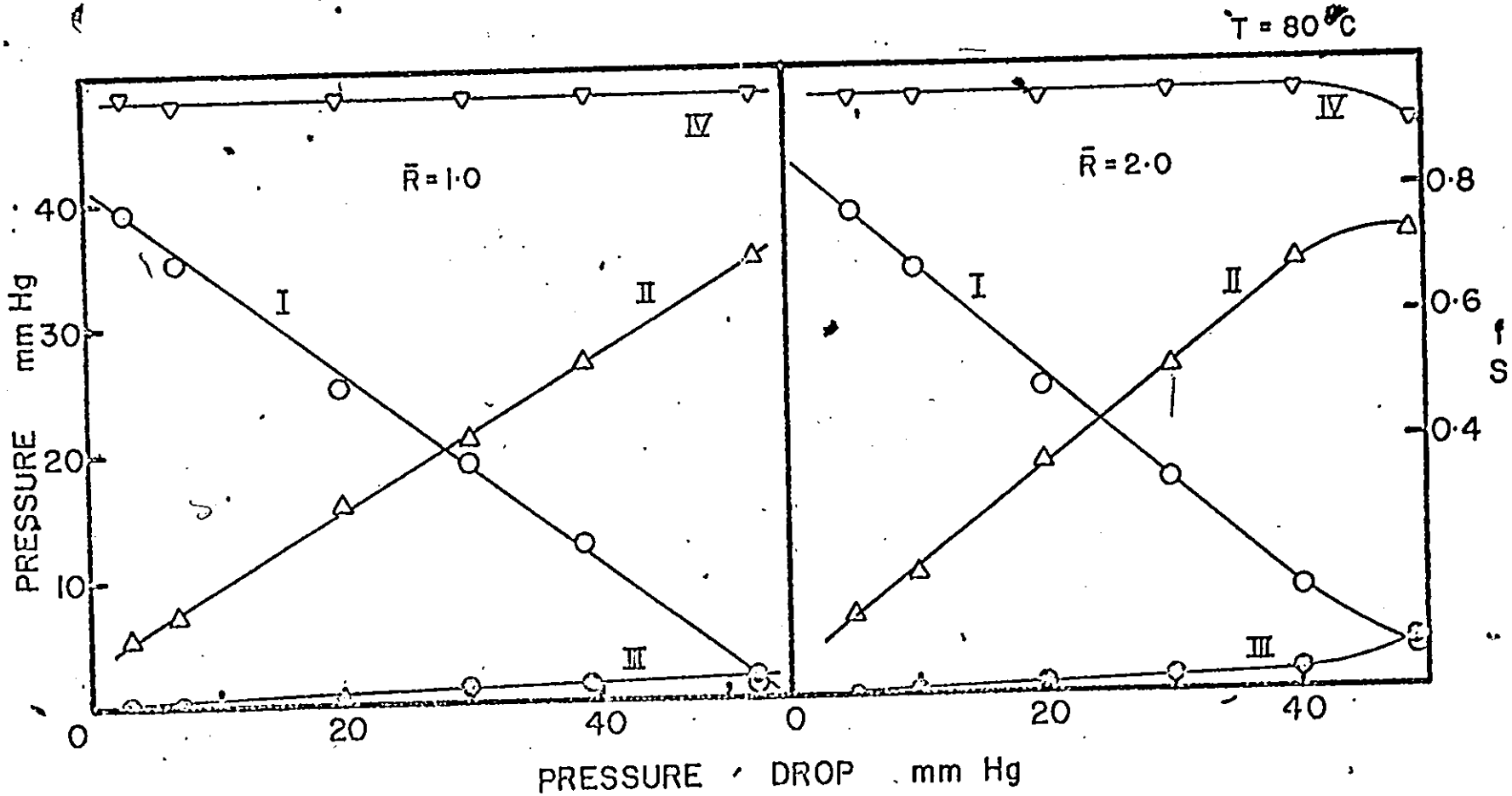

Fig. 27. Product distribution during the course of reaction (Co catalyst). I = allene, II = propylene, III = propane, IV = selectivity.

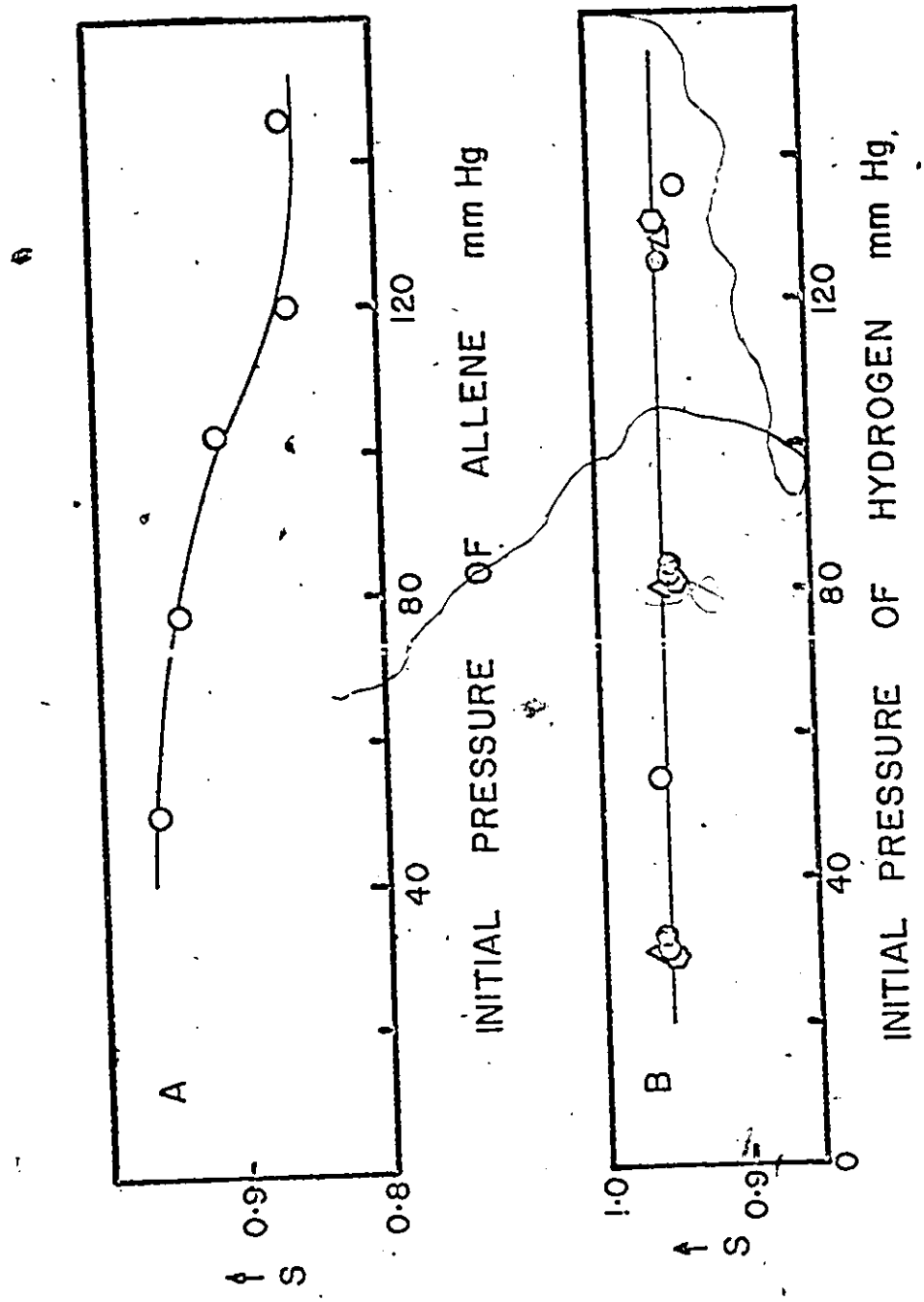

Fig. 28. Dependence of selectivity (Co catalyst).

5.3 ISOMERIZATION

Preliminary studies of allene isomerization over unsupported and silica supported copper, nickel-copper alloy and the transition metals of Group VIII, showed that only silica supported iron and cobalt were active for the isomerization reaction.

Equilibrium between allene and methylacetylene was studied over silica supported 5% iron (wt=0.67585 gm) catalysts between 165 to 200°C. Starting with a pure sample of allene (50 mm), the distribution of isomers was followed by analyzing the samples at various time intervals. The results of these studies are given in Appendix C. The analysis showed that the equilibrium could be obtained in about 12 hrs. and the equilibrium values were nearly constant within the studied temperature range (Fig. 29). Similar values were obtained for the equilibrium distribution when methylacetylene was taken as the reactant (Table C.2) and the samples were analyzed after a time interval of 12, 24 and 36 hrs.

5.3.1 Kinetics over Iron Catalyst

Varying amounts of allene were introduced into the reactor and the samples analyzed after various time intervals. No pressure change was observed during the course of reaction thus eliminating the presence of polymerization reaction. Analysis showed the presence of only two compounds, i.e. allene and methylacetylene, thus removing the possibility of the fragmentation of either isomer. The results of the isomerization of allene over iron catalysts are given in Table C.3. To establish the kinetics, results were analyzed using two different approaches.

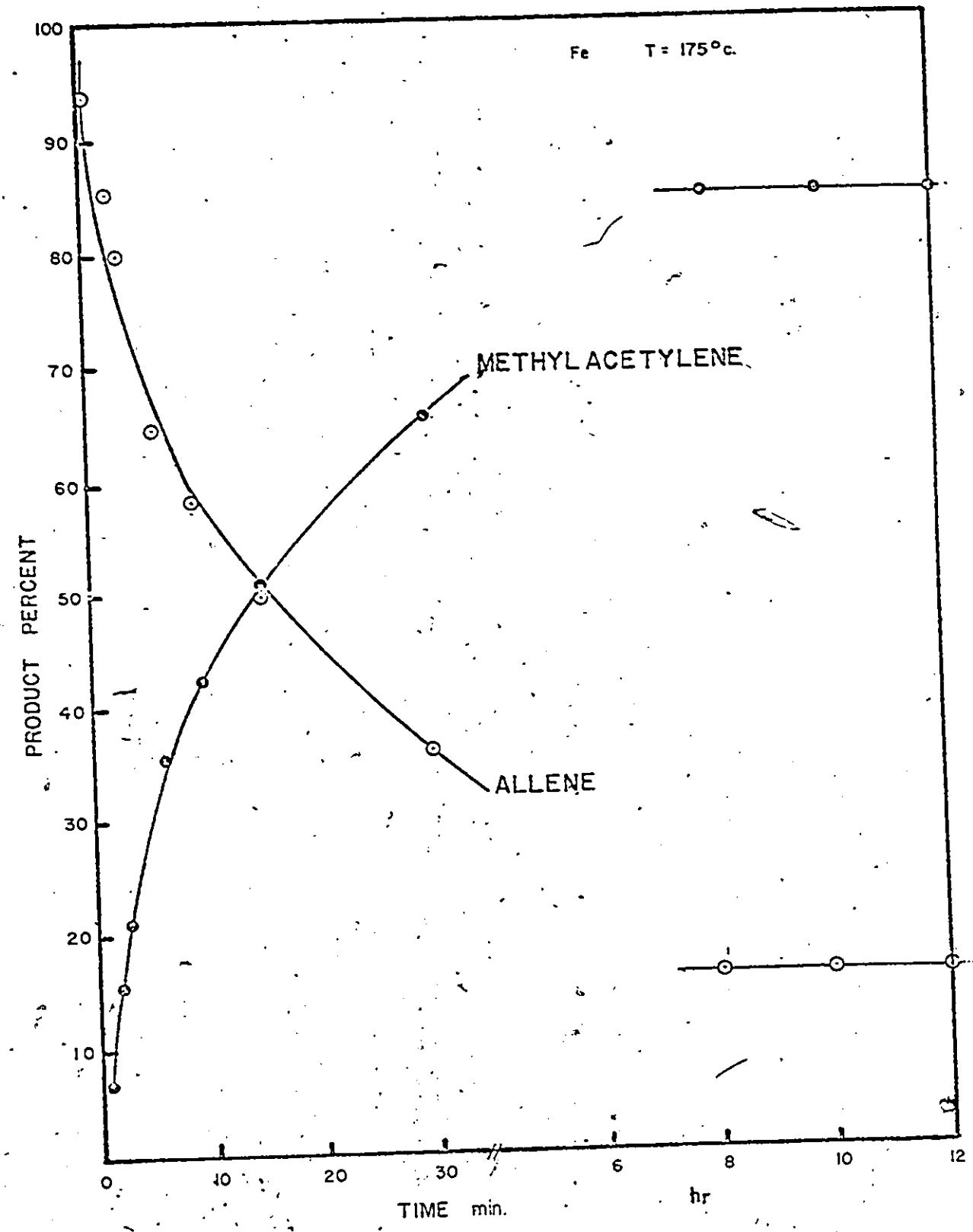

Fig. 29. Allene-methylacetylene distribution.

A) Assuming a first order reversible reaction

allene $\rightleftharpoons$ methylacetylene (5.3)

and using the following equation to calculate the rate of reaction

$$r = (1-y_e)\frac{P_A}{t}\ \ell n\ \frac{1-y_e}{y-y_e} \qquad (5.4)$$

where

r = initial rate of isomerization reaction

y = fraction of allene left after time t

y_e = fraction of allene at equilibrium

P_A = initial pressure of allene, mm

t = time, min.

The rate of reaction was fairly constant for all the runs. A typical analysis is given in Table 5.3.

TABLE 5.3.
Calculation of initial rate of isomerization.
T=135°C P_{allene}=50±2 mm

TIME min	A mm	M mm	A+M	% A	% M	r_i	$r_{i\ ave}$	r_i graph
1/2	40.9	0.3	41.2	99.25	0.75	0.6206		
3	40.1	2.2	42.3	94.87	5.13	0.7465	0.6861	0.71
5	42.0	3.4	45.5	92.49	7.51	0.7148		
5/2	38.6	4.7	43.3	89.13	10.87	0.6723		
10	39.5	6.2	45.7	86.43	13.57	0.6762		

B) Initial rate method

Partial pressures of methylacetylenes were plotted against time and the initial rates were determined by drawing a tangent on the pressure time curves at t=0 (Fig. 30). The dependence of initial rate on initial pressures is shown in Fig. 31. The order of reaction was calculated to be

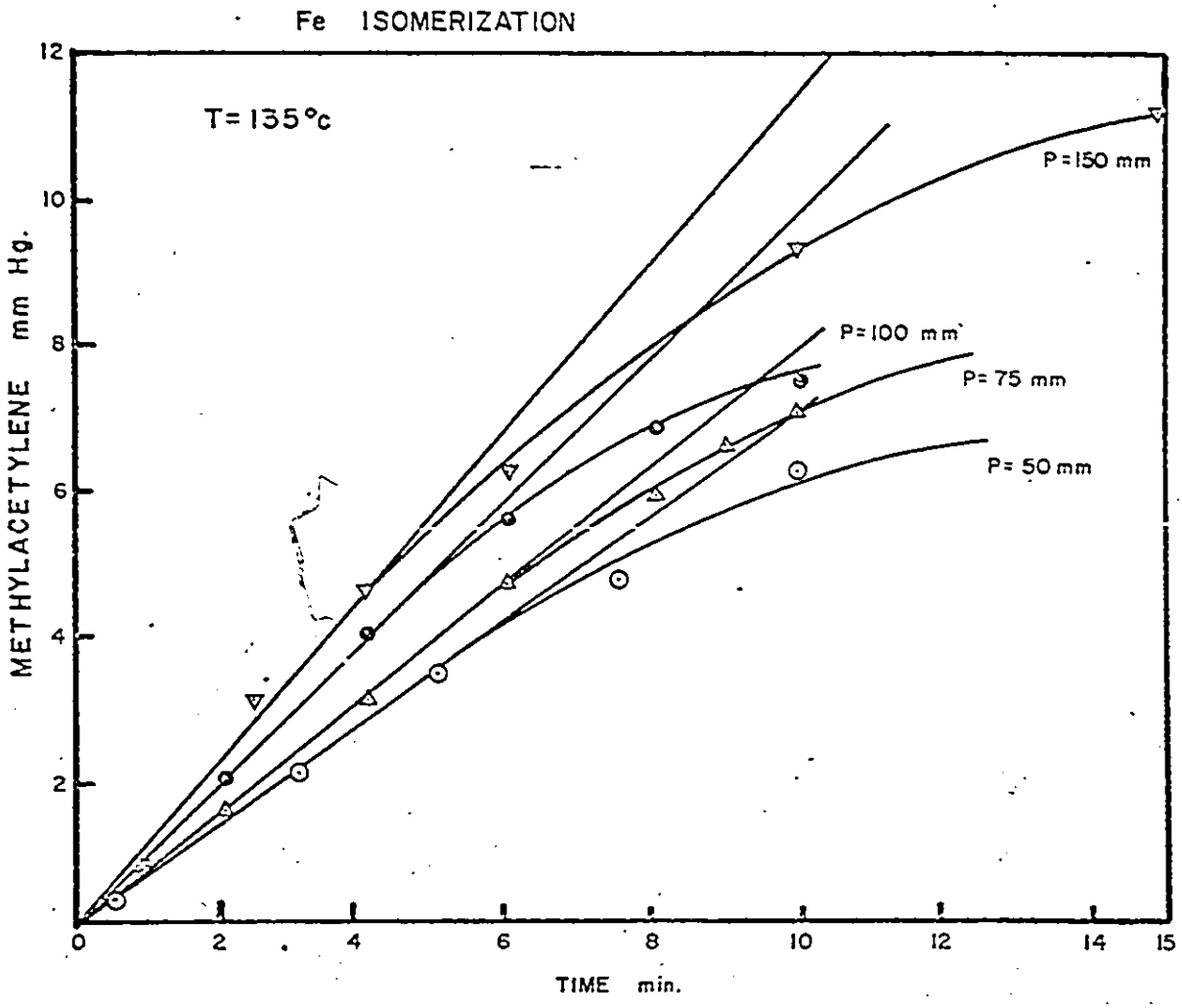

Fig. 30. Methylacetylene pressure with time (Fe catalyst).

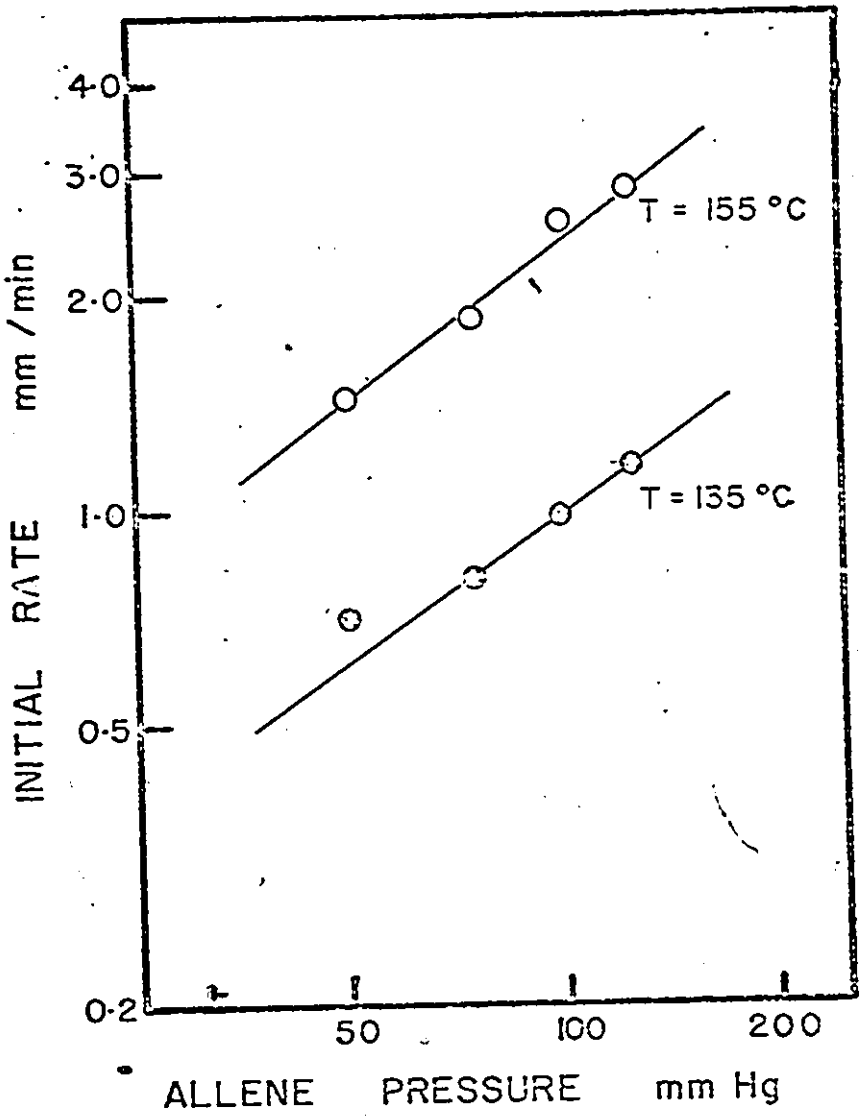

Fig. 31. Dependence of initial rate on initial allene pressure (Fe catalyst).

0.8 (≈1) and was temperature independent. The apparent energy of activation was calculated to be 11.8 k cal/mole (Fig. 32). The initial rate expression can be written as:

$$r_o = k P_{allene}$$

5.3.2 Cobalt Catalyst

Similar results as observed for iron catalysts were obtained on cobalt catalysts (Table C.4). Assuming a first order reversible reaction, fairly constant reaction rates were calculated. Fig. 33 shows the methylacetylene presure-time curves for different initial allene pressures at 116°C. Fig. 34 shows the dependence of initial rate on initial allene pressures. The order of reaction was one. Apparent energy of activation was calculated to be 11.2 k cal/gm mole.

5.4 ADSORPTION STUDIES

10% nickel catalyst pallet (wt=0.05483 gm)was placed in the cell and was reduced at 400°C. After reduction, the cell was evacuated for 6 hrs. at 400°C and was cooled to room temperature under vacuum.

Curve I, Fig. 35, shows the adsorption of hydrogen at room temperature on freshly reduced catalysts. Following to the last point shown for run I, the catalyst was saturated with 100 mmof hydrogen for 12 hrs. and was evacuated for 6 hrs. at room temperature. Curve II (circles) shows the adsorption of hydrogen on hydrogen saturated catalysts. The cell was again evacuated for 12 hrs. at 400°C and cooled to room temperature under evacuation. Adsorption isotherms on freshly reduced and hydrogen saturated catalysts were obtained by repeating the above procedure. Curve I and II (triangles Fig. 35) show the reproducibility of data.

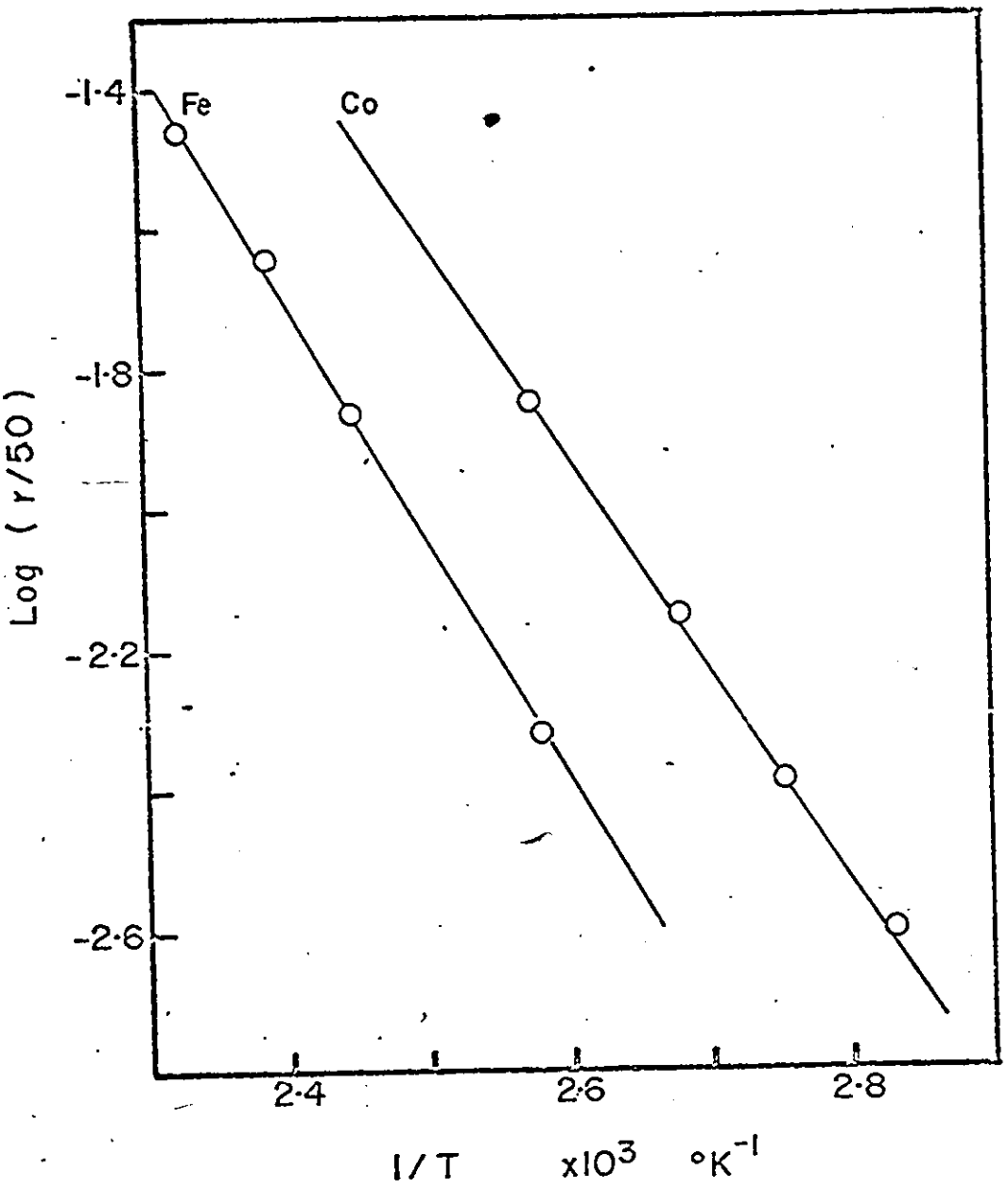

Fig. 32. Arrhenius plot (isomerization).

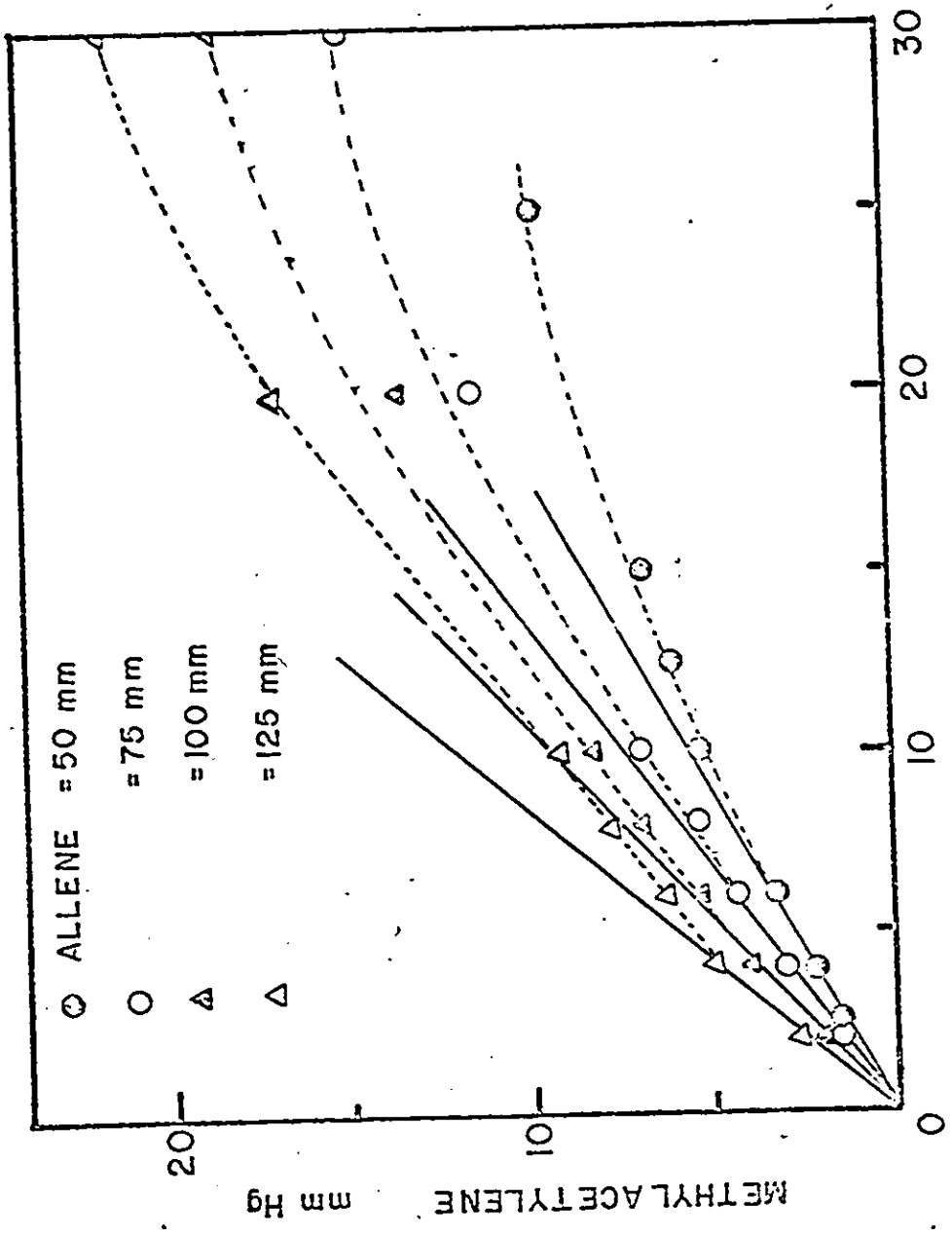

Fig. 33. Methylacetylene pressure with time (allene isomerization over Co catalyst).

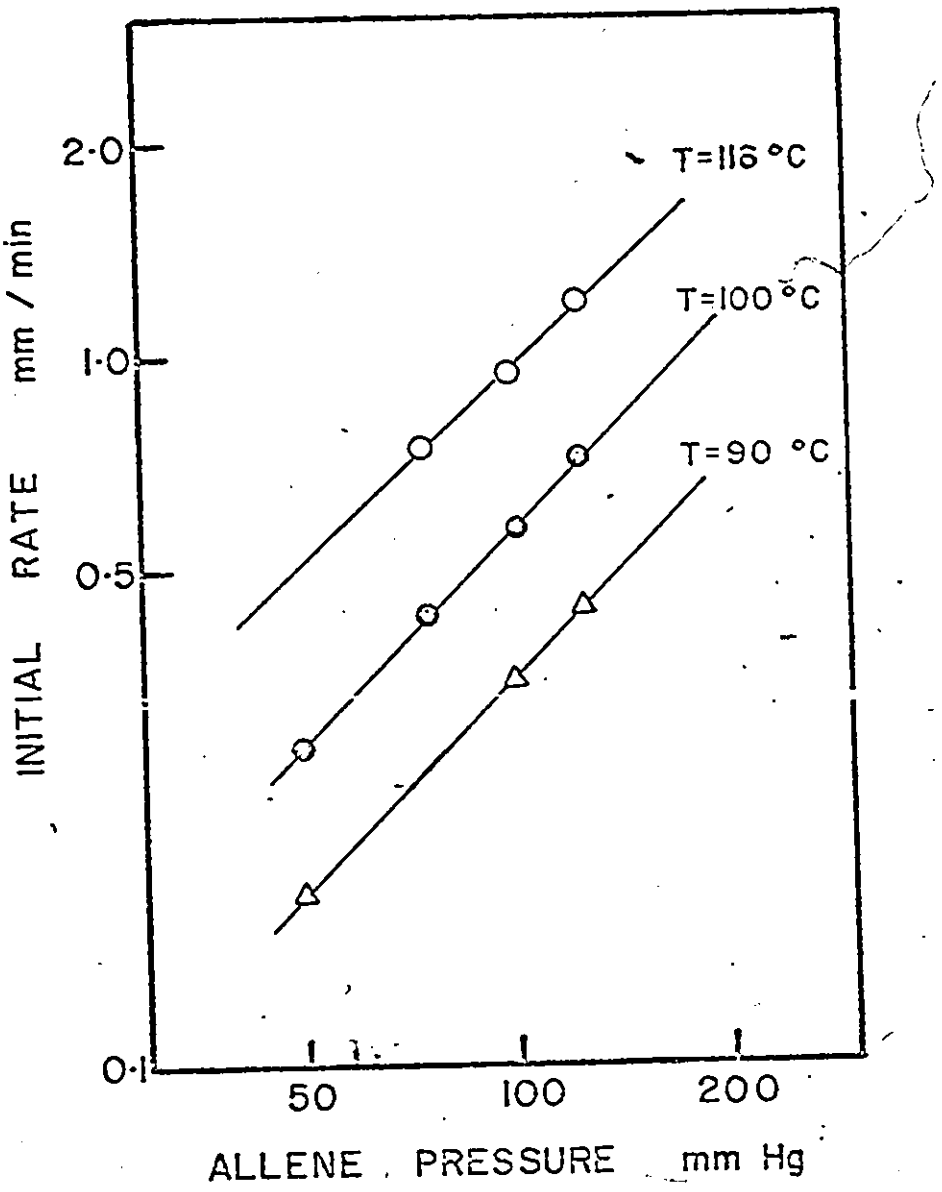

Fig. 34. Dependence of initial rate on initial pressure of allene (isomerization of allene on Co catalyst).

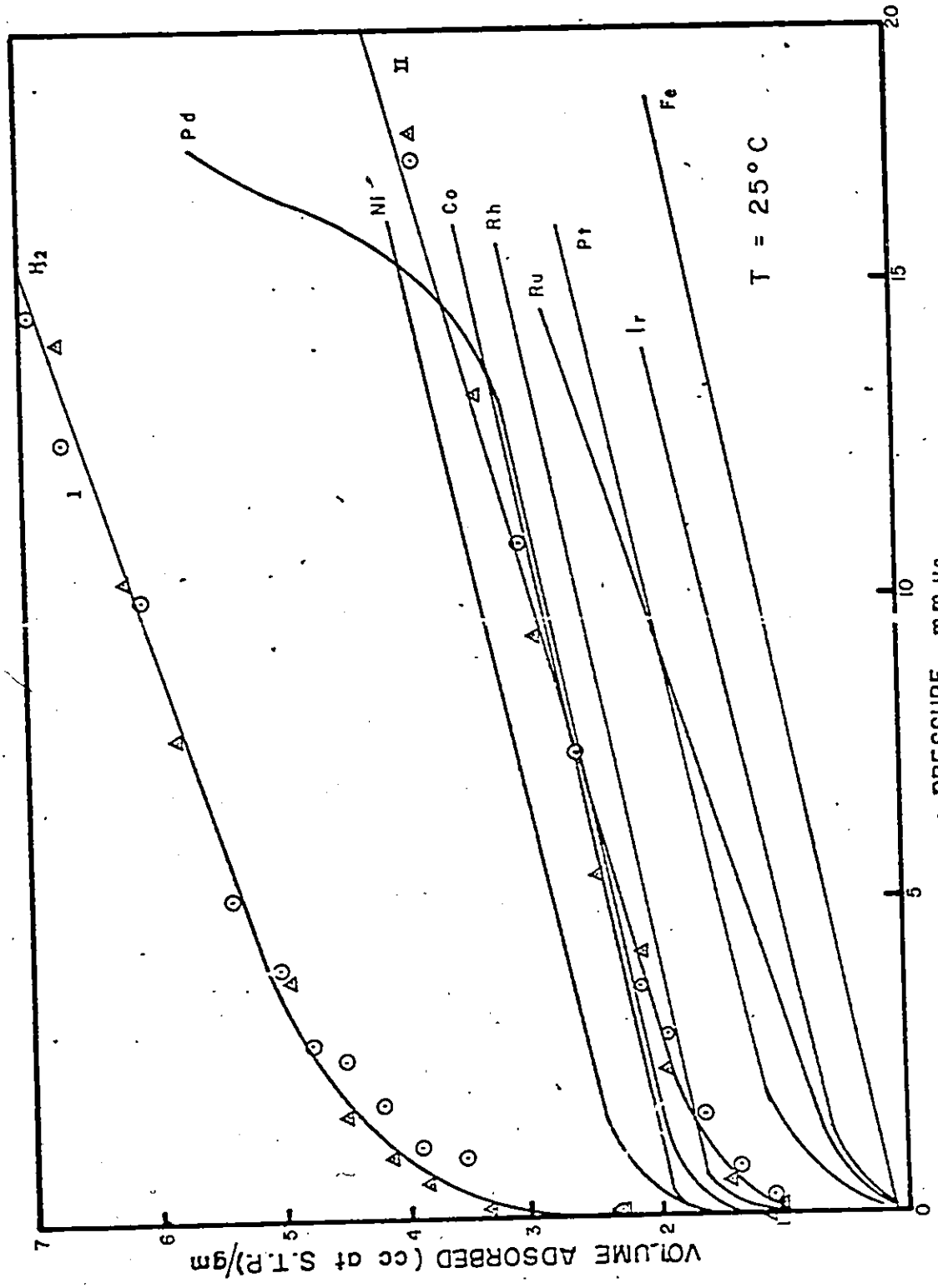

Fig. 35. Adsorption isotherms of H_2.

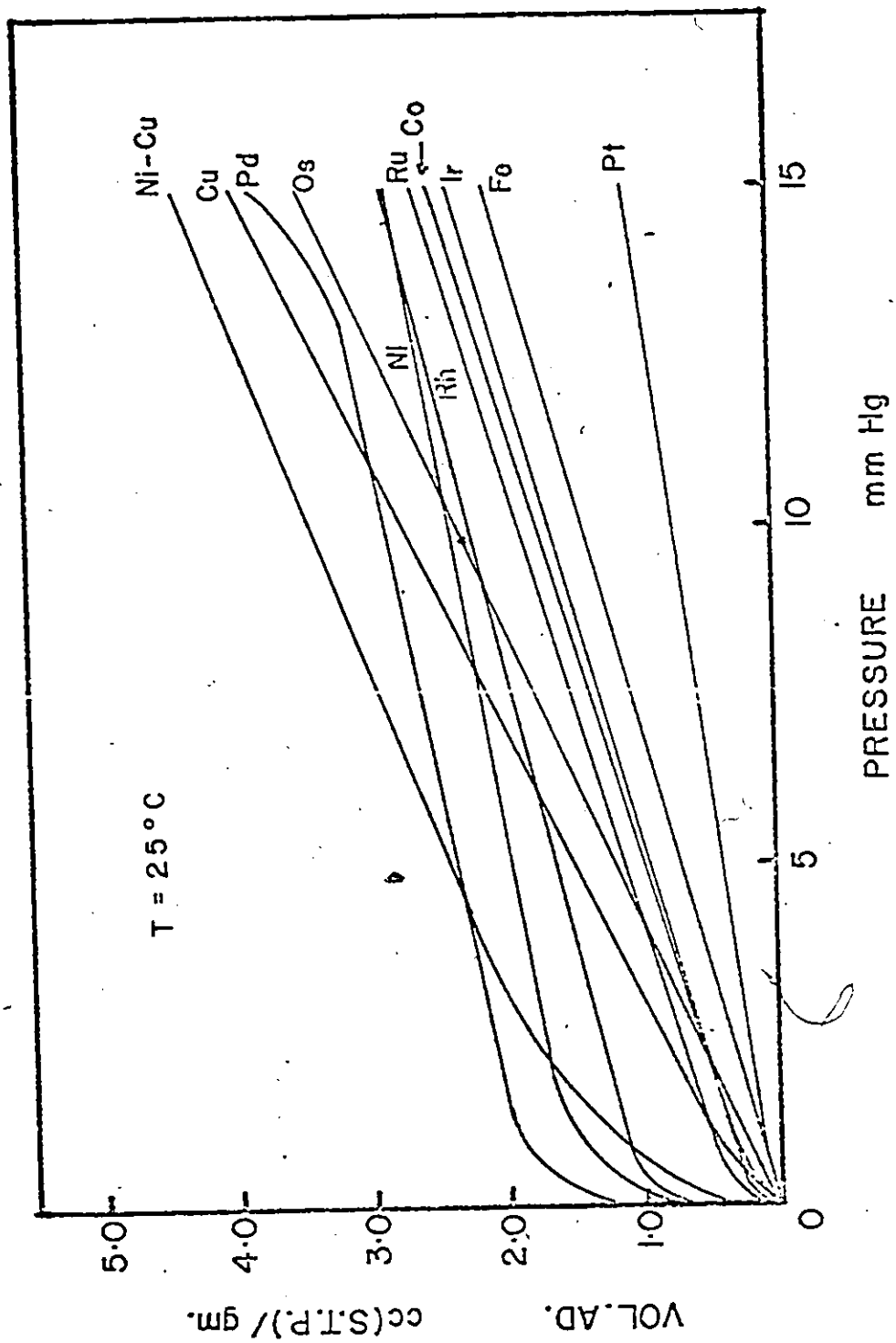

Fig. 36a. Weakly adsorbed hydrogen.

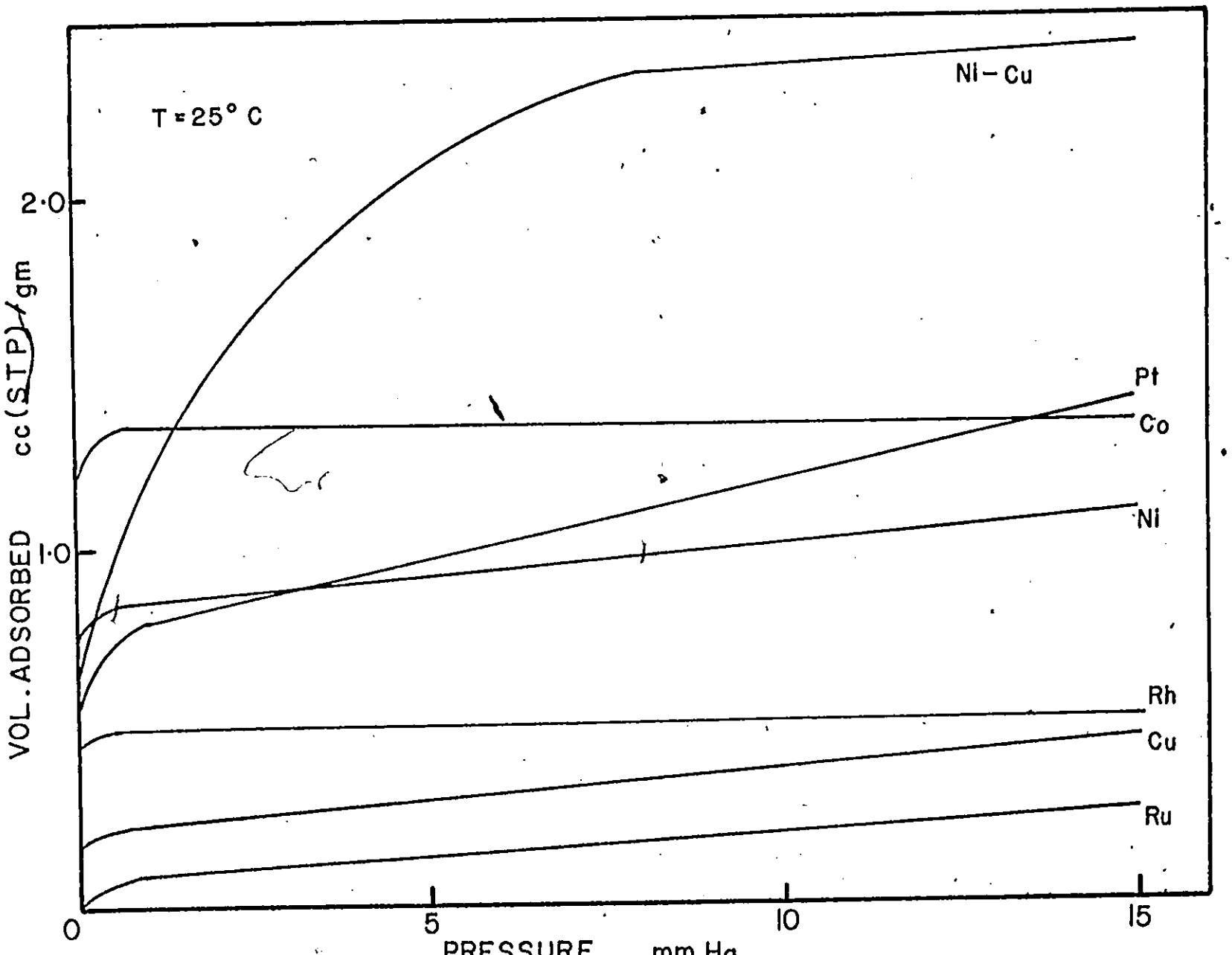

Fig. 36b. STRONGLY HELD HYDROGEN

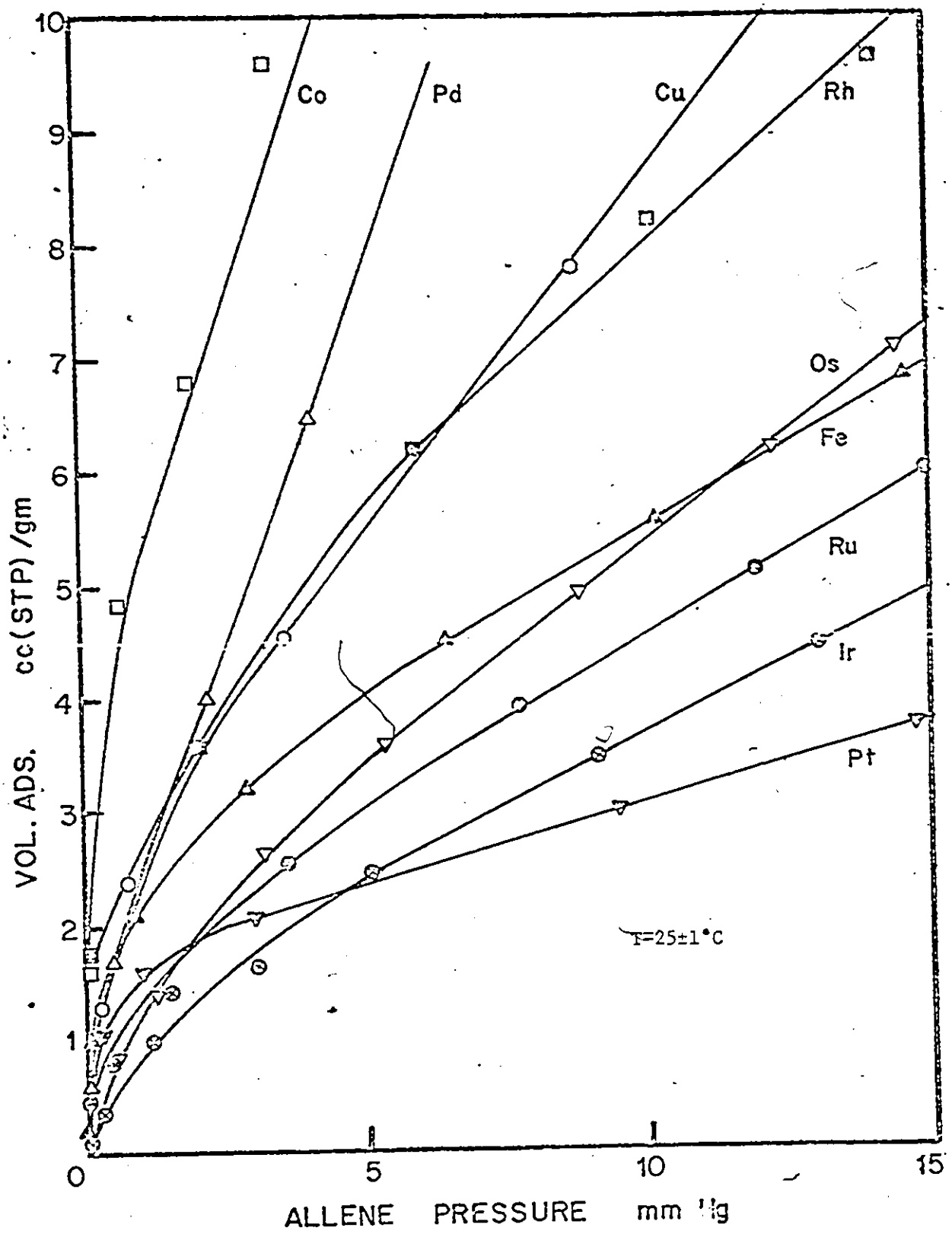

Fig. 37. Adsorption isotherms of allene.

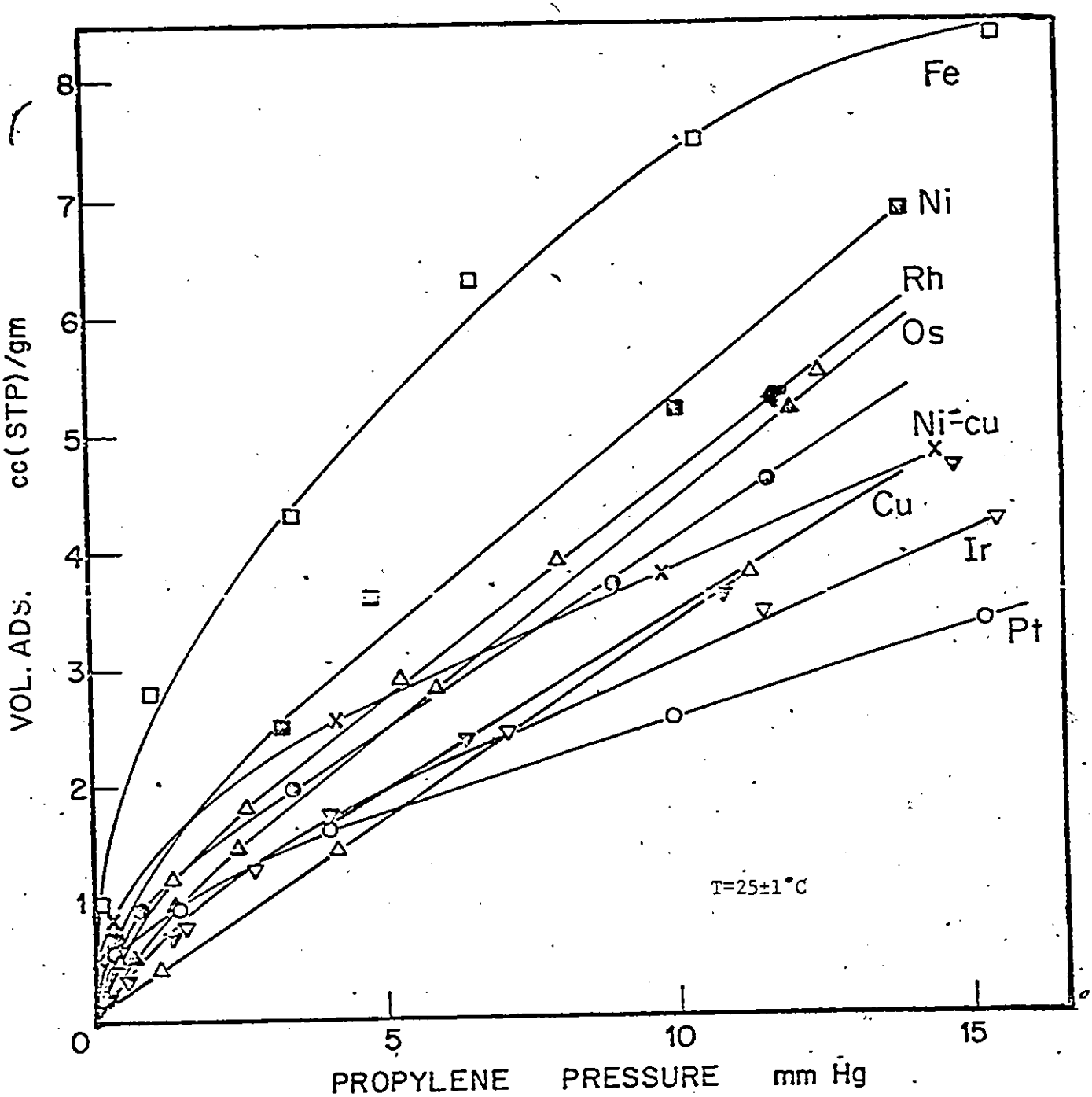

Fig. 33. Adsorption isotherms of propylene.

These and other results (46,47) show that the hydrogen adsorption is of two types: Type I - chemisorption which is removed by evacuation at room temperature; Type II - chemisorption which is not removed by evacuation at room temperature.

Figs. 35, 36a, 36b, 37 and 38 show the total adsorption of hydrogen, weakly adsorbed hydrogen, strongly adsorbed hydrogen, adsorption isotherms of allene and propylene on various catalysts, respectively.

5.5 INFRARED STUDIES

Infrared studies were carried out for all the catalysts following the adsorption studies and reducing the catalyst at 400°C, until no absorption bands were observed for hydrocarbon groups or the spectra resembled with the base line. To balance the bands due to the support, all studies were carried out with a silica pellet (treated similarly with the catalyst) in the reference cell. Reasonably straight base line was obtained in the interested frequency range for all the catalysts.

5.5.1 Nickel Catalyst

No absorption bands were observed for adsorbed hydrogen at room temperature on nickel catalysts (wt=0.075 gm). Fig . 39, Curve II shows the spectrum of adsorbed allene (15 mm saturated for 12 hrs.). Absorption bands at 3076 and 2985 cm^{-1} represent the asymmetric and symmetric CH stretching in $C=CH_2$ group where as bands at 2900 and 2840 cm^{-1} are assigned to lowered (as) and (s) CH_2 stretching due to the attachment with surface nickel. Bands at 2920 and 2845 cm^{-1} are assigned to CH_2 stretching mode in hydrocarbons. The adsorption bands at 1627 and 1427 cm^{-1} represent a C=C stretching and $=CH_2$ deformation mode. The bands

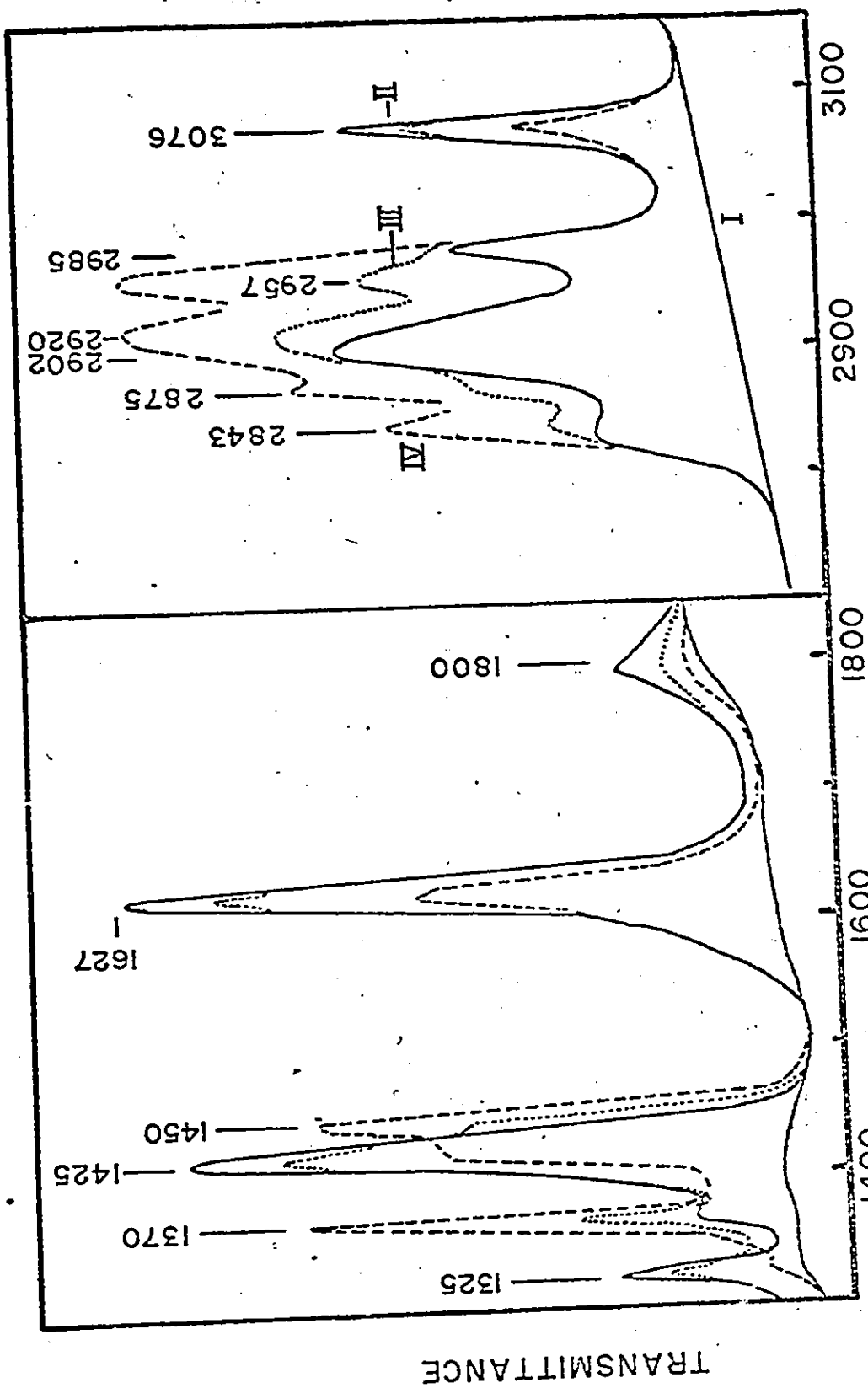

Fig. 39. Infrared spectra of allene. (Ni catalyst)
I - Base line; II - adsorbed allene; III - H_2=10 mm;
IV - H_2=20 mm.

at 1800 and 1325 cm^{-1} may be due to the overtone of $=CH_2$ deformation in the lower frequency. Evacuation had no effect on the spectrum.

Stepwise addition of hydrogen (P_{H_2} =10 and 20mm) to the evacuated sample of adsorbed allene resulted in the appearance of new bands at 2957, 2875, 1450 and 1370 cm^{-1} which are assigned to different modes of the CH_3 group (Fig. 39, curves III and IV). The bands at 2902 and 2840 cm^{-1} shifted to 2920 and 2943 cm^{-1}. The spectra obtained for the hydrogenated species of allene on nickel resembled the one obtained for surface hydrogenated products of chemisorbed propylene attached to nickel atoms (72). Nearly equal intensities of the bands at 2920 and 2957 cm^{-1} suggest the presence of $CH_3(CH_2)_2$-M group (85).

Fig. 40a shows the spectra of adsorbed propylene (10 mm) and after evacuation. Absorption bands at 2955 and 2875 cm^{-1} belong to the asymmetric and symmetric stretching vibration of the CH_3 group. The hydrogenation of surface species produced a more intense spectra (Curve III) which could be ascribed to a propyl group attached to the metal atom. ($CH_3(CH_2)_2$-M, Ref. 82).

5.5.2 Nickel-Copper Alloy

The spectra of adsorbed allene on nickel-copper alloy (wt.=0.08 gm, silica=0.074 gm) were similar to the one obtained for nickel catalysts. Fig. 41 shows the spectra of adsorbed allene for various pressures. At very low pressures (P_{allene}=0.02 mm, curve II) absorption bands were also observed at 2960, 2875 and 1360cm^{-1} which indicates the presence of CH_3 group may be due to the self-hydrogenation of allene. Evacuation had no effect on the spectra. Fig. 42 shows the spectra of adsorbed allene and stepwise addition of hydrogen. Fig. 43 shows the spectra of

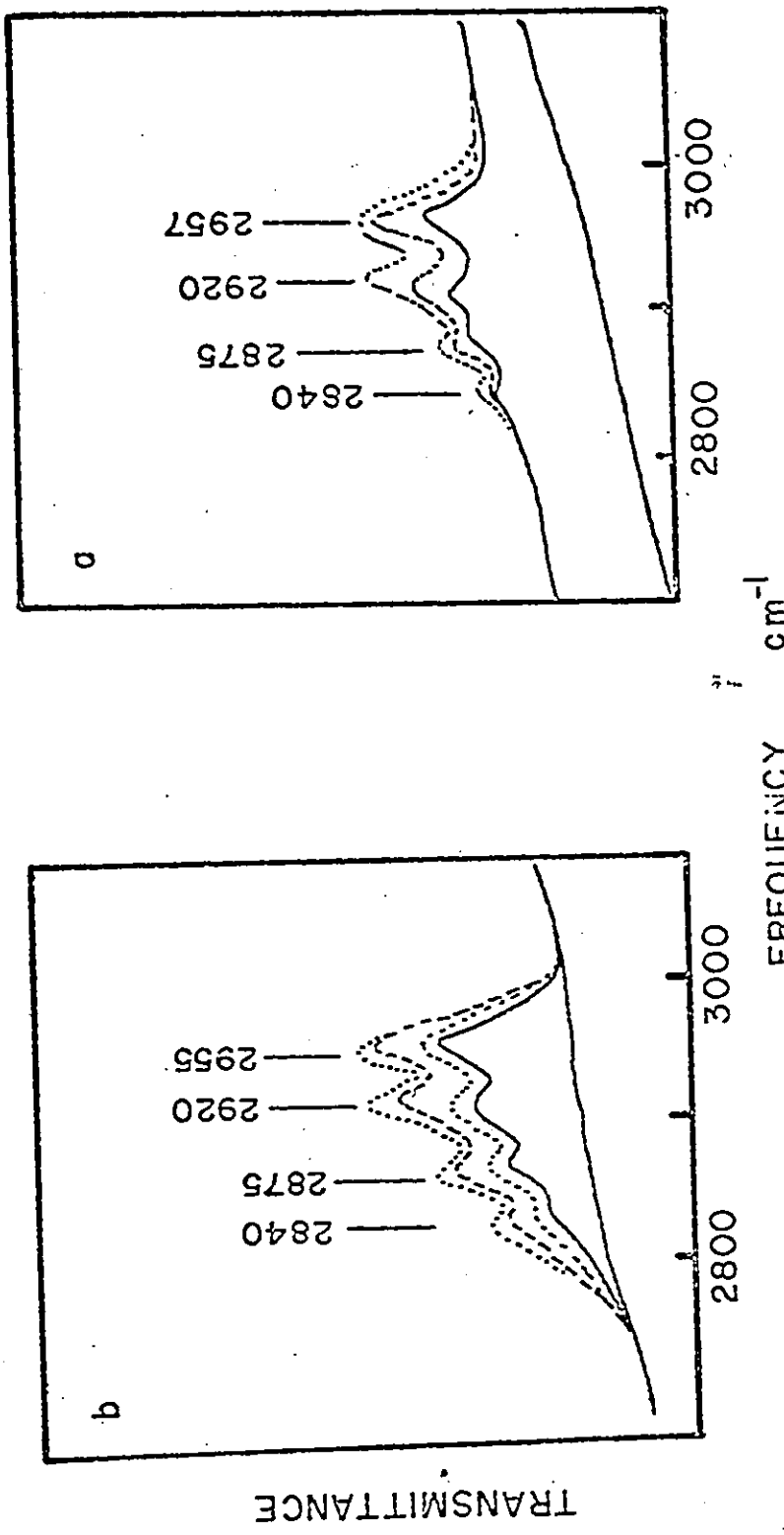

Fig. 40. Infrared spectra of propylene.
a) Ni catalyst I = base line; II - propylene (10 mm); III - H_2=10 mm; IV - H_2=20 mm.
b) Ni-Cu alloy catalyst I = base line, II - propylene (10 mm); III - H_2=10 mm; IV - H_2=20 mm.

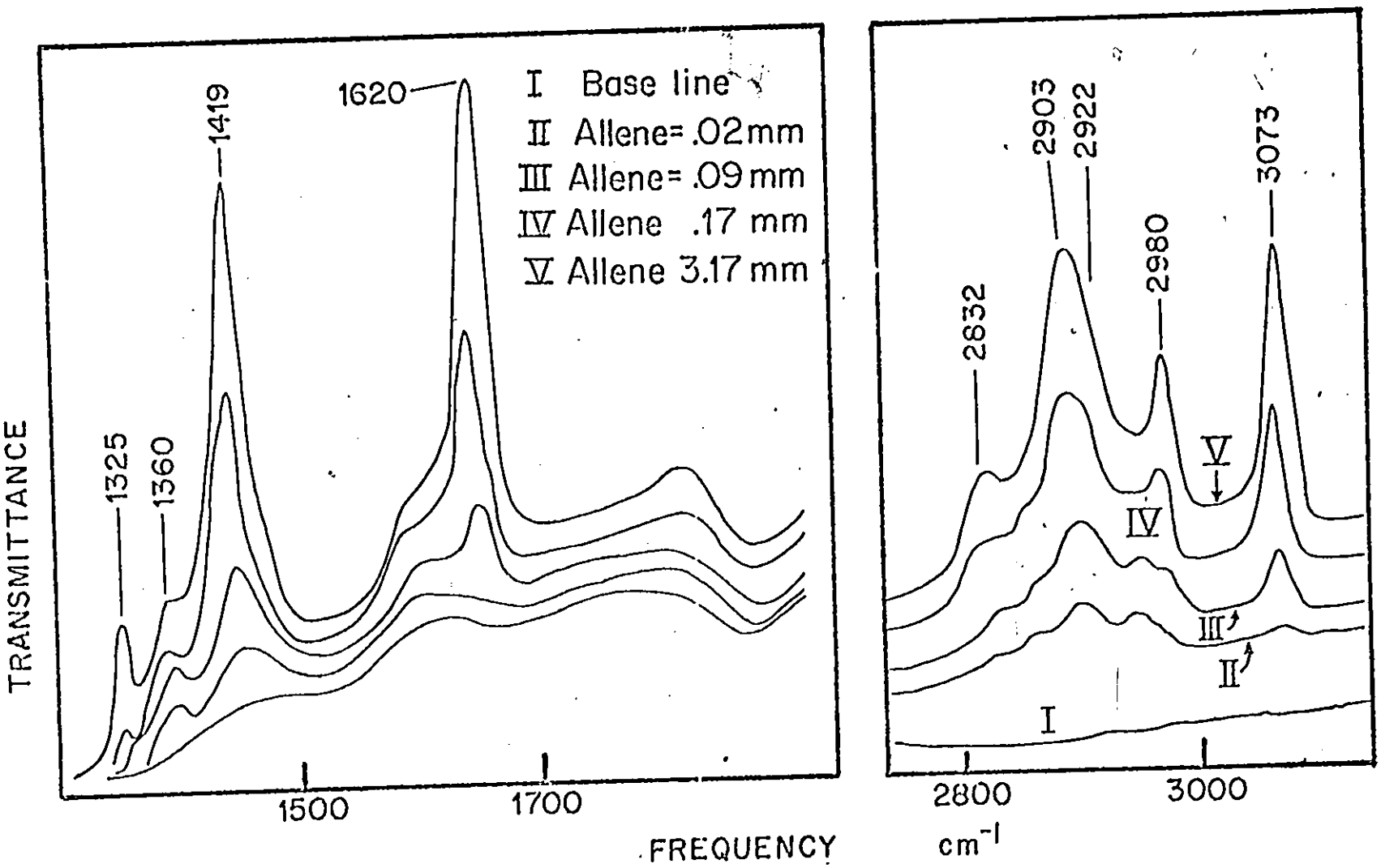

Fig. 41. Infrared spectra of adsorbed allene (Ni-Cu alloy catalyst).
I - base line; II - 0.02 mm; III - 0.09 mm; IV - 2.0 mm; V - 10 mm.

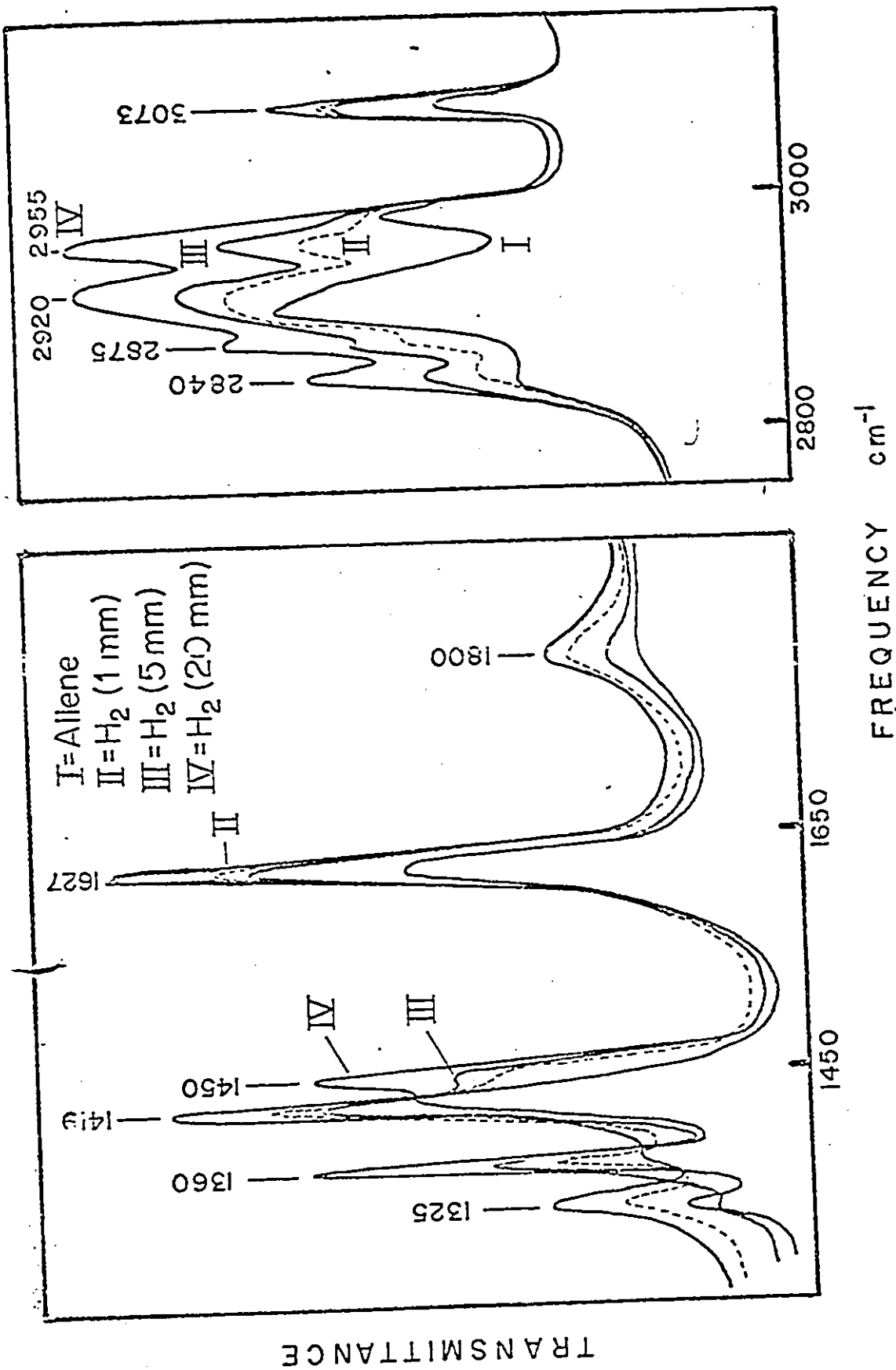

Fig. 42. Infrared spectra of adsorbed allene and stepwise addition of hydrogen. (Ni-Cu catalyst).

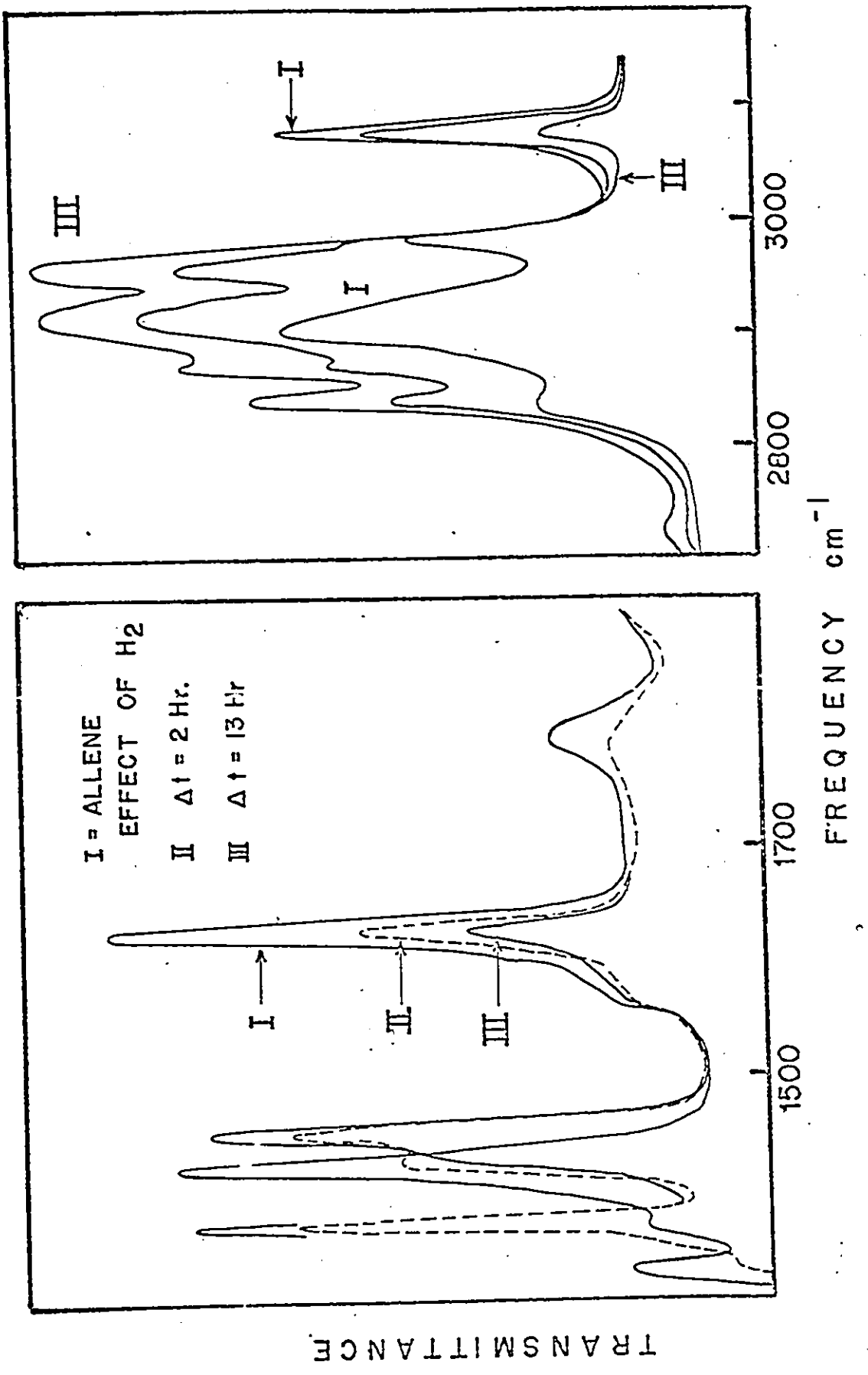

Fig. 43. Infrared spectra of adsorbed allene.

adsorbed allene and 30 mm of hydrogen at different time intervals (curve II, Δt=2 hr., curve III, Δt=13 hr.). Fig. 40b shows the spectra of adsorbed propylene and effect of hydrogen.

5.5.3 Copper Catalyst

Fig. 44 shows the spectra of adsorbed allene. Curves II, III and IV show the spectra of allene at pressures of 100, 200 and 300 mm saturated for 12 hr. While no absorption bands were observed in the lower frequency range, weak absorption bands were observed in the CH stretching range. Evacuation had no effect on the spectra. Due to poorly defined spectra, it is very difficult to assign any structure to the adsorbed species. Addition of hydrogen (10, 20 or 30 mmHg) yielded an intense spectra (curves IV, V and VI) resembling the one obtained for hydrogenated allene on nickel. No absorption bands could be obtained for adsorbed propylene or hydrogenated propylene.

5.5.4 Cobalt Catalyst

Fig. 45 shows the spectra of adsorbed allene (curves II to V) on cobalt catalysts (wt.=0.100 gm, silica=0.0865 gm). No bands were observed at lower frequency ranges. As the pressure of allene increased, bands appeared at 3076, 2980, 2900 and 2834 cm^{-1}. Curve V shows the spectrum of 30 mm of allene saturated for 24 hrs. The spectrum was similar to the one obtained for nickel catalysts. Evacuation had no effect on the spectra. Curves VI and VII show the spectra on addition of 30 mmHg of H_2 after ½ hr. and 12 hr. Curve VIII shows the spectra after heating sample VII at 250°C for ½ hr. The bands due to $C=CH_2$ group (3076 and 2480 cm^{-1}) disappeared completely on heating the sample. Fig. 46 shows the spectra of adsorbed propylene before and after hydrogen addition.

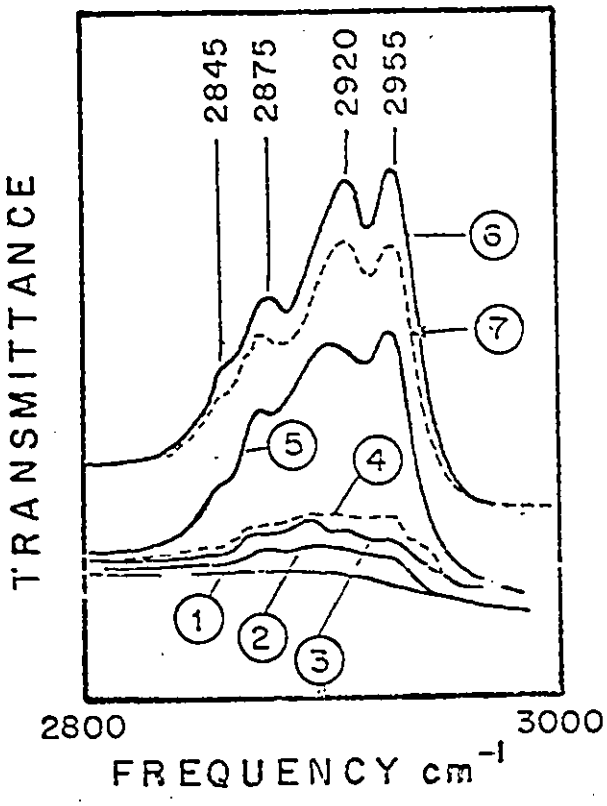

Fig. 44. Infrared spectra of adsorbed allene and effect of hydrogen on Cu catalyst.
I - base line, allene; II - 100 mm; III - 200 mm; IV - 300 mm; Hydrogen: V - 10 mm; VI - 20 mm; VII - 30 mm.

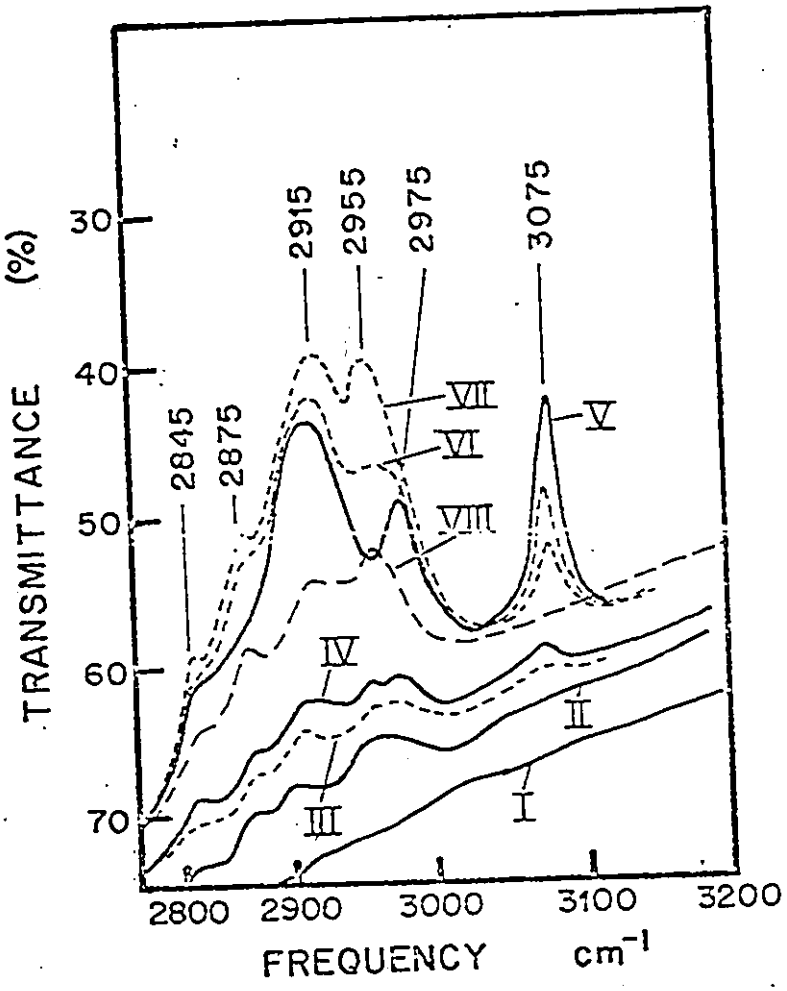

Fig. 45. Infrared spectra of allene on Co catalyst. I - base line, allene: II - 1 mm; III - 2 mm; IV - 5 mm; V - 30 mm; Hydrogen: 30 mm; VI - $\Delta t = \frac{1}{2}$ hr.; VII - Δt=12 hr; VIII - spectra of sample VII after heating it for ½ hr. at 250°C.

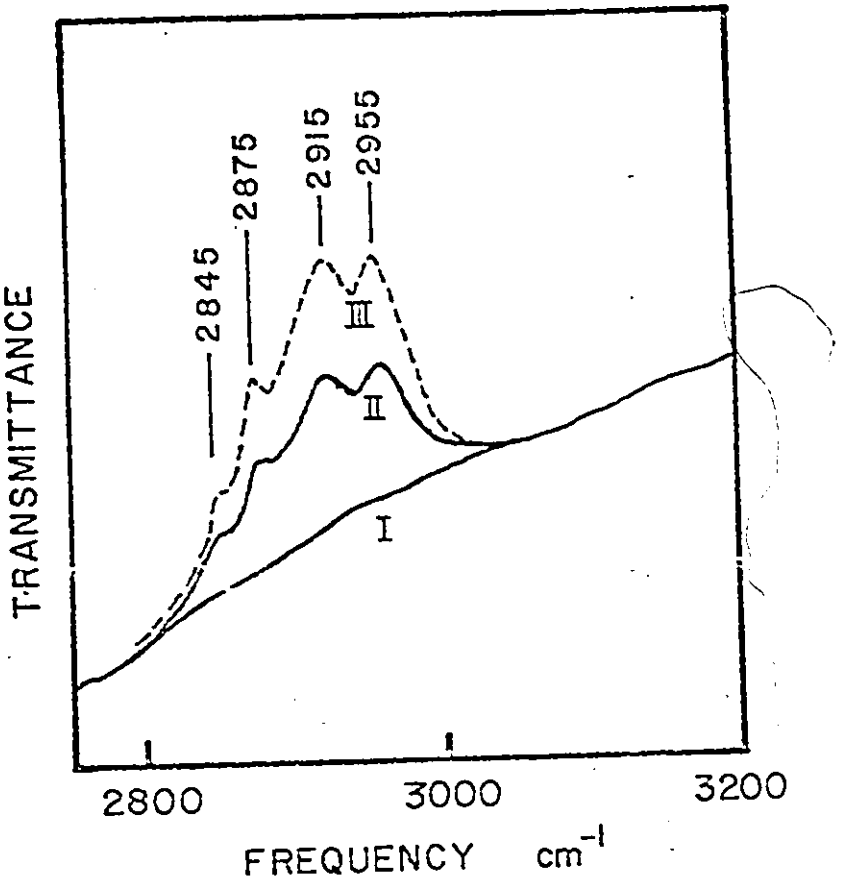

Fig. 46. Spectra of adsorbed propylene.
I - base line; II - propylene=20 mm;
III - adsorbed propylene + 30 mm H_2.

Nearly equal intensity of bands at 2920 and 2955 cm^{-1} indicates the presence of $CH_3(CH_2)_2$-M species.

5.5.5 Rhodium Catalyst

At low pressures, no absorption bands for adsorbed allene were observed. However, saturating the catalyst with 10.5 mm pressure of allene for 24 hr. yielded the spectrum shown in Fig. 47a, curve II. Saturating the catalyst with 100 mm of allene for 72 hr. yielded an intense spectrum (curve III) with absorption bands at 3076, 2982, 2902 and 2838 cm^{-1}. Evacuation had no effect on the spectra. Addition of 15 mm hydrogen at room temperature yielded curves IV and V ($\Delta t=\frac{1}{2}$ hr., $\Delta t=12$ hr.). Fig. 47a shows the spectra of 100mm Hg of propylene saturated for 12hr. (curve II) and the effect of hydrogen addition (curve III).

5.5.6 Palladium Catalyst

Fig. 48 shows the spectra of allene (300 mm Hg) saturated for 72 hr. before and after evacuation (curve II). No absorption bands were observed in the lower frequency range. The addition of 30 mm of hydrogen at room temperature yielded more intense spectra with two new bands at 2958 and 2873 cm^{-1} ($\Delta t=\frac{1}{2}$ hr., $\Delta t=12$ hr.). While saturating the catalyst with propylene (100 mm) produced no bands, on heating the catalyst with 15 mmHg of propylene and 15 mmHg of hydrogen gave a spectrum shown in Fig. 48b (curve II). Evacuation had no effect on this spectrum.

5.5.7 Platinum Catalyst

Fig. 49a shows the spectra of adsorbed hydrogen on platinum catalysts. Two bands were observed at 2115 and 2055 cm^{-1}. With increasing pressures of hydrogen, the band at 2115 cm^{-1} became sharper. These bands

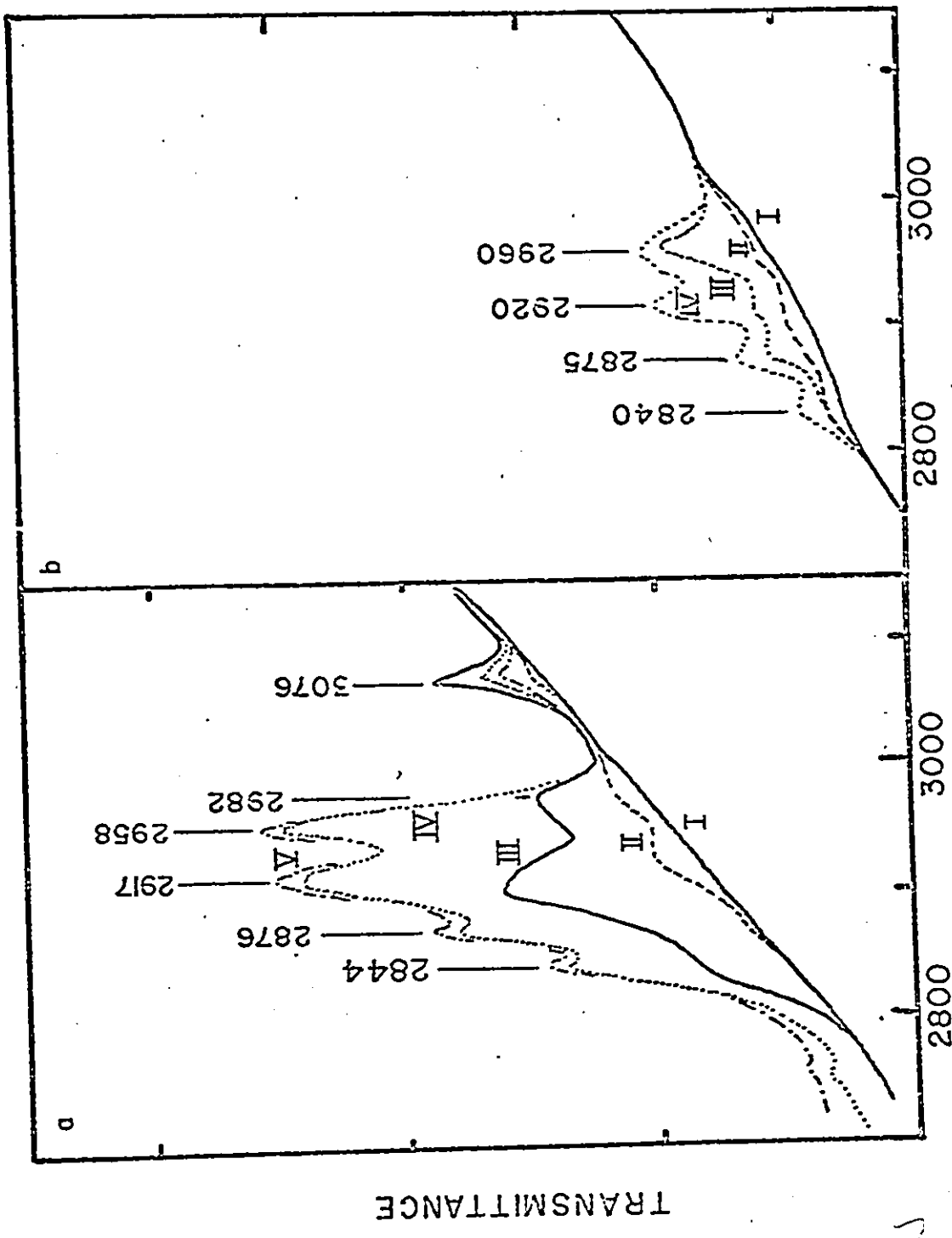

Fig. 47. Infrared spectra of allene and propylene on Rh catalyst.
A - Allene: I - base line; II - 10.5 mm; III - 100 mm; IV - Hydrogen: 15 mm,
V - $\Delta t=\frac{1}{2}$ hr.; V - $\Delta t=12$ hr.; B) I - base line; II propylene = 100 mm; III - $H_2=15$ mm;
IV - $H_2=30$ mm.

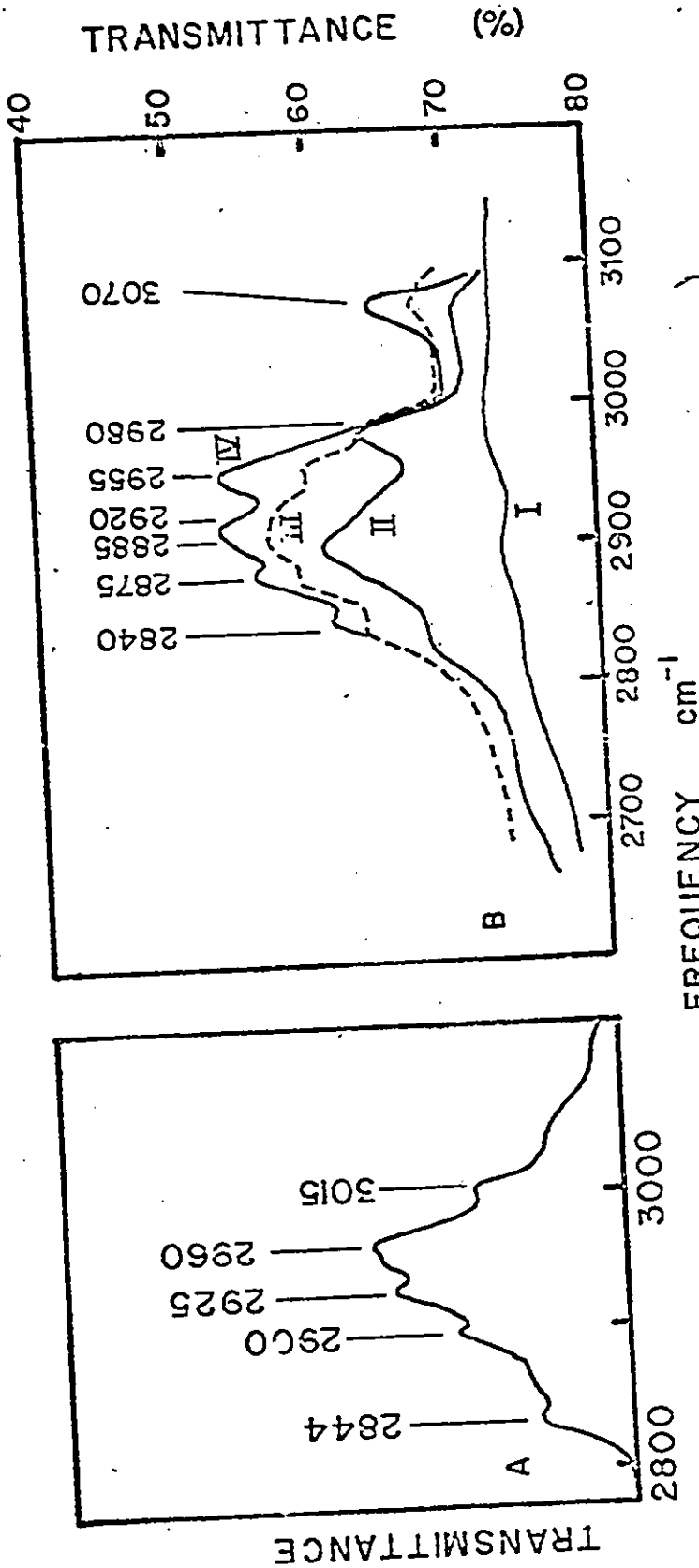

Fig. 48. Infrared spectra of allene and propylene on Pd catalyst.
A) I - base line; II - allene=100 mm; III - H_2=30 mm, Δt=½ hr.;
IV - H_2=30 mm, Δt=12 hr.
B) Mixture of 15 mm propylene and 15 mm hydrogen.

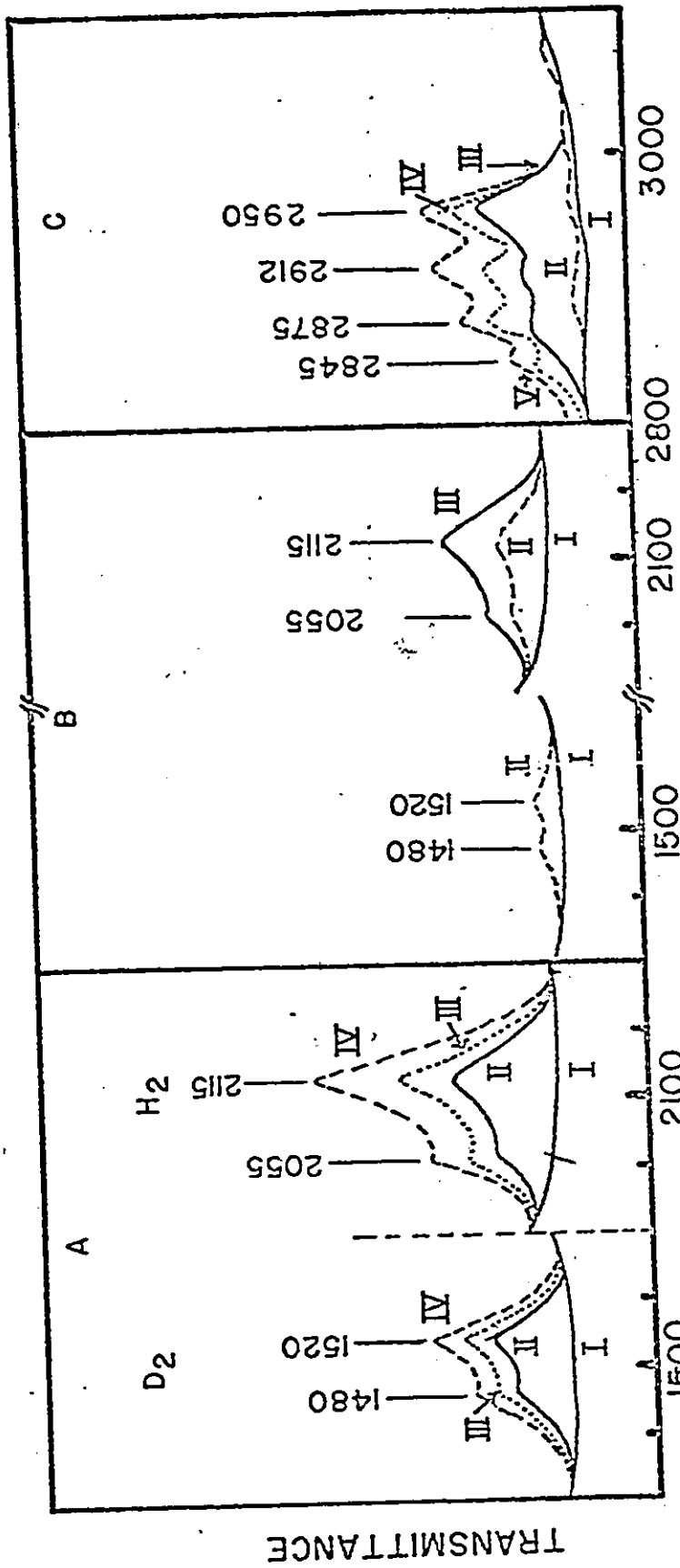

Fig. 49. A) Infrared spectra of hydrogen and deuterium.
I - base line; II - H_2=200 mm; III - H_2=300 mm; IV - H_2=400 mm.
B) I - base line; II - H_2=200 mm; III - 200 mm H_2 + 200 mm D_2
C) I - base line; II - 200 mm allene; III - H_2=30 mm, Δt=6 hr.;
IV - Δt=12 hr; V - Δt=24 hr.

disappeared completely on degassing the catalyst for a few minutes at room temperature. Introduction of deuterium (200 mm) to the hydrogen (200 mm) exposed sample resulted in a decrease in the intensities of these bands, and appearance of two new bands at 1520 and 1480 cm^{-1} (Fig. 49b) suggesting the bands to be due,not to molecular hydrogen or deuterium but to adsorbed atomic hydrogen on the surface. Fig. 49c shows the spectra of allene (200 mm) saturated for 72 hr. (curve II) and after evacuation. Curves III, IV and V show the effect of H_2 (30 mm) after a time interval of 6, 12 and 24 hrs. at room temperature.

5.5.8 Iridium Catalyst

While no absorption bands were obtained for adsorbed allene, a mixture of allene and hydrogen when heated to 200°C yielded the spectra shown in Fig. 50 (curve II - P_{allene}=3 mm, P_{H_2}=30 mm, curve III; P_{allene}=15 mm, P_{H_2}=15 mm). On evacuation, all the bands disappeared. On addition of hydrogen (15 mm) to the evacuated sample, curve II was reproduced.

As the transmittance was poor, no infrared studies could be carried on Ru, Os and Fe catalysts.

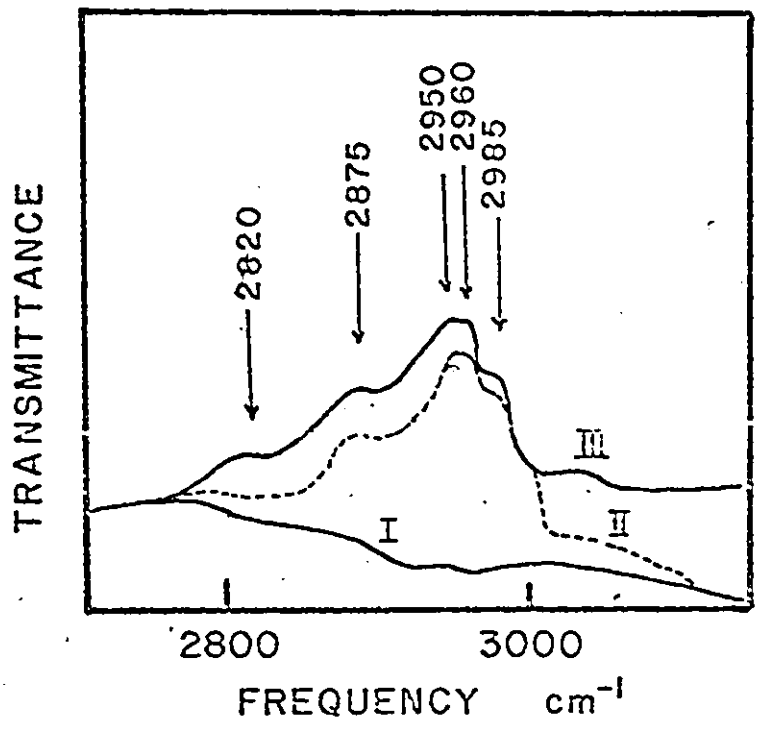

Fig. 50. Infrared spectra of allene and hydrogen mixture at 250°C.
I - base line; II - allene=3 mm, H_2=30 mm;
III - allene=15 mm, H_2=15 mm.

6. DISCUSSION

The kinetic form of the pressure drop-time curve depends on the nature and more significantly on the concentration of the species, in the reactive layer, on the surface of the catalyst when the massive reaction begins. It also depends on the order of admission of the reactants, into the reaction vessel, pretreatment of the catalyst and the method of the preparation of the catalyst.

Bond (15) has classified the observed pressure-time curves into different categories, which is based on the hydrogenation of acetylene over nickel pumice. Mann and To (29), Mann and Tiu (30) and Mann and Shah (31) observed type III curves on pumice supported group VIII transition metals and unsupported group VIII transition metals and nickel-copper alloy catalysts.

In the present study, type III curves (Fig. 3b) were observed for all reactant ratios except for platinum where type II (Fig. 3a) curves were observed for the reactant ratios less than 1.5. For a reactant ratio greater than 1.5, the pressure-time curves consisted of two linear portions (Fig. 3a), the rate (r) increased in the second portion due to the further hydrogenation of propylene which is supported by the fact that after a certain pressure drop, the pressure of propylene decreased in the product stream whereas the pressure of propane increased (Fig. 16).

The order of reaction with respect to hydrogen was always one, which is in agreement with the findings of other works (24,30,31). In the case of platinum, palladium and ruthenium catalysts, in the initial rate-pressure plot, an inflection point occurred after which the rate increased (Fig. 8). In the hydrogenation of acetylene on nickel catalysts, Bond (15) and Bond and Mann (16) observed type III pressure-time curves

when acetylene was added first and the initial hydrogen/acetylene ratio was less than about 2. For an initial hydrogen/acetylene ratio greater than 2, type I pressure-time curves were obtained. An accelerated initial rate was obtained as soon as the pressure-time curves changed its shape. For type III curves, the order was always 1 and the initial rate was expressed as:

$$-\frac{dP}{dt} = k_A P_{H_2} \tag{6.1}$$

It was concluded that type I curves were due to a complex rate equation expressed as:

$$-\frac{dP}{dt} = k_A P_{H_2} + k_B(P_{H_2} - P^o_{H_2}) \tag{6.2}$$

where $P^o_{H_2}$ was hydrogen pressure in mm Hg at which inflection occurred. $P^o_{H_2}$ was nearly equal to two folds of acetylene pressure. The calculated values of k_A/k_B increased markedly with increasing temperatures. In the present study, irrespective of initial hydrogen/allene ratios, type II curves on platinum and type III curves on palladium and ruthenium were obtained. The values of $P^o_{H_2}$, k_A, k_B and k_B/k_A are given in Table 6.1.

It is clear from the table that while $P^o_{H_2}$ is dependent on temperature, $P^o_{H_2}/P_{allene}$ decreased from about 2 to 1 within the studied temperature range. In the case of platinum, k_B/k_A decreased with increasing temperature while on palladium and ruthenium, k_B/k_A increased with increasing temperature.

For platinum, the rate of formation of propylene (Fig. 16) was nearly constant for all the ratios of P_{H_2}/P_{allene}, but the rate of formation of propane increased with increasing reactant ratios or initial hydrogen pressures ($P_{C_3H_4}$=50 mm). While the reactant ratio was equal to 1.5,

TABLE 6.1
Calculated values of k_A, k_B and k_B/k_A.
P_{allene}=50± mm

CATALYST	T°C	$k'_B x10^2$	$k_A x10^2$	$k_B x10^2$	k_B/k_A	$P^o_{H_2}/P_{allene}$	$P^o_{H_2}$
	84	3.3	1.1	2.2	2.0	1.9	95
Pt	94	5.45	2.23	3.22	1.405	1.17	58.5
	100	8.65	3.7	4.95	1.33	0.92	46
	105	10.65	4.65	6.0	1.295	0.90	45
	10	2.8	1.525	1.275	0.834	2.0	100
Pd	20	4.6	2.0	2.6	1.3	1.66	83
	30	7.4	2.5	4.9	1.96	1.18	59
	65	2.45	1.22	1.23	1.008	2.3	115
Ru	75	3.225	1.475	1.85	1.254	1.8	90
	85	3.85	1.7	2.15	1.264	1.5	75
	100	5.0	1.875	3.125	1.667	1.14	57

the amounts of propylene and propane formed were nearly equal at $\bar{R}$=2.0 the main product was propane. In the hydrogenation of allene on pumice supported platinum, Bond and Sheridan (21) observed that at a reactant ratio of 1.0, the rate of formation of propylene and propane was constant till all allene was removed and after that propylene started to hydrogenate. It appears that for reactant ratios less than 1.0, the rate was governed by the formation of propylene and for higher reactant ratios, the rate was governed by the formation of propane directly from allene.

Assuming a simple rate expression with nth order with respect to hydrogen, the rate expression could be written as:

$$-\frac{dP}{dt} = k'_B P^n_{H_2} \qquad (6.3)$$

or

$$-\frac{dP}{dt} = (k_A P_{H_2} + k_B P^n_H) \qquad (6.4)$$

The values for n, from the initial rate method, were calculated to be 2.0, 1.85, and 1.5 for platinum, palladium and ruthenium, respectively.

The zero order with respect to allene and positive order with respect to hydrogen indicate that while the former was strongly adsorbed on the surface and its surface coverage was extensive, the latter (hydrogen) was weakly adsorbed and its surface coverage was low. The relative strength of adsorption of the reactants is also supported by the low pressure adsorption isotherms of allene and hydrogen.

In the chemisorption of ethylene over nickel surface, Jenkins and Rideal (83) observed that 80% of the surface was covered with acetylene residue. In the hydrogenation of ethylene, Tuul and Fransworth (84) observed that the catalyst deactivated slightly during the course of reaction. However, a marked increase in the activity was observed the following day on treating the catalyst overnight with hydrogen. Khulbe (85) observed similar behaviour for the hydrogenation of 2-butyne over pumice supported iron catalysts. In the present investigation, iron and osmium catalysts deactivated continuously with each successive run. The continuous deactivation of the catalyst even at higher temperatures (>200°C) made it impossible to study the kinetics.

The rate of reaction expressed in mm Hg per unit time per unit metal weight can be used in correlating the activity of the metals provided all the catalysts are prepared in the same manner. Since the rate of reaction is dependent on pressure and temperature, it is not suitable to correlate the catalytic activity. Considering the k_{100} (specific rate constant at 100°C/m^2) as a measure of the catalytic

activity, the order of the catalytic activities for metals was in the following sequence:

Pd>Rh>Pt>Ni>Ni-Cu>Co>Ru>Cu>Ir

Since iron and osmium deactivated continuously, the activity of these metals could not be compared.

Many attempts have been made in the past to explain the variation in the catalytic activities of the metals. In order to get a proper perspective with respect to the new trends in correlating the catalytic activity with different parameters, it may be well to review the various theories that have been proposed as to the properties of solids that are important in making them active as catalysts.

Sabatier (86) suggested that the mechanism for the metal catalysts like nickel might involve a chemical factor namely the nickel hydride. At present, it has been customary to speak of the reactants as chemisorbed intermediates and not specifically as metallic hydrides.

Taylor (87) while proposing the theory of active centres considered that in heterogeneous catalysis only certain points on the surface of a metallic catalyst were active for a given reaction. Subsequently, active centres were given geometric interpretation and were considered to be the corners or edges of crystals. Later, they came to be interpreted as representing the different faces of crystals. Balandin (88) suggested that the activity of the catalyst depended to a large measure on the presence of correctly spaced groups of atoms to accommodate the various reactant molecules. He proposed that for the hydrogenation of benzene, properly spaced face centred cubic metals, which hydrogenate benzene, should not be active catalysts for hydrogenating 5 and 7 membered rings.

Long et al (89) found that only those bimetallic alloys of nickel, cobalt and iron which had a face centred cubic structure were actually capable of causing the conversion of benzene to cyclohexane at temperatures below 200°C.

Beeck (90) made a systematic study of ethylene hydrogenation on evaporated metals and related the activities of the catalysts to their crystal parameters. Fig. 51 shows the plot of log k_{100} against lattice distance for the hydrogenation of allene. With the exception of copper and iridium, all the metals lie in a smooth curve with a maximum for palladium. If the activity depended on lattice parameters, then the activity of iridium catalysts should be nearly equal to platinum or rhodium or it should be greater than nickel or copper whereas iridium was the least active catalyst.

Boudart (91) suggested that the variation of the activity of metals for the hydrogenation of ethylene could be correlated with Paulings (92), percent-d character. Considering Boudart's view, the activity of iridium should be greater than rhodium. However, if log k_{100} is plotted against percent-d character (Fig. 52), with the exception of iridium, all the metals lie on a smooth curve. The activity increases reaching a maximum and then decreases. To (93) also observed a dome shaped curve for the hydrogenation of allene on pumice supported group VIII transition metals. The activity was in the following sequence.

Pt>Pd>Rh>Ir>Ni>Co>Fe>Ru>Os

The activity of unsupported transition metals (31) was in the following sequence.

Pd>Ir>Rh>Pt>Ru,Os

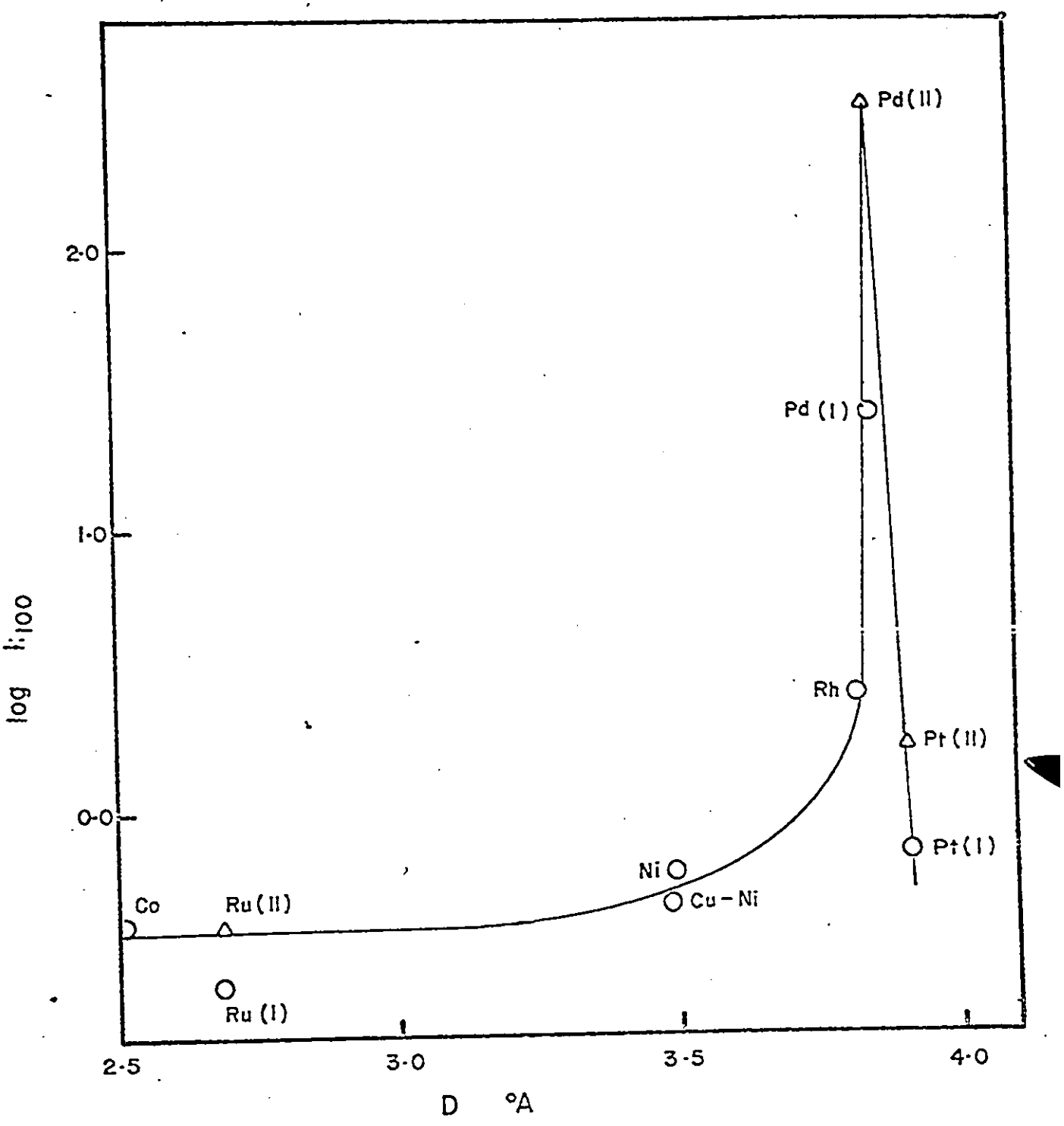

Fig. 51. Dependence of $\log_{10}k$ on lattice distance.

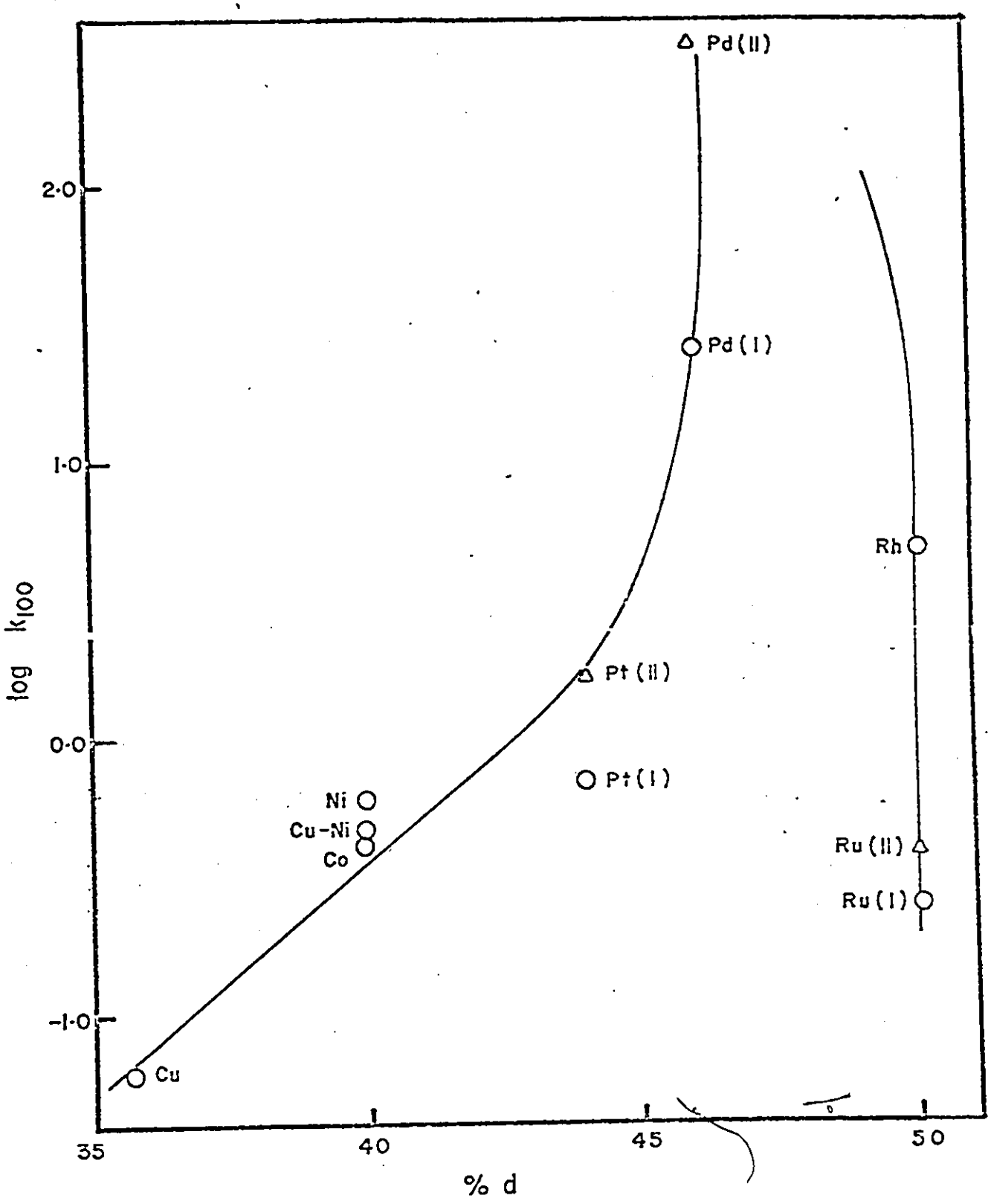

Fig. 52 Dependence of $\log_{10}k$ on % d character.

These results and present investigations show a close similarity in the catalytic activity of supported and unsupported metals to those obtained by Mann and Khulbe (23) for methylacetylene hydrogenation. Palladium was found to be most active catalyst for allene and methylacetylene hydrogenation. Pumice supported palladium was less active than platinum, which indicates that the support also plays some part in the catalytic activity.

There seems to be no simple correlation between E, A and other physical properties of the catalyst.

Activity variation shown by a series of related catalysts may be due to either a variation in the frequency factor or the activation energy or in both. For a given reaction over a series of related catalysts, the relationship between the activation energy E and the frequency factor A is of great significance. It is usually of the form:

$$\log A = mE + C \tag{6.5}$$

and is referred to as "compensation effect" (4), while an increase in the value of log A at constant E implies a higher rate, an increase in E at constant log A implies a lower rate. Simultaneous increase or decrease in E and log A tend to compensate the rate.

For the hydrogenation of allene, the Arrhenius parameter for silica supported transition metals (Fig. 53) can be correlated by the equation:

$$\log A = 0.6E - 0.9 \tag{6.6}$$

On the basis of the analysis during the course of reaction, these catalysts can be classified into the following two categories:

1) active for consecutive reactions like

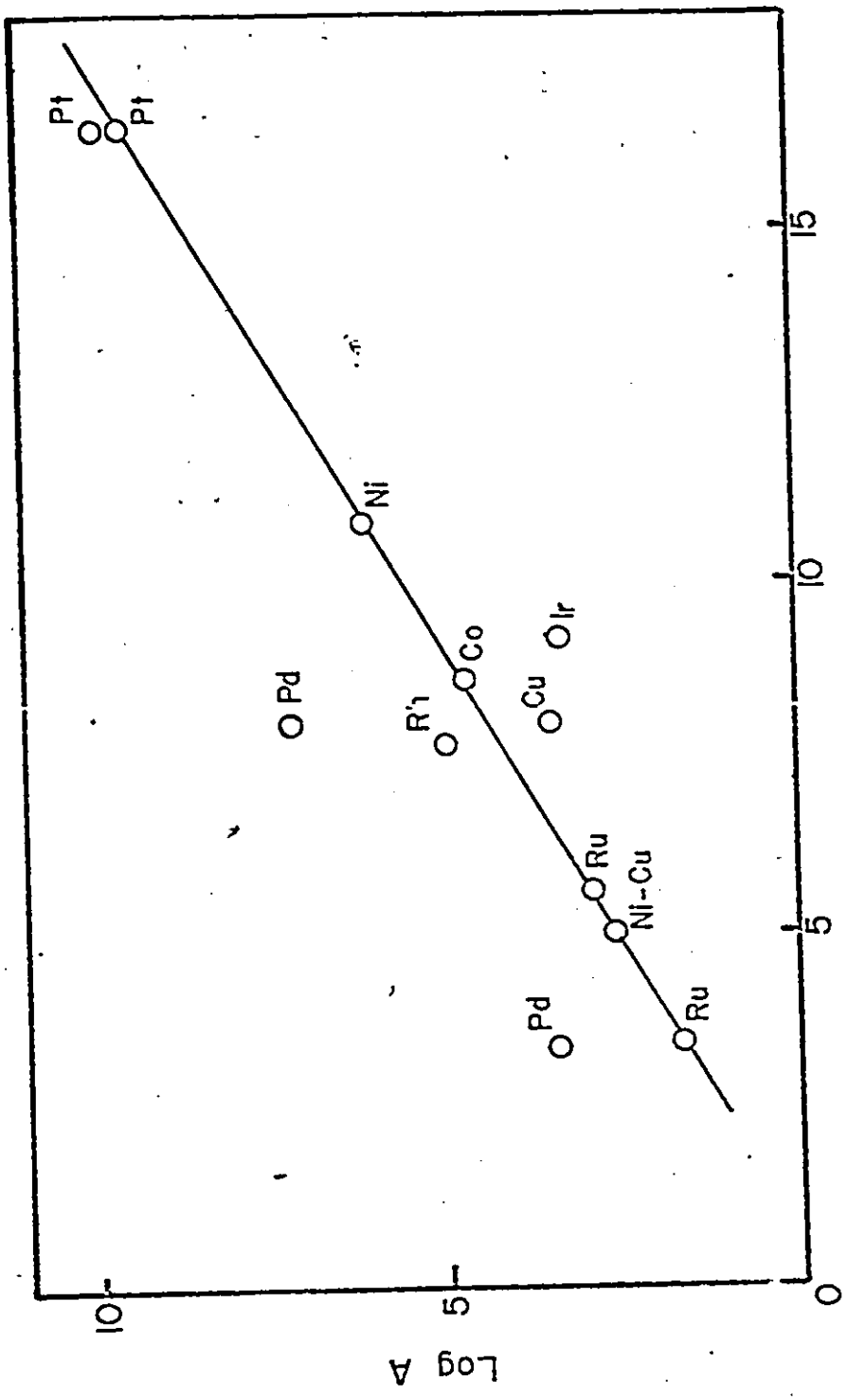

Fig. 53. Dependence of log E on energy of activation.

$$A \xrightarrow{k_1} B \xrightarrow{k_2} C$$

2) active for simultaneous reactions like

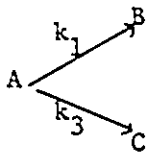

Nickel, copper and nickel-copper alloys fall in the first category as the initial product of the reaction was propylene. When a major amount of allene was removed, formation of propane started with the hydrogenation of propylene. Other catalysts fall in the second category where propane and propylene both were the initial products of the reaction.

Fig. 54 shows the variation of selectivity with pressure drop. For a reactant ratio of one, the selectivity was almost independent of pressure fall except for platinum where it decreased slightly with pressure fall. For a reactant ratio of two, the selectivity decreased after a pressure fall of about 50 mm due to the further hydrogenation of propylene into propane. Fig. 55 shows the variation of selectivity with initial hydrogen pressure at two different temperatures. In the case of platinum and palladium, the selectivity decreased sharply with increasing amounts of hydrogen. It is clear from the analysis of the products during the course of reaction for different reactant ratios that the rate of formation of propane increased and rate of formation of propylene was constant with increasing reactant ratios resulting in a decrease in the selectivity with increasing hydrogen pressures. The selectivity of nickel-copper alloy catalysts increased with increasing temperatures. It is possible that the rate of desorption of propylene increased more compared to that of allene, with increasing temperatures, resulting in

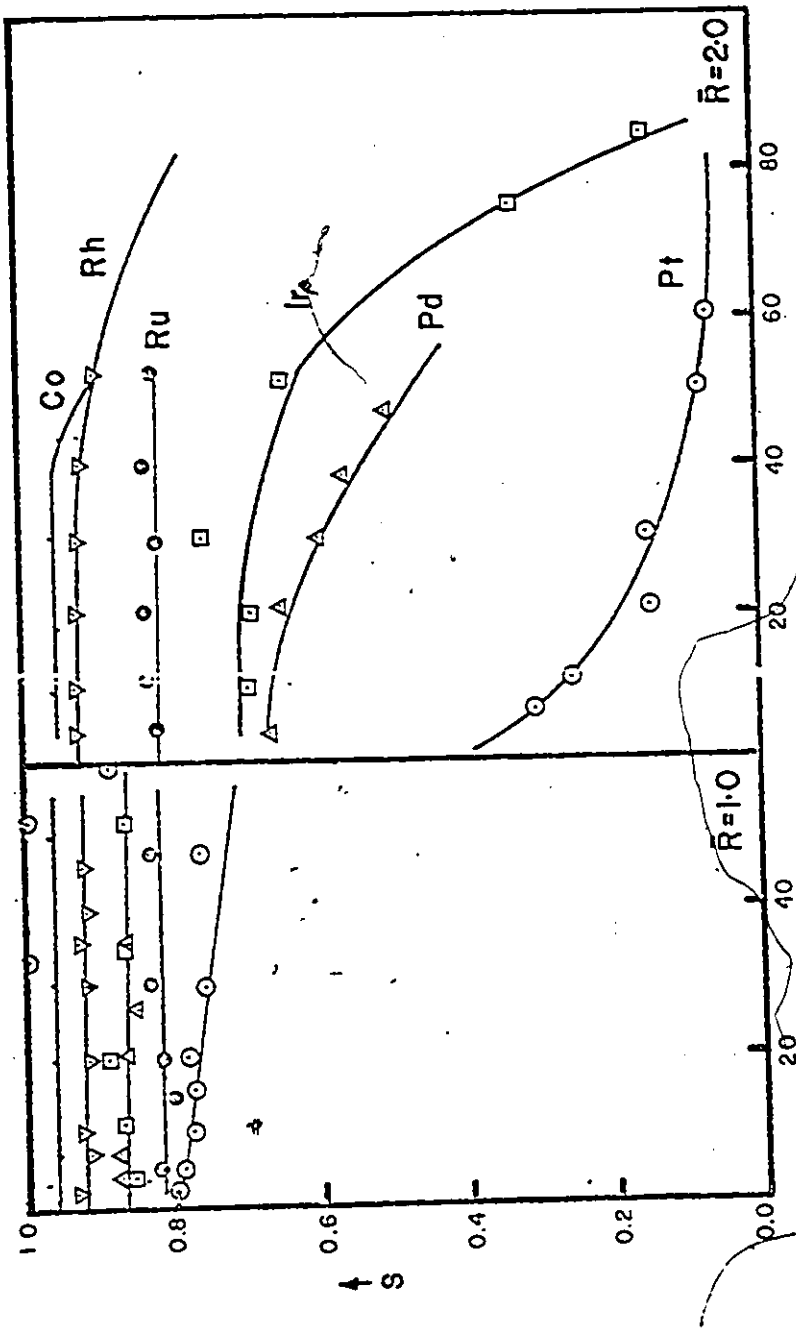

Fig. 54. Dependence of selectivity on pressure drop.

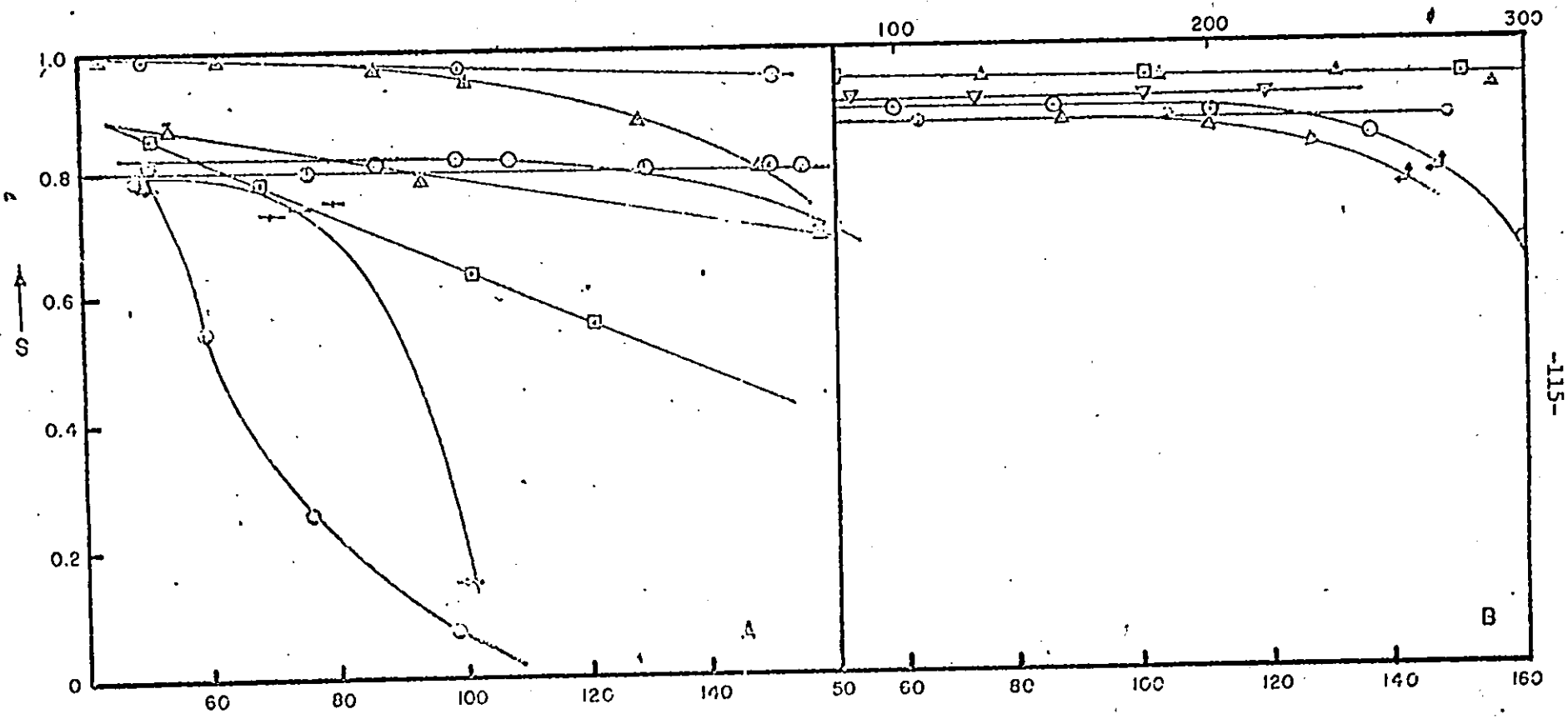

Fig. 55. Dependence of selectivity on initial pressure of hydrogen.

A) Ni, ⊙ - 91, △ - 120; Pt, ⊣ - 100, ○ - 105; Pd, ⧊ -20, □-40; Ru, ◐ - 75, ⊖ 100°C. B) Ir, ⊙ -230, △- 260; Rh, ◎ -30, ▽-50, and Co, □ -50, △ -80°C.

lesser chances for adsorbed propylene to hydrogenate into propane.

Kamentzy and Markovich (94) calculated isomerization equilibrium for the isomerization of allene.

at different temperatures by the statistical method using spectroscopic data obtained by Linnett and Avery (95) for allene, and by Crawford (96) for methylacetylene, and the heat of hydrogenation obtained by Kistiakovsky and co-workers (26). The values of equilibrium constants and the percentage of allene in equilibrium mixture at various temperatures are tabulated below.

TABLE 6.2
Equilibrium constants for allene-methylacetylene isomerization.

T°K	K	% of allene
355	15.5	6.0
473	9.9	10.0
673	5.5	15.3
773	4.7	17.4
873	4.2	19.2

At 200°C, the equilibrium mixture should contain about 90% methylacetylene. Slobodine (97) studied the equilibrium of allene-methylacetylene isomerization by passing these substances over "Floridine" between 167 and 350°C. Starting with methylacetylene as the initial substance, the resulting mixture contained about 61.5 to 67.8% methylacetylene at 325°C. On the other hand, starting with allene as the initial substance except at 325°C, the resulting mixture contained a much lower percentage of methylacetylene. However, at 325°C, the resulting mixture contained

about 61.5 to 67.8% of methylacetylene. As the methylacetylene content of the resulting mixture was much lower than 61.5% except at 325°C, it is doubtful whether the true equilibrium had been reached even at 325°C. No direct determination of the allene content of the mixtures were carried out. The polymerization and decomposition reactions must have proceeded to a considerable extent and their products diluting the resulting mixture. It seems, therefore, quite natural that the methylacetylene contents of the mixture were, in all cases, lower than the theoretical value. Cordes and Gungler (98) obtained an equilibrium mixture containing 20% allene and 80% methylacetylene at 300°C by heating these isomers as the initial substance in the presence of activated charcoal. In the present study, starting with allene or methylacetylene, an equilibrium mixture containing about 16% allene and 84% methylacetylene was obtained in the studied temperature range. This is fairly close to the calculated values (94).

On the basis of the equilibrium data calculated by Kamenetzy and Markovich (94), Bond and Sheridan (21) suggested that the reaction should occur on supported or unsupported metals. In the hydrogenation of allene on pumice supported nickel, palladium and platinum (21), they could not obtain even traces of methylacetylene. Though the rearrangement of allenes and acetylenes could be obtained by different means, nothing has been reported about allene-methylacetylene isomerization reaction catalyzed by supported or unsupported metals. Hence, no direct comparison can be made. However, Kokes et al (70,71) observed a first order methylacetylene-allene isomerization reaction catalyzed by ZnO.

In the present study, silica supported iron and cobalt were found

to be active for the isomerization reaction. In the hydrogenation of allene on silica supported cobalt catalysts, traces of methylacetylene were observed at higher allene pressures. No such mention is made by previous workers (21,23,29,31,31) in the hydrogenation of allene or methylacetylene.

The order of reaction for isomerization was always one. In the case of cobalt, the initial rate determined by pressure-time curves was slightly lower than the initial rate calculated by using Equation (5.4). While, in the former case the initial rate was obtained for the formation of methylacetylene, in the latter case it was calculated for the disappearance of allene which was slightly more due to the polymerization. The energy of activation was calculated to be 11.8 and 11.2 k cal/mole for iron and cobalt, respectively. The activity (defined as the rate constant per gm of the catalyst for initial allene pressure of 50 mm at 127°C) was nearly equal for iron and cobalt catalysts. No direct comparison can be made with other catalysts or their physical characteristics as only iron and cobalt were active for the reaction.

The thermal isomerization of alkadienes apparently involve "detachment" of hydrogen (99).

$$H_2C{=}C{=}CH_2 \rightleftharpoons \left[\bar{H}C{=}\bar{C}{-}\bar{C}H_2{+}H\right] \longrightarrow HC{\equiv}C{-}CH_3$$

$$H_2C{=}C{=}\underset{\displaystyle CH_3}{\underset{|}{C}}{-}CH_3 \rightleftharpoons \left[H_2C{=}\bar{C}{-}\underset{\displaystyle CH_3}{\underset{|}{\bar{C}}}{-}\bar{C}H_2{+}H\right] \rightleftharpoons H_2C{=}\underset{\displaystyle H}{\underset{|}{C}}{-}\underset{\displaystyle CH_3}{\underset{|}{C}}{-}CH_2$$

When allene was heated with ether and sodium at 100°C, allene yielded the sodium derivative of methylacetylene (97). Allene, treated for 12 hrs. at 160 to 170°C with alcoholic potash, gave methylacetylene and ethyl isopropenyl ether (intermediate product) together with unreacted

allene (43).

$$H_2C{=}C{=}CH_2 + CH_3OH \longrightarrow H_2C{=}C(OC_2H_5){-}CH_3 \rightleftharpoons HC{\equiv}C{-}CH_3 + C_2H_5OH$$

The reaction path for the base catalyzed acetylene-allene isomerization is presumed to be (44):

$$RCH_2{-}C{\equiv}CH + \overline{B} \longrightarrow RCH{=}C{=}\overline{CH} + HB$$
$$\Updownarrow$$
$$RCH{=}C{=}CH_2 + \overline{B}$$

On ZnO, Kokes (70,71) observed that a) adsorbed methylacetylene gives an OH band and a hydrocarbon species characterized in part by a band at 1865 cm^{-1}; b) 1-deuterio methylacetylene adsorbs to give an OH band rather than OD band; c) identical spectra for adsorbed allene and methylacetylene. These results show that hydrogen was removed from the CH_3 group of methylacetylene by yielding a band at 1865 cm^{-1} ($CH_2{-}C{=}CH$) which was too high to be a simple double band. Also, it was much lower in frequency than that for the triple bond in gaseous methylacetylene (2142 cm^{-1}). Dynamic (at different time intervals) infrared spectra of $CH_3{-}C{\equiv}CD$ on ZnO suggests the reaction to be taking place as:

$$CH_3{-}C{\equiv}CD\ (g) \underset{+H}{\overset{-H}{\rightleftharpoons}} CH_2{=}C{=}CD \quad (1833\ cm^{-1})$$
$$\Updownarrow +H \quad -H$$

$$CH{=}C{-}CDH \underset{+H}{\overset{-H}{\rightleftharpoons}} CH_2{=}C{=}CHD$$
$$-D \Updownarrow +D$$
$$CH_2{-}C{=}CH \quad (1865\ cm^{-1})$$

For many years, it was generally believed that the support was inert and simply acted as a carrier for the metal in a finely divided high area form. There are now growing evidences that the support may

not be inert but may influence the catalytic activity in any of several ways:

a) it may interact chemically with the metal thereby modifying the properties of the metal

b) the support may exert an influence on the actual structure of the metal

c) the support may act either as a source of reactive intermediates or as a seat of reaction, through the migration of adsorbed species between metal and support.

The phenomenon of surface migration between metal and support "Spill-over" (100) has been shown to be of particular importance with hydrogen on supported metals. Altham and Webb (101) who used tritium and radioactive approach to monitor the extent of hydrogen spill-over on platinum-silica and platinum alumina catalysts, observed that in the absence of platinum, neither alumina nor silica was active for olefin exchange at temperatures below 250°C. However, when the metal was present, both silica and alumina possessed an appreciable activity for olefin and hydrogen exchange at ambient temperatures, although neither oxide was active for olefin hydrogenation.

Evidence for the participation of the support in the reaction of olefins and acetylenes over supported metals have been obtained by the use of catalyst poisons. Webb and MacNab (102) have studied the hydrogenation, hydroisomerization and deuterium exchange of 1-butene over rhodium-silica in the temperature range 0-69°C. The catalysts were progressively poisoned with mercury. The extent of mercury coverage was measured by a radioactive counting technique. While the rate of hydrogenation and

deuterium exchange decreased with increasing mercury coverage, the rate of 1-butene isomerization remained constant up to a fractional coverage (θ_{Hg}) of about 0.8. These results can be satisfactorily interpreted by considering the hydrogenation and 1-butene exchange to be confined to the surface of metals only, and the isomerization occuring on the support and involving the migration of hydrocarbon from the metal to the support. Since in the absence of rhodium, silica itself showed no isomerization activity in the temperature range studied and the reversible adsorption of 1-butene on silica did not occur to any appreciable extent, rhodium must have therefore activated the surface of silica by adsorbing the hydrocarbon which then migrated to the support before undergoing reaction.

In the present study, silica showed no activity for the isomerization reaction. The absence of the isomerization reaction on pure metals suggests that metals are not active for this reaction. Thus, it can be assumed that the isomerization reaction occurs on the surface of silica activated by metals. The nearly equal activity and energy of activation for both the catalysts suggests that the reaction occurs on the same active site and that the rate determining step is also the same. Considering all the above-mentioned assumptions, the isomerization reaction can be represented as follows:

$$\text{Allene (g)} \underset{k_b}{\overset{k_a}{\rightleftharpoons}} \text{allene (adsorbed on metal)}$$

$$k_n \quad \Big\downarrow\uparrow \quad k_n'$$

$$\left[\overset{- - - - - -}{CH_2\text{-}C\equiv CH}\right]^- \underset{+H}{\overset{-H}{\rightleftharpoons}} \text{allene (adsorbed on silica)}$$

$$+H \Big\downarrow\uparrow -H$$

$$CH_3\text{-}C\equiv CH \text{ (adsorbed)} \longrightarrow CH_3\text{-}C\equiv CH \text{ (gas)}$$

Two types of adsorbed hydrogen were obtained on all the catalysts; Type I, chemisorbed hydrogen which could be removed by evacuation at room temperature, Type II, which could not be removed even after several hours of evacuation at room temperature. Similar behaviour of H_2 adsorption on ZnO was observed by Sholten and Montfoort (47), Kokes and Dent (46) and on silica supported platinum at 25°C by Komers et al (48). The amount of hydrogen adsorbed on silica supported platinum was less than the amount of hydrogen adsorbed in the present study. The lesser amount of hydrogen adsorbed on the catalyst surface could be due to the treatment of the catalyst at 650°C. The amount of strongly held hydrogen was nearly constant in the pressure range studied.

Different types of adsorbed hydrogen were observed by several workers (49,50,51). Recently, Dixon et al (51) while studying the adsorption isotherms at 295 and 77°K on wet and dry catalyst samples, have obtained five kinds of hydrogen adsorption on alumina supported platinum.

The present study could reveal only two types of adsorbed hydrogen since all the adsorption studies were made at room temperature. Type II adsorption covers all metal surface and can not be removed by pumping at room temperature. Fig. 35b shows the amount of strongly held hydrogen on the surface and is independent of hydrogen pressure. Different types of hydrogen adsorbed on catalyst surface, observed by several workers at very low temperatures, are removable at room temperature by degassing the catalyst for a few minutes.

The following table shows the amounts of gases adsorbed (CC(STP)/gm) on various silica supported catalysts at 10 mm pressure and 25±1°C.

There seems to be no simple relationship between the amount of gas adsorbed to the catalytic activity or the physical properties of the metals.

TABLE 6.3
Amounts of gases adsorbed. T=25°C, P=10 mmHg

CATALYST	TOTAL HYDROGEN ADSORPTION CC(STP)/gm	WEAKLY ADS. HYDROGEN CC(STP)/gm	H_s	Allene CC(STP)/gm	Propylene CC(STP)/gm
Ni	3.35	2.50	0.85	-	5.2
Co	2.85	1.50	1.35	13.5	4.0
Fe	1.10	1.10	0	5.4	7.4
Pd	2.85	2.85	0	16.0	3.35
Rh	2.55	2.05	0.50	8.15	4.55
Ru	2.05	1.35	0.70	4.55	3.40
Pt	2.00	1.15	0.85	3.08	2.55
Ir	1.55	1.30	0.25	3.70	3.05
Os	1.35	1.25	0.10	5.40	4.40
Cu	1.55	1.25	0.30	8.55	7.55
Ni-Cu	4.55	2.45	2.10	-	3.80

In the present investigation, the method used to obtain the low pressure hydrogen (up to 15 mm) adsorption isotherms at room temperature was similar to the one used by Sinfelt and Yates (60). The hydrogen uptake was obtained by extrapolating the linear portion of the isotherm to zero pressure thus avoiding the contribution of physical adsorption and adsorption of hydrogen by the support. Table 6.4, page 124, shows the results of these calculations.

Table 6.5, pg.124,shows the catalytic activity (k_{100} per square metre per gm of the catalyst) dispersion and other metallic properties of group VIII transition metals.

TABLE 6.4
Metal surface area and H/M calculated from adsorption isotherms.
T=25±1°C

CATALYST	TOTAL VOLUME OF H_2 ADSORBED AT ZERO PRESSURE CC STP/gm	NO. OF H ATOMS ON THE SURFACE $x10^{-19}$	METAL ON SURFACE $x10^4$ gm	METAL SURFACE AREA m^2/gm	H/M
Ni	2.25	12.103	117.94	7.262	0.24
Co	1.80	9.682	94.73	5.809	0.19
Fe	0.10	0.538	4.99	0.323	0.01
Pd	1.85	9.951	175.75	5.971	0.35
Rh	1.55	8.338	139.92	5.003	0.28
Ru	0.45	2.421	41.34	1.453	0.08
Pt	0.96	5.164	167.22	3.098	0.33
Fr	0.44	2.367	75.51	1.420	0.15
Os	0.30	1.614	50.95	0.968	0.10
Cu	0.55	2.958	31.20	1.775	0.06
Ni-Cu	3.50	18.827	184.22	11.297	0.37

TABLE 6.5
Dispersion and other properties of group VIII metals

METAL	SPECIFIC ACTIVITY	$\frac{H}{M}$	$\frac{H_W}{M}$	$\frac{H_s}{M}$	% d (92)	ATOMIC RADIUS A^o
First Triad						
Ni	$11.18x10^{-2}$	.24	.16	.18	40	1.24
Co	$3.587x10^{-2}$	.19	.05	.14	39.5	1.25
Fe	-	.01	.01	.0	39.7	1.24
Second Triad						
Pd (I)	5.772	.35	.35		46	1.37
Pd (II)	9.48	-				
Rh	$9.05x10^{-1}$	.28	.29	.09	50	1.34
Ru (I)	$3.83x10^{-1}$	.08	.06	.02	50	1.32
Ru (II)	$1.51x10^{-1}$					
Third Triad						
Pt (I)	$4.5x10^{-1}$	.33	.05	.29	44	1.38
Pt (II)	1.007					
Ir	$9.35x10^{-3}$	.15	.10	.05	49	1.35
Os	-	.10	.07	.03	49	1.34

M(I) and M(II) represent reactions before and after the inflection point.

The results of the present investigation present a clear pattern of the catalytic behaviour of the group VIII transition metals for the hydrogenation of allene. Considering the triad of ruthenium, rhodium and palladium in the second long period of the Periodic Table, it can be noted that the catalytic activity increases from left to right, i.e. Ru<Rh<Pd. Furthermore, the increase in the activity is accompanied by an increase in the dispersion or H/M ratio. Exactly analogous behaviour is observed with cobalt and nickel, from the triad of iron, cobalt and nickel, i.e. nickel is more active than cobalt, and with iridium and platinum from the triad of osmium, iridium and platinum. The most striking observation is the extremely high activity of palladium compared to other transition metals of group VIII, the difference amounting to a factor of 10^2 to 10^3. At room temperature (after 15 mm of hydrogen pressure), palladium absorbs a large amount of hydrogen yielding H/Pd ranging from 1 to 4 at 20 to 400 mm hydrogen pressure (103). The high sorption value may be responsible for extremely high activity of palladium.

If the catalytic activity depends on the dispersion of the metal, the catalytic activity of transition metals of group VIII should be in the following decreasing sequence:

Pd>Pt>Rh>Ni>Co>Ir>Ru>Os>Fe

which is in fairly good agreement to the observed one.

Platinum silica catalysts with 200 mm hydrogen at room temperature yielded a sharp absorption band at 2115 cm^{-1} and a shoulder at 2055 cm^{-1}. On increasing the hydrogen pressure, the band at 2115 cm^{-1} became sharper and more intense compared to the band at 2055 cm^{-1}. Both bands disappeared completely on degassing the catalyst for a few minutes at room

temperature. This is in full agreement with the findings of Dixon et al (104). Repeating the experiments with deuterium, two absorption bands were obtained at 1520 and 1480 cm^{-1}. If one of these bands could be assigned to the molecular hydrogen or deuterium adsorbed on the catalyst surface, the addition of a mixture of hydrogen and deuterium should give rise to an absorption band between these frequencies, due to the formation of HD. Introduction of D_2 to the sample exposed to hydrogen resulted in a decrease in the intensity of the bands at 2115 cm^{-1} and 2055 cm^{-1} and the appearance of two new bands at 1520 and 1480 cm^{-1}. This suggests that these bands were not due to the adsorbed molecular hydrogen or deuterium on the surface. It can, therefore, be concluded that hydrogen adsorption takes place with the dissociation of hydrogen molecules. These adsorbed species of hydrogen on platinum silica catalysts can be assigned to as Type III and Type IV observed by Dixon et al (51,104) on $Pt-Al_2O_3$ catalysts.

The bands observed for chemisorption of allene on nickel catalysts are given in Table 6.6.

Evacuation at room temperature had no effect on the spectra. Absorption bands at 3076 and 2985 cm^{-1} were assigned to fundamental asymmetric and symmetric CH stretching in $C=CH_2$ groups (6,72). These bands are forbidden in gaseous allene (105). The absorption bands near 2900 and 2835 cm^{-1} were assigned to $-\underset{M}{CH_2}$ or $-\underset{M}{\overset{H}{C}}-\underset{M}{CH_2}$ groups by Eischens and Pliskin (53). Sheppard and Ward (72) obtained spectra of different ethyl, propyl and n-butyl compounds of tin and iron.

The spectra of these compounds consistently showed prominent bands

TABLE 6.6.
Infrared frequencies (observed) for allene chemisorption in nickel.

Allene Frequency cm^{-1}	Group	Allene adsorbed $+H_2$	Group
3076	$C=CH_2$ (as)	reduced	
2985	$C=CH_2$ (s)	reduced	
		2957	$C-CH_3$(as)
		2920	CH_2 (as)
2902	$-\underset{\vert}{\overset{M}{CH_2}}$ (as)	2875	CH_3 (s)
		2843	CH_2 (s)
2840 sh	$-\underset{\vert}{\overset{M}{CH_2}}$ (s)		
1800	δCH_2 overtone	reduced	
1627	C=C	reduced	
		1450	δCH_3 (as)
1425	$=CH_2$ deformation	reduced	
		1370	δCH_3 (s)
1325	may be overtone of δCH_2 at lower frequencies		

sh = shoulder

as = asymmetric

s = symmetric

in the 2920 and 2895 cm^{-1} region and weaker ones between 2835 and 2815 cm^{-1}. The former was attributed to a $-CH_2-M$ group representing either a lowered νCH_2 asymmetric stretching or a raised νCH_2 symmetric fundamental compared with hydrocarbons. The latter was associated to a δCH_2 overtone. In the present case, bands near 2900 and 2840 cm^{-1} represent a lowered CH_2 as. and s. fundamental respectively due to the attachment with the surface nickel atoms. The absorption band at 1627 cm^{-1} represents a C=C in a monosubstituted hydrocarbon (6) whereas the band at 1427 cm^{-1} represents a $=CH_2$ deformation mode. Absorption bands at 1800 and 1325 cm^{-1} may be the overtone of $=CH_2$ deformation in the lower frequency range. Absence of a band near 3025 cm^{-1} (=CH-) removes the possibility of dissociative adsorption of allene. If the following structure is given to the adsorbed species of allene, the bands observed are consistent to the expected bands.

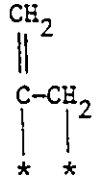

I

Stepwise addition of hydrogen to the evacuated sample decreased the intensity of the bands at 3076, 2895, 1627 and 1425 cm^{-1}. Heating the sample in a hydrogen atmosphere resulted in the complete disappearance of these bands. New bands with large intensities at 2955, 1450, 1370 cm^{-1} and a weak band at 2875 cm^{-1} appeared on addition of hydrogen to the adsorbed allene sample. These bands are assigned to different modes of CH_3 group (Table 4.1). The bands at 2900 and 2840 cm^{-1} shifted to 2920 and 2843 cm^{-1} which represents the asymmetric and symmetric vib-

ration modes of $>CH_2$ group. The spectra obtained for the hydrogenated species of allene on nickel was similar to the one observed by Sheppard and Ward (72) for surface hydrogenation products of chemisorbed propylene attached to nickel atom. While taking the spectra of different dialkyl compounds of platinum, Morrow (82) observed $\nu(as)CH_2/\nu_{as}CH_3$ equal to 0.83 for a propyl group. Nearly equal intensities of the bands at 2920 and 2955 cm^{-1} suggests the presence of $CH_3(CH_2)_2$ group as surface hydrogenated product of allene chemisorbed on nickel.

The spectra of chemisorbed and hydrogenated propylene on nickel silica was similar to the one obtained for surface hydrogenated species of allene on nickel-silica.

At low pressures, no absorption bands were observed for chemisorbed allene on Pd and Rh. As the amount of allene adsorbed was much less than nickel or cobalt, it seems that at low pressures the concentration of the adsorbed species was not sufficient to be observed by infrared. However, at higher pressure, the spectra of adsorbed allene consisted of four bands (3070, 2980, 2895 and 2835cm^{-1}). Addition of hydrogen had an effect similar to the one observed on nickel. These bands indicate the same adsorbed species of allene on Pd and Rh. The spectrum obtained after initial adsorption was weak and poorly defined on Pt. Although the observed bands occurred at positions similar to those obtained on palladium, the weakness of the spectrum makes it unreliable to estimate the surface composition from the results. After hydrogenation, an intense spectrum in the region 3000 to 2800 cm^{-1} was obtained and the nearly equal intensity of the bands at 2955 and 2920 cm^{-1} suggests the same hydrogenated species as observed on palladium or nickel. From the

great intensity increase on hydrogenation, it is clear that initial adsorption on this metal gives rise to a much higher proportion of surface carbides or other hydrogen-deficient surface grouping, i.e. that a high degree of dissociative adsorption has occurred. Sheppard and Ward (72) and Clark (73) observed very weak spectra for initial adsorption of acetylene on platinum supported on silica and porous glass. Similar behaviour was observed on copper catalysts.

The zero order in allene and the positive order in hydrogen show that the former was the more strongly adsorbed reactant and that its surface coverage was high, whereas hydrogen was weakly adsorbed, by comparison and its surface coverage was correspondingly low. Consider the following equations:

$$H_2 + 2* \underset{k_{-1}}{\overset{k_1}{\rightleftharpoons}} 2 \begin{vmatrix} H \\ | \\ * \end{vmatrix} \qquad (1)$$

$$C_3H_4 \underset{k_{-2}}{\overset{k_2}{\rightleftharpoons}} CH_2 = \underset{*}{C} - \underset{*}{CH_2} \qquad (2)$$

$$CH_2 = \underset{*}{C} - \underset{*}{CH_2} + \begin{vmatrix} H \\ | \\ * \end{vmatrix} \underset{k_{-3}}{\overset{k_3}{\rightleftharpoons}} CH_2 = C - CH_3 + \begin{vmatrix} H \\ | \\ * \end{vmatrix} + * \qquad (3)$$

Equations (1) and (2) describe the adsorption of each reactant at a pair of adjacent vacant sites. Such adsorption takes place competitively for a given pair of sites. When a surface is highly covered with adsorbate requiring two adsorption sites, single sites will remain vacant. Adsorbed hydrogen atoms and adsorbed allene will compete for these single sites.

Hydrogen adsorption may take place at such sites, as shown in Eqn. (3), by a quasi-Rideal Eley mechanism. Alternatively, the sites of adsorption may be a pair of adjacent metal atoms, if these are not available for allene adsorption because of the operation of some geometric factor (i.e., either the adjacent metal atoms form a forbidden lattice spacing or the introduction of a further allene molecule would produce intolerable intermolecular repulsions). Thus, the requirement of the 'single site' in step (3) is that it must be capable of activating a hydrogen molecule. Bond and Wells (106) have considered this type of mechanism in the hydrogenation of acetylene over platinum catalyst. They showed that step (3) is irreversible and the concentration of weakly adsorbed hydrogen molecule is proportional to the hydrogen pressure. These adsorbed hydrogen molecules react with an adsorbed allene molecule according to step (3). Langmuir equation can not be used to relate the surface coverage of hydrogen, θ_H, to its pressure in the gas phase. For the adsorption process:

$$\text{rate of hydrogen consumption} = k_1 P_{H_2} [**] + k_3 \theta_{C_3H_4} [*] P_{H_2} = K P_{H_2} \qquad (A)$$

since $\theta_{C_3H_4} \longrightarrow 1$ and the concentration of single sites and of pair of sites will be constant for a given allene pressure at a given temperature. Consequently, the hydrogen surface coverage is directly proportional to hydrogen pressure.

The hydrogen atom from step (3) either reacts with an adsorbed allene molecule giving half-hydrogenated state of reacts with other species.

$$CH_2 = \underset{*}{C} - \underset{*}{CH_2} + \underset{*}{H} \underset{k_{-4}}{\overset{k_4}{\rightleftharpoons}} CH_2 = \underset{*}{C} - CH_3 + 2* \qquad (4)$$

From the stepwise addition of hydrogen to adsorbed allene, it is clear that as the intensity of the bands representing the CH_3 group increases, the intensity of the bands representing $C{=}CH_2$ group decreases indicating that the half-hydrogenated state from step (3) is unstable and it reacts with a vacant site and changes its structure.

$$CH_2 = \underset{|}{\overset{*}{C}} - CH_3 + * \xrightarrow{k_5} CH_2 - \underset{|}{\overset{*}{\overset{\bullet}{C}}} - CH_3 \qquad (5)$$

The half-hydrogenated state formed in step (3) or the radical formed in step (4) then reacts with a neighbouring hydrogen atom or molecule. From step (3), the nearest reactant is a hydrogen atom which further reacts with the half-hydrogenated state or the radical.

$$CH_2 = \underset{|}{\overset{*}{C}} - CH_3 + \underset{|}{\overset{*}{H}} \xrightarrow{k_6} CH_2 = CH - CH_3(g) + 2* \qquad (6)$$

$$CH_2 - \underset{|}{\overset{*}{C}} - CH_3 + \underset{|}{\overset{*}{H}} \xrightarrow{k_7} CH_2 - \underset{|}{\overset{*}{CH}} - CH_3 + 2* \qquad (7)$$

$$CH_2 = CH - CH_3(g)$$

Steps (5), (6) and (7) are not shown reversible as $CH_2 - \underset{|}{\overset{*}{\overset{\bullet}{C}}} - CH_3$ formed in step (5) either reacts with a hydrogen atom to form adsorbed propylene which deadsorbs from the surface to give gaseous propylene leaving two adjacent sites for the adsorption of allene or the radical reacts with another radical to from polymer.

The rate of formation of propylene from steps (6) and (7)

$$= k_6 \theta_{C_3H_5} \theta_H + k_7 \theta^{\bullet}_{C_3H_5} \theta_H \qquad (B)$$

where $\theta_{C_3H_5}$ and $\theta^{\bullet}_{C_3H_5}$ are surface covered by C_3H_5 and $C^{\bullet}{}_3H_5$ respectively.

Applying steady state assumption for C_3H_5 and $C^{\bullet}{}_3H_5$,

$$k_3 \theta_{C_3H_4} P_{H_2} + k_4 \theta_{C_3H_4} \theta_H = k_{-3} \theta_{C_3H_5} \theta_H [*] + k_{-4} \theta_{C_3H_5} [*]^2$$

$$+ k_5 \theta_{C_3H_5} [*] + k_6 \theta_{C_3H_5} \theta_H \qquad (C)$$

$$k_5 \theta_{C_3H_5} [*] = k_7 \theta^{\bullet}_{C_3H_5} \theta_H \qquad (D)$$

Combining Eqns. (B) and (D),

$$\text{rate} = k_6 \theta_{C_3H_6} \theta_H + k_5 \theta_{C_3H_5} [*]$$

$$= \left[k_6 \theta_H + k_5 [*] \right] \theta_{C_3H_5} \qquad (E)$$

From Eqn. (C),

$$\theta_{C_3H_5} = \frac{k_3 P_{H_2} + k_4 \theta_H}{k_{-3} \theta_H [*] + k_{-4} [*]^2 + k_5 [*] + k_6 \theta_H} \qquad (F)$$

Substituting the value of $\theta_{C_3H_5}$ in Eqn. (E),

$$\text{rate} = \left[k_6 \theta_H + k_5 [*] \right] \frac{k_3 P_{H_2} + k_4 \theta_H}{k_{-3} \theta_H [*] + k_{-4} [*]^2 + k_5 [*] + k_6 \theta_H} \qquad (G)$$

if $k_6 \theta_H + k_5 [*] >> k_{-3} \theta_H [*] + k_{-4} [*]^2$

$$\text{rate} = k_3 P_{H_2} + k_4 \theta_H$$

$$= [k_3 + k_4] P_{H_2}$$

$$\propto P_{H_2}$$

The order of reaction reduces to first order which is in agreement with the experimentally obtained order.

On other catalysts, the initial products of the reaction were both propane and propylene. The formation of propane may be from the hydrogenation of adsorbed propylene.

$$CH_2(*) - CH(*) - CH_3 + H(*) \underset{k_{-8}}{\overset{k_8}{\rightleftharpoons}} CH_2(*) - CH_2 - CH_3 + 2* \qquad (8)$$

$$CH_2(*) - CH_2 - CH_3 + H(*) \xrightarrow{k_9} CH_3 - CH_2 - CH_3(g) + 2* \qquad (9)$$

Total rate of allene consumption

$$= k_6 \theta_{C_3H_5} \theta_H + k_7 \theta_{C_3H_5} \theta_H + k_9 \theta_{C_3H_7} \theta_H \qquad (H)$$

Rate of formation of propane

$$= k_9 \theta_{C_3H_7} \theta_H \qquad (I)$$

Applying steady state assumption for C_3H_7 and C_3H_6

$$k_8 \theta_{C_3H_6} \theta_H = k_{-8} \theta_{C_3H_7} [*]^2 + k_9 \theta_{C_3H_7} \theta_H \qquad (J)$$

$$k_7\theta_{C_3H_5}\theta_H + k_{-8}\theta_{C_3H_7}[*]^2 = k_7\theta^*_{C_3H_5}\theta_H \quad (K)$$

On addition,

$$k_9\theta_{C_3H_7}\theta_H = k_7\theta^*_{C_3H_5}\theta_H$$

$$= k_5\theta_{C_3H_5}[*] \quad (L)$$

From Eqns. (H) and (L),

$$\text{total rate} = k_6\theta_{C_3H_5}\theta_H + 2k_5\theta_{C_3H_5}[*] \quad (M)$$

Substituting the value of $\theta_{C_3H_5}$ from Eqn. (F),

$$= \left[k_6\theta_H + 2k_5[*]\right]\left[\frac{k_3P_{H_2} + k_4\theta_H}{k_{-3}\theta_H[*] + k_{-4}[*]^2 + k_5[*] + k_6\theta_H}\right]$$

if $k_6\theta_H \gg k_{-3}\theta_H[*] + k_{-4}[*]^2 + k_5[*]$

$$\text{Total rate} = k_3P_{H_2} + k_4\theta_H \quad (N)$$

$$= k\,P_{H_2} \propto P_{H_2}$$

the equation reduces to first order.

If $k_{-4}[*]^2 \gg k_5[*] + k_6\theta_H + k_{-3}\theta_H[*]$

$$\text{Total rate} = \frac{\left[k_6\theta_H + 2k_5[*]\right]}{k_{-4}[*]^2}\left[k_3P_{H_2} + k_4\theta_H\right] \quad (O)$$

$$= k_1 P_{H_2}^2 + k_2 P_{H_2} \qquad (P)$$

$$= \left[k_2 + k_1 P_{H_2}\right] P_{H_2}$$

When the contribution due to the first term ($k_2 P_{H_2}^2$) is much more than the contribution due to the second term ($k_1 P_{H_2}$), the equation reduces to a second order reaction which is in full agreement to the present findings.

7. CONCLUSION

The catalytic hydrogenation and isomerization of allene over silica supported transition metals, Cu and Cu-Ni alloys, was investigated over a wide range of temperature and the initial reactant ratios in a constant volume reactor.

The orders of reaction were mostly one and zero with respect to hydrogen and allene respectively and were independent of temperature. In the case of Pt, Pd and Ru, in the initial rate - initial hydrogen pressure plot, an inflection point occurred after which the rate accelerated. The orders of reaction in the accelerated region were 2.0, 1.8 and 1.5, respectively.

The apparent activation energy for the first order reaction varied between 3.4 to 16.4 k cal/mole and for the second order reaction it was 16.4, 8.7 and 3.4 on Pt, Ru and Pd, respectively. There seems to be no simple relation between energy of activation and other parameters of the catalyst. A satisfactory "Compensation effect" appears to exist for allene hydrogenation and the Arrhenius parameter can be correlated as:

$$\log A = 0.6E - 0.9$$

The catalytic activity was in the following sequence:

Pd>Rh>Pt>Ni>Ni-Cu>Co>Ru>Cu>Ir

On the basis of analysis, these catalysts can be categorized as:

a) active for consecutive reaction

$$\text{Allene} \xrightarrow{H_2} \text{Propylene} \xrightarrow{H_2} \text{Propane}$$

b) active for simultaneous reaction

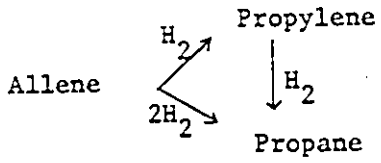

Nickel, copper and nickel-copper alloy fall into the first category where only propylene was obtained as the initial product of the reaction; other catalysts fall into the second category.

Only iron and cobalt were active for the isomerization reaction. Nearly equal activity and energy of activation (11.2 and 11.8 k cal/mole) suggested that the support, in the presence of metal, was active for isomerization reaction.

Except for palladium and iron, two types of hydrogen adsorption were obtained on all catalysts:

1) chemisorbed hydrogen which could be removed on evacuating at room temperature
2) chemisorbed hydrogen which could not be removed on evacuation at room temperature.

The amount of different gases adsorbed was in the following sequence:

H2	Ni-Cu>Ni>Co = Pd>Rh>Ru>Pt>Ir = Cu>Os>Fe
Allene	Pd>Co>Cu>Rh>Fe,Os>Ir>Ru>Pt
Propylene	Fe>Ni>Rh>Os>Co>Cu-Ni>Cu>Ru>Pd>Ir>Pt

The dispersion or H/M was in the following sequence:

Ni-Cu>Pd>Pt>Rh>Ni>Co>Ir>Os>Ru>Cu>Fe

For group VIII transition metals, the activity pattern was fairly close to the dispersion.

Infrared studies showed the presence of $CH_2{=}\overset{*}{C}{-}\overset{*}{CH_2}$ and $CH_3(CH_2)_2{-}^*$ species as the initial adsorption and hydrogenated products of allene on the surface.

A possible mechanism, based on the reaction product analysis, infrared studies of adsorption and hydrogenation of allene over all the catalysts investigated has been postulated. The mechanism satisfactorily explains the observed kinetics of the reaction.

8. SIGNIFICANT CONTRIBUTIONS

The present investigation "Hydrogenation, isomerization, adsorption and infrared studies of allene on silica supported transition metals of group VIII copper and copper-nickel alloy" has been of great importance in the understanding of the reaction mechanism and catalytic activity of various catalysts. In summary, the following significant contributions are made by the present study:

1) For the first time, the isomerization of allene to methylacetylene in the presence of metal catalysts (silica supported cobalt and iron) has been observed.

2) For the first time, using infrared techniques, the following structure has been assigned to the adsorbed species of allene:

$$CH_2 = \underset{*}{C} - \underset{*}{CH_2}$$

3) The proposed mechanism for the hydrogenation reaction fully explains the kinetic behaviour of the reaction on silica supported metals.

4) The following sequence is observed for the catalytic activity of different catalysts for the hydrogenation of allene:

Pd>Rh>Pt>Ni>Ni-Cu>Co>Ru>Cu>Ir

5) The catalytic activity can be correlated to H/M.

6) These catalysts can be divided into two groups:

   i) catalysts active for consecutive reaction (Ni,Ni-Cu,Cu)

   ii) catalysts active for simultaneous reaction (Pd,Pt,Ru,Rh, Co and Ir).

9. RECOMMENDATIONS

Though the detailed study of allene hydrogenation over group VIII transition metals suggested the dependence of activity on dispersion or H/M ratio, the method of preparation, support and molecular structure play an important role in governing the activity of the catalyst for a particular reaction. In order to obtain a better correlation of the activity and to explain the reaction mechanism more closely, it is suggested that the following studies should be made:

1) Hydrogenation of allene over these catalysts prepared by different methods. This would explain the variation of the activity with the method of preparation of the catalysts.
2) Hydrogenation of allene, adsorption and infrared studies on these metals on other supports.
3) The reaction of allene with deuterium in order to obtain further information regarding the reaction mechanism.
4) Adsorption and infrared studies of partially deuterated allene in order to confirm the nature of the adsorbed species.
5) More information of the adsorbed state should be collected by EPR, NMR and tracer techniques.
6) Hydrogenation, adsorption, EPR and infrared studies of the isomers (methylacetylene and cyclopropylene) and partially deuterated compounds of these isomers should be made.

10. REFERENCES

1. Rideal, E.K., "Concept in Catalysis", Academic Press, London and New York, 1968.

2. Thomson, S.J. and Webb, G., "Heterogeneous Catalysis", Oliver and Boyd, Edinburg, 1968.

3. Anderson, R.B., "Experimental Methods in Catalytic Research", Academic Press, London and N.Y., 1968.

4. Bond, G.C., "Catalysis by Metals", Academic Press, London and New York, 1962.

5. Bond, G.C., "Hydrogenation Review", Cat. Prog. Res. Proces. NATO, Sci. Comm. Conf., 1972, Pub. 1973, p. 141.

6. Little, L.H., "Infrared Spectra of Adsorbed Species", Academic Press, London and New York, 1966.

7. Sabatier and Senderens, J.B., Compt. Rend., 128, 1173 (1899).

8. Ross, W.H., Culbertson, T.B., and Parson, J.P., Ind. Engg. Chem., 13, 775 (1921).

9. Yoshikawa, K., Bull. Chem. Soc. Japan, 7, 201 (1932).

10. Petrov, A.D. and Antsus, L.T., J. Appl. Chem. USSR, 6, 1145 (1933).

11. Dupont, G., Bull. Soc. Chem., France, 3, 1030 (1936).

12. Dupont, G. and Lombard, R., Ibid, 8, 851 (1941).

13. Sheridan, J., J. Chem. Soc. 373 (1944), 133, 301, 305, 470 (1945).

14. de Pauw, F. and Jungers, J.C., Bull. Soc. Chim., Beld., 57, 618 (1948).

15. Bond, G.C., J. Chem. Soc., 2705 (1958).

16. Bond, G.C. and Mann, R.S., Ibid, 4738 (1958).

17. Tamaru, K., Bull. Chem. Soc. Japan, 23, 180 (1950).

18. Bond, G.C., Dowden, D.A. and Mackenzie, N., J. Chem. Soc., 1538 (1958).

19. Bond, G.C. and Mann, R.S., Ibid, 3566 (1959).

20. Sheridan, J. and Reid, W.D., Ibid, 2962 (1952).

21. Bond, G.C. and Sheridan, J., Trans. Faraday Soc., 48, 651 (1952), 48, 658 (1952).

22. Mann, R.S. and Naik, S.C., Can. J. Chem., 45, 1023 (1967).

23. Mann, R.S. and Khuble, K.C., Ibid, 45, 2755 (1967), 46, 623 (1968), 47, 215 (1969), Paper 29, 4th International Congress on Catalysis Moscow, 1968.

24. Meyer, E.F. and Burwell, R.L., Jr., J. Am. Chem. Soc., 85, 2881 (1963).

25. Mann, R.S. and Khulbe, K.C., J. Cat., 10, 401 (1968), 13, 25 (1969), 17, 46 (1970), Indian J. of Technology, 9, 471 (1971).

26. Kistiakowsky, Ruhoff, Smith and Vaughan, J. Am. Chem. Soc., 58, 146 (1936).

27. Wells, P.B., Platinum Metals Rev., 7, 18 (1963).

28. Bond, G.C., Webb, G., Wells, P.B. and Winterbottom, J.M., J. Catal., 1, 74 (1962).

29. Mann, R.S. and To, D.E., Can. J. Chem., 46, 161 (1968).

30. Mann, R.S. and Tiu, D.E. Ibid, 46, 3249 (1968).

31. Mann, R.S. and Shah, A.M., Ibid, 48, 3324 (1970), 50, 1793 (1972).

32. Phillipson, J.J., Wells, P.B. and Wilson, G.R., J. Chem. Soc. A., 9, 1351 (1969).

33. Bond, G.C., "Advances in Catalysis", edited by Eley, D.D., Vol. 15, p. 92 (1964).

34. Phillipson, J.J. and Wells, P.B., Proc. Chem. Soc. 227 (1964).

35. Ragaini, V., J. Cat., 34, 1 (1974).

36. Ballaivet, D., Barthoeuf, D. and Trambouze, Y., J. Cat., 34, 423 (1974).

37. Gati, Gy and Knozinger, H., 5th International Congress on Catalysis, Paper 57, 1972.

38. Hightower, J.W. and Hall, K., Trans. Faraday Soc., 66, 477 (1970).

39. Amenomiya, Y., J. Res. Inst. for Catalysis, Hokkaido Uni., 9, 1 (1961).

40. Macnab, J.I. and Webb, G., J. Cat., 10, 19 (1968).

41. Bond, G.C., Webb, G. and Wells, P.B., Trans. Faraday Soc., 64, 3077 (1968).

42. Jacobs, T.L., Akawie, R. and Cooper, R.G., J. Am. Chem. Soc. 73, 1273 (1951).

43. Favorsky, A., J. Prakt. Chem., 37, 382 (1888), 44, 208 (1891).

44. Iwai, "Mechanism of Molecular Migrations", Vol. 2, p. 73 (B.S. Thyagarajan ed.), Wiley, New York, 1969.

45. Chang, C.C. and Kokes, R.J., J. Cat., 28, 92 (1973).

46. Kokes, R.J. and Dent, A.L., "Advances in Catalysis", 22, 1 (1972) J. Phys. Chem., 75, 887 (1971).

47. Sholten, J.J. F. and van Montfoort, A., 5th International Congress on Catalysis, Paper 22, 1952.

48. Komers, R., Amenomiya, Y. and Cvetanovic, R.J., J. Cat., 15, 293 (1969).

49. Tsuchiya, S. Amenomiya, Y. and Cvetanovic, R.J., J. Cat., 19, 245 (1970).

50. Stephen, J.J., Ponee, V. and Sachtler, W.M.H., Ibid, 37, 81 (1975).

51. Dixon, L.T., Barth, R., Kokes, R.J. and Gryder, J.W., J. Cat., 37, 376 (1975).

52. Toya, T., J. Res. Inst. Catal. Hokkaido Univ., 10, 236 (1962). Suppl. Prog. Theoret. Phys., 23, 250 (1962).

53. Eischenes, R.P. and Pliskin, W.A., "Advances in Catalysis", Vol. 10, p. (1966), Z. Physik. Chem., 24, 11 (1960), J. Chem. Phys., 24, 482 (1956).

54. Primet, M. Bassat, J.M., Mathieu, M.V. and Pettre, J.M., J. Cat., 28, 368 (1973).

55. Primet, M., Bassat, J.M. and Mathieu, M.V., J. Chem. Soc., Faraday Trans. I, 70, 293 (1974).

56. Clewley, J.D., Lynch, J.F. and Flanagan, T.B., J. Cat., 36, 291 (1975).

57. Dalla Betta, R.A., J. Cat., 34, 57 (1974).

58. Brooks, C.S. and Christopher, G.L.M., J. Cat., 10, 211 (1968).

59. Vannice, M.A., Benson, J.E. and Boudart, M., J. Cat. 16, 348 (1970).

60. Sinfelt, J.H. and Yates, D.J.C., J. Cat., 10, 362 (1968), Ibid, 8, 82 (1967), Ibid 8, 348 (1967).

61. Webb, G., Surface and Defect Properties of Solids, 3, 184 (1974).

62. Little, L.A., Sheppard, N. and Yates, D.J.C., Pros. Roy. Soc., 259A, 242 (1960).

63. Peri, J.B., Disc. Faraday Soc., 41, 121 (1966).

64. Lucchesi, P.J. Carter, J.L. and Sinfelt, J.H., J. Am. Chem. Soc., 86, 1494 (1964).

65. Carter, J.L., Lucchesi, P.J., Sinfelt, J.H., Yates, D.J.C., Proc. Intern. Congr. Catalysis 3rd Amsterdam, 1964, p. 644 (1965).

66. Morrow, B.A. and Sheppard, N., Proc. Roy. Soc. A311, 391 (1969). Ibid A311, 415 (1969), J. Phy. Chem. 70178, 2404 (1966).

67. Erkelens, J., Liefkens, Th. J., J. Cat. 8, 36 (1967), 27, 165 (1972).

68. Ivery, N.R., Ibid, 19, 15 (1970).

69. Pickering, H.L. and Eckstrom, H.C., J. Phy. Chem., 63, 521 (1959).

70. Kokes, R.J., Accounts of Chemical Research, 6(7), 262 (1973).

71. Kokes, R.J., Dent, A.L., Cheng, C.C. and Dixon, L.T., J. Am. Chem., Soc. 94, 4429 (1972).

72. Sheppard, N. and Ward, J.W., J. Cat., 15, 50 (1969).

73. Clark, M., Ph.D. Thesis, Cambridge University, 1960.

74. Randhava, S.S. and Rehmat, A., Trans. Faraday Soc., 66, 235 (1970).

75. Sheppard, N., Pure and App. Chem., 4, 71 (1962).

76. Palazov, A.N., Harson, M.S. and Shopov, D.M., J. Cat., 36, 251 (1975).

77. Schuit, G.C.A. and Van Reijen, L.L., "Advances in Catalysis", 10, p. 26 (1941).

78. Arrhenius, S., Z. Phys. Chem., 4, 226 (1889).

79. Bellamy, L.T., "Infrared Spectra of Complex Molecules", 2nd Ed., Chpts. 2, 3 and 4. Methuen, London (1968).

80. Wexler, A.S., Appl. Specty. Rev., 1, 29 (1969).

81. Mann, R.S. and Khulbe, C.P., Can. J. Chem., 48, 2075 (1970).

82. Morrow, B.A., Can. J. Chem., 48, 2192 (1970).

83. Jenkins, G.I. and Rideal, E., J. Chem. Soc., 2496 (1955).

84. Tuul, J. and Fransworth, H.E., J. Chem. Soc., 2490 (1955).

85. Khulbe, C.P., M.A.Sc. Thesis, Ottawa University (1969).

86. Sabatier, P., "La Catalysis in Chemie Organique", Librarie Polytechnique, Paris (1913).

87. Taylor, H.S., Proc. Roy. Soc. A108, 105 (1925).

88. Balandin, A.A., Z. Phys. Chem., 132, 289 (1924).

89. Long, J.H., Frazer, J.C.W. and Ott, E., J. Am. Chem. Soc., 56, 1101 (1934).

90. Beeck, O., Rev. Mod. Phys., 17, 61 (1945).

91. Boudart, M., J. Am. Chem. Soc., 72, 1040 (1950).

92. Pauling, L., Phys. Rev., 54, 899 (1938), Proc. Roy. Soc. London, Sec. A. 196, 343 (1943).

93. To, D.E., M.A.Sc. Thesis, University of Ottawa (1967).

94. Kamentzy, D.A.F. and Markovich, Acta. Phys. Chim., USSR, 17, 308 (1942).

95. Linnett, J.W. and Avery, W.H., J. Chem. Phys., 58, 146 (1936).

96. Crawford, J. Chem. Phys., 7, 140 (1939).

97. Slobodine, Y.M., Journ. Gen. Chem. (Rus), 6, 1892 (1936), 9, 272 (1939), 7, 1664 (1937).

98. Cordes, J.F. and Gunzler, H., Z. Naturforsch, 156, 933 (1966).

99. Egloff, G., Hulla, G. and Komarewoky, V.I., "Isomerization of Pure Hydrocarbons", Am. Chem. Soc. Monograph, Reinhold Pub. Co., Chapter 2, p. 70, New York, 1942.

100. Sermon, P.A. and Bond, G.C., Cat. Rev., 8, 211 (1974).

101. Altham, J.A. and Webb, G., J. Cat., 18, 133 (1970).

102. Webb, G. and MacNab, J.I., J. Cat., 26, 226 (1972).

103. Aben, P.C., J. Cat., 10, 224 (1968).

104. Dixon, L.T., Barth, R. and Gryder, J.W., J. Cat., 37, 368 (1975).

105. Lord, R.C. and Venkateswarbe, P., J. Chem. Phys., 20, 1237 (1952).

106. Bond, G.C. and Wells, P.B., J. Cat., 4, 211 (1965).

107. Washburn, E.W., "Interational Critical Tables", Vol. I, McGraw Hill (1926).

APPENDIX A

TABLE A-1
Physical characteristics of the catalysts.

CATALYST	LATTICE STRUCTURE	LATTICE PARAMETER °A (107)	%d CHARACTER (92)	ATOMIC RADIUS °A
Ni	f.c.c.	3.49	40.0	1.24
Co	f.c.c. c.p.h.	2.51 4.10	39.5	1.25
Fe	b.c.c.	2.85	39.7	1.24
Pd	f.c.c.	3.85	46.0	1.37
Rh	f.c.c.	3.82	50.0	1.34
Ru	c.p.h.	2.68,4.27	50.0	1.32
Pt	f.c.c.	3.91	44.0	1.38
Ir	f.c.c.	3.82	49.0	1.35
Os	c.p.h.	2.71,4.32	49.0	1.34
Cu	f.c.c.	3.61		
Cu-Ni	f.c.c.			

f.c.c. = face-cubic centred

b.c.c. = body-cubic centre

c.p.h. = close-packed hexagonal

TABLE A-2
Properties of the catalysts used.

CATALYST	E k cal/mole	k_{100} min^{-1}/gm	A min^{-1}/gm	log A	S m^2/gm	H/M
Ni	10.81	0.8119	1.75×10^{6}	6.242	7.262	0.24
Co	8.64	0.2084	2.4×10^{4}	4.38	5.809	0.19
Fe	-	-	-	-	0.323	0.01
Pd	8.0	566.19	2.75×10^{7}	7.43	5.971	0.35
Pd	3.4	34.10	3.04×10^{2}	2.48	-	-
Rh	7.73	4528	1.53×10^{5}	5.184	5.003	0.28
Ru	5.64	0.556	1.1×10^{3}	3.049	1.453	0.08
Ru	4.0	0.2203	4.8×10^{1}	1.686	-	-
Pt	16.4	3.120	1.27×10^{10}	10.10	3.098	0.33
Pt	16.4	1.420	5.77×10^{9}	9.76	-	-
Ir	8.89	0.0133	2.1×10^{3}	3.33	1.420	0.15
Os	-	-	-	-	0.968	0.10
Cu	7.94	0.0961	4.31×10^{3}	3.63	1.775	0.06
Cu-Ni	5.63	0.5585	1.1×10^{3}	3.045	11.297	0.37

APPENDIX B

EXPERIMENTAL DATA AND KINETIC RESULTS

TABLE B-1
Nickel-Silica Catalyst

Weight of the catalyst = 0.02585gm
Weight of reduced catalyst = 0.02158gm

B-1.1 Dependence of initial rate on hydrogen pressure.

$P_{C_3H_4}$=50±1 mm Hg

TEMP °C	P_{H_2} mmHg	r_o mm/min	TEMP °C	P_{H_2} mmHg	r_o mm/min
70	49.5	0.45	80	45.5	0.50
	71.0	0.65		50.0	0.55
	88.5	0.80		61.0	0.65
	96.5	0.90		71.5	0.75
	114.0	1.00		90.0	0.95
	145.0	1.30		110.0	1.20
91	50.0	0.70	100	42.0	0.75
	71.0	0.95		49.5	0.90
	80.0	1.15		70.0	1.20
	90.0	1.25		89.0	1.45
	131.0	1.80		111.0	1.95
				130.0	2.30
110.5	25.0	0.55	110.5	74.5	1.70
	39.0	0.90		100.0	1.20
	50.0	1.15		113.0	2.55
	63.0	1.45		142.0	3.20
				155.0	3.50

B-1.2. Dependence of initial rate on allene pressure.
P_{H_2} =50±1 mm

TEMP °C	$P_{C_3H_4}$ mm	r_o mm/min	TEMP °C	$P_{C_3H_4}$ mm	r_o mm/min
80	50.0 75.0 117.5	0.55 0.55 0.55	91	50.0 55.0 70.0 102.5 125.0	0.70 0.70 0.75 0.75 0.75
100	49.5 75.0 100.0 152.5	0.90 0.90 0.90 0.90	110.5	50.0 71.0 85.0 100.0 125.5	1.25 1.25 1.25 1.25 1.25

B-1.3 Summary of the results.

TEMP °C	$1/Tx10^3$ $°K^{-1}$	n	m	$kx10^2$ min^{-1}/gm	log k	E k cal/mole
70	2.9155	1.0	0.0	0.90	-2.1458	
80	2.8329	1.0	0.0	1.05	-1.9788	
91	2.7473	1.0	0.0	1.37	-1.8633	10.81
100	2.6810	1.0	0.0	1.75	-1.7570	
110.5	2.6076	1.0	0.0	2.30	-1.6289	

B-1.4. Product distribution during the course of reaction.
T=120°C $P_{C_3H_4}$=50±1 mm

P_{H_2}=50±1 mm

ΔP	C_3H_8	C_3H_6	C_3H_4	S
11.0	0.0	5.8	31.0	1.0
20.0	0.0	9.5	25.5	1.0
32.5	0.2	15.8	17.7	0.99
43.0	0.2	20.0	8.7	0.99
51.5	0.6	24.7	3.0	0.98
62.5	3.0	22.4	0.4	0.88

P_{H_2}=100±1 mm

ΔP	C_3H_8	C_3H_6	C_3H_4	S
3.0	0.0	3.3	36.9	1.0
7.5	0.0	6.0	34.0	1.0
10.0	0.4	7.0	32.0	0.95
20.0	0.6	11.3	25.7	0.95
30.0	1.5	16.5	18.0	0.91
41.5	3.0	25.0	12.0	0.89
60.0	7.9	23.3	3.9	0.75

B-1.5 Dependence of selectivity on initial reactant pressure.
$P_{C_3H_4}$=50±1 mm, ΔP=20 mm

T°C	P_{H_2}	C_3H_8	C_3H_6	C_3H_4	S
120	148.5	2.5	8.44	27.09	0.77
	128.5	1.75	10.44	27.88	0.83
	112.0	0.96	10.67	29.06	0.92
	101.5	0.77	9.50	25.75	0.94
	87.5	0.58	14.89	27.88	0.96
	62.5	0.20	12.00	25.92	0.98
101	44.5	0.40	9.11	28.11	0.96
	101.0	0.77	11.11	29.06	0.94
	157.0	2.40	9.55	29.25	29.25

T°	P_{H_2}	C_3H_8	C_3H_6	C_3H_4	S
110	51.0	0.31	8.22	25.91	0.97
	99.0	0.77	11.78	24.73	0.94
	149.0	2.50	10.67	25.13	0.81
91	51.5	0.20	10.67	29.05	0.98
	100.0	0.77	11.38	29.45	0.94
	151.0	1.0	11.78	28.00	0.92

P_{H_2}=50±1 mm, ΔP=20 mm

$P_{C_3H_4}$

120	88.0	0.2	6.4	59.5	0.97
	76.0	0.2	8.2	48.3	0.98
	61.0	0.1	9.1	36.5	0.99

$P_{C_3H_4}$

120	41.0	0.3	16.0	27.5	0.98
	80.0	0.2	9.7	51.5	0.98

TABLE B-2
Nickel-Copper-Silica Catalyst

Weight of the catalyst = 0.02500gm
Weight of the reduced catalyst = 0.02092gm

B-2.1. Dependence of initial rate on initial hydrogen pressure.
$P_{C_3H_4}$ =50±1 mm

TEMP °C	P_{H_2} mm	r_o mm/min	TEMP °C	P_{H_2} mm	r_o mm/min
97.0	50.0	0.55	109.5	50.5	0.75
	80.0	0.90		77.0	1.10
	109.5	1.15		101.5	1.45
	135.0	1.45		127.0	1.80
	148.0	1.65		146.0	2.05
121.0	50.0	0.90	131.0	50.5	1.10
	65.0	1.20		60.0	1.30
	75.0	1.35		65.0	1.50
	96.0	1.75		77.0	1.70
	110.0	2.20		94.0	2.15
142.5	47.5	1.25	142.5	99.0	2.50
	70.0	1.75		123.0	2.90
	99.0	2.25			

B-2.2. Dependence of initial rate on initial allene pressure.
P_{H_2} =50±1 mm

TEMP °C	$P_{C_3H_4}$ mm	r_o mm/min	TEMP °C	$P_{C_3H_4}$ mm	r_o mm/min
109.5	50.0	0.75	121.0	50.0	0.90
	75.0	0.75		72.0	0.90
	105.0	0.75		102.5	0.90
				130.0	0.90
131.0	50.0	1.10	142.5	50.0	1.25
	75.0	1.10		100.0	1.25
	100.5	1.10		150.5	1.25
	150.0	1.10		199.5	1.25

B-2.3. Summary of the results.

TEMP °C	$1/Tx10^3$ $°k^{-1}$	n	m	$kx10^2$ min^{-1}/gm	log k	E k cal/mole
97.0	2.7031	1.0	0.0	1.10	-1.9568	
109.5	2.6132	1.0	0.0	1.40	-1.8539	
121.0	2.5385	1.0	0.0	1.82	-1.7399	5.63
131.0	2.4372	1.0	0.0	2.22	-1.6378	
142.5	2.4074	1.0	0.0	2.55	-1.5935	

B-2.4. Product distribution during the course of reaction.
T=142°C, $P_{C_3H_4}$=50±1 mm

P_{H_2}=50±2 mm

ΔP mm	C_3H_8	C_3H_6	C_3H_4	S
5.0	0.0	3.4	37.0	1.0
10.0	0.0	6.0	30.0	1.0
15.0	0.0	8.5	27.0	1.0
20.0	0.0	10.8	24.0	1.0
41.0	0.0	21.5	9.0	1.0
2.0	0.0	2.5	40.0	1.0
10.0	0.2	8.5	35.0	0.98
16.0	0.2	11.5	29.1	0.98
20.0	0.2	16.0	26.7	0.99

P_{H_2}=150±1 mm

ΔP	C_3H_8	C_3H_6	C_3H_4	S
5.0	0.4	4.9	38.6	0.93
10.0	0.8	8.0	35.4	0.91
20.0	1.9	14.2	28.3	0.88
30.0	2.7	21.1	18.9	0.88
41.0	4.2	25.6	11.0	0.86
51.0	5.8	26.9	9.5	0.82
28.0	0.6	21.0	22.0	0.97
35.0	1.1	24.0	16.5	0.95
43.0	1.9	25.8	8.7	0.93
54.5	3.6	29.3	4.7	0.89

B-2.5. Dependence of selectivity on initial reactant pressure.
$P_{C_3H_4}$=50±1 mm, ΔP=20 mm

TEMP °C	P_{H_2} mm	S	TEMP °C	P_{H_2} mm	S	TEMP °C	P_{H_2} mm	S
97.0	50.0	1.0	109.5	50.0	1.0	121.0	50.0	1.0
	150.0	0.84		100.0	0.96		100.0	0.96
				150.0	0.86		150.0	0.87
131.0	50.0	1.0	142.0	50.0	1.0	142.0	150.0	0.88
	100.0	0.98		100.0	0.99			
	150.0	0.90		133.0	0.97			

P_{H_2}=50±1 mm

TEMP °C	$P_{C_3H_4}$ mm	S	TEMP °C	$P_{C_3H_4}$	S	TEMP °C	$P_{C_3H_4}$ mm	S
142.0	50.0	1.0	142.0	130.5	1.0	142.0	178.5	1.0
	96.0	1.0		150.0	1.0			

TABLE B-3
Copper-Silica Catalyst

Weight of the catalyst = 0.11271gm
Weight of the reduced catalyst = 0.09886gm

B-3.1. Dependence of initial rate on initial reactant pressure.
$P_{C_3H_4}$ =50±1 mm

TEMP °C	P_{H_2} mm	r_o mm/min	TEMP °C	P_{H_2} mm	r_o mm/min
98.0	51.0	0.45	115.0	48.5	0.75
	69.0	0.60		77.5	1.25
	93.0	0.85		100.5	1.65
	130.0	1.15		126.0	2.00
	166.0	1.50		166.0	2.65
125.0	51.5	1.15	135.0	50.5	1.35
	57.0	1.25		76.0	1.90
	98.0	2.15		93.0	2.40
	186.0	4.05		111.0	2.75
	140.0	3.05		145.0	3.60
145.0	30.0	1.10	145.0	91.0	2.90
	56.0	1.80		120.0	3.80
	65.0	2.00			

P_{H_2} =50±1 mm

TEMP °C	$P_{C_3H_4}$ mm	r_o mm/min	TEMP °C	$P_{C_3H_4}$ mm	r_o mm/min
115.0	50.0	0.75	125.0	50.5	1.15
	101.5	0.75		98.5	1.16
	150.0	0.75		149.5	1.15
135.0	50.0	1.35	145.0	48.0	1.70
	99.5	1.45		88.5	1.70
	150.0	1.35		126.5	1.70

B-3.2. Summary of the results.

TEMP °C	$1/Tx10^3$ $°K^{-1}$	n	m	$kx10^2$ min^{-1}/gm	log k	E k cal/mole
98	2.695	1.0		0.9	-2.046	
115	2.577	1.0	0.0	1.30	-1.886	
125	2.513	1.0	0.0	2.15	-1.668	7.94
135	2.451	1.0	0.0	2.50	-1.612	
145	2.398	1.0	0.0	3.20	-1.497	

B-3.3. Product distribution during the course of reaction.
T=145°C, $P_{C_3H_4}$=50±1 mm

P_{H_2}=50±1 mm

ΔP	C_3H_8	C_3H_6	C_3H_4	S
10.0	0.0	5.0	32.5	1.0
20.0	0.0	9.0	26.0	1.0
30.0	0.0	15.0	17.0	1.0
40.0	0.0	21.5	6.0	1.0

P_{H_2}=100±1 mm

ΔP	C_3H_8	C_3H_6	C_3H_4	S
10.0	0.0	5.0	35.0	1.0
20.0	0.0	12.0	29.0	1.0
39.5	0.0	24.0	12.5	1.0
55.0	0.0	35.0	2.0	1.0

TABLE B-4
Platinum-Silica Catalyst

Weight of the catalyst = 0.02580gm
Weight of the reduced catalyst = 0.02488gm

B-4.1. Dependence of initial rate on initial pressure of hydrogen.
$P_{C_3H_4}$ = 50±1 mm

TEMP °C	P_{H_2}	r_o	P_{H_2}	r_o	P_{H_2}	r_o
74.5	35.5 50.0	0.25 0.35	66.5 84.5	0.42 0.52	107.0 136.0	0.65 0.95
84.0	18.0 36.0 50.0	0.22 0.42 0.57	70.0 78.5 102.0	0.75 0.85 1.25	118.0 143.0	1.82 2.60
94.0	9.5 29.5 36.5 44.0	0.25 0.70 0.85 1.00	50.0 53.0 62.0 70.0	1.15 1.25 1.50 2.00	78.0 99.0 119.0	2.40 3.60 4.70
100.0	5.0 16.0 25.0 31.5	0.20 0.60 0.95 1.15	41.0 48.0 51.5 61.5	1.60 1.75 2.15 3.00	69.0 80.5	3.70 4.70
105.0	10.0 14.5 22.0 26.5	0.50 0.65 1.00 1.20	38.0 42.0 51.0 57.0	1.70 2.00 2.60 3.25	61.5 65.0 74.5	3.75 4.15 5.15

B-4.2. Dependence of initial rate on initial pressure of allene.
P_{H_2} =50±1 mm

TEMP °C	$P_{C_3H_4}$ mm	r_o mm/min	TEMP °C	$P_{C_3H_4}$ mm	r_o mm/min
84.0	50.0	0.57	94.0	44.0	1.20
	88.0	0.55		50.0	1.15
	133.5	0.57		74.5	1.15
	194.5	0.57		100.0	1.15
	41.0	0.57		200.0	1.15
100.0	45.0	2.20	105.0	43.5	2.70
	50.5	2.15		50.5	2.60
	174.5	2.15		198.0	2.60
	100.5	2.15		68.5	2.60
	136.5	2.15		109.5	2.60

B-4.3. Summary of the results.

TEMP °C	$1/Tx10^3$ $°K^{-1}$	m	n	$kx10^2$	$\log_k$	E k cal/mole
74.5	2.8776	1.0	0.0	0.675	-2.1703	
84.0	2.8011	1.0	0.0	1.1	-1.9582	16.4
		2.0		3.3	-1.4812	
94.0	2.7247	1.0	0.0	2.35	-1.6286	
		2.0		5.45	-1.2634	
100.0	2.6809	1.0	0.0	3.7	-1.4315	
		2.0		8.65	-1.0628	
105.0	2.6455	1.0	0.0	4.6	-1.3370	
		2.0		10.65	-0.9725	

B-4.4. Product distribution during the course of reaction.
T=100°C; $P_{C_3H_6}$=50±1 mm

P_{H_2}=25±1 mm

ΔP	C_3H_8	C_3H_6	C_3H_4	S
2.0	0.5	2.0	40.0	0.85
7.0	0.6	4.0	37.0	0.84
12.5	1.0	6.5	34.0	0.83
17.0	1.5	9.0	31.0	0.83
21.5	2.0	10.6	28.0	0.84

P_{H_2}=75±1 mm

ΔP	C_3H_8	C_3H_6	C_3H_4	S
10.0	2.0	8.0	31.5	0.78
20.0	3.5	10.5	27.0	0.76
30.0	5.5	15.5	20.0	0.73
40.0	7.5	19.0	14.0	0.72
50.0	11.0	20.0	7.5	0.64
57.5	15.5	17.0	6.5	0.52
75.0	30.0	10.0	5.0	0.25

P_{H_2}=50±1 mm

2.5	0.5	2.0	41.5	0.79
5.0	1.0	4.0	38.5	0.79
12.0	1.5	5.3	36.0	0.77
15.5	2.0	7.8	33.0	0.76
20.0	2.5	9.0	30.5	0.77
30.0	4.5	14.0	24.0	0.75
45.5	6.7	21.0	11.0	0.76

P_{H_2}=100±1 mm

7.0	10.0	4.0	6.0	0.30
10.5	12.5	4.0	31.5	0.24
20.0	16.3	3.2	26.0	0.14
30.0	18.7	3.0	21.0	0.14
50.0	25.0	2.0	15.0	0.08
60.0	29.0	1.7	11.0	0.06

B-4.5. Dependence of selectivity on initial reactant pressure.
$P_{C_3H_4}$=50±1 mm, ΔP=20 mm

T	H_2	S	T	H_2	S	T	H_2	S
85	25.0	0.76	95	25.0	0.81	100	25.0	0.83
	50.0	0.72		50.0	0.78		50.0	0.79
	75.0	0.69		75.0	0.73		70.0	0.74
	100.5	0.66		101.0	0.70		75.0	0.75
							91.0	0.76
							101.0	0.15
105	25.0	0.85	75	25.0	0.71			
	50.0	0.80		50.0	0.65			
	59.0	0.55		75.5	0.62			
	75.0	0.24		99.5	0.59			
	98.0	0.01						

P_{H_2}=50±1 mm

T	C_3H_4	S	T	C_3H_4	S
100	20.0	0.67	300	60.0	0.80
	30.0	0.75		75.0	0.80
	40.0	0.77		120.0	0.81
	50.0	0.79			

TABLE B-5
Palladium Silica Catalyst

Weight of the catalyst = 0.00025gm
Weight of the reduced catalyst = 0.00017gm

B-5.1. Dependence of initial rate on initial hydrogen pressure.
$P_{C_3H_4}$=50±1 mm

TEMP °C	H_2 mm	r_o mm/min	H_2 mm	r_o mm/min	H_2 mm	r_o mm/min
0.0	53.0	0.60	98.0	1.10	115.0	1.35
	80.0	0.90	153.0	1.75		
10.0	50.0	0.75	123.0	2.20	102.0	1.60
	84.0	1.30	164.0	3.30		
	69.5	1.05	140.0	2.60		
20.0	27.5	0.55	64.5	1.35	120.0	3.35
	50.0	1.00	90.0	2.00	140.0	4.30
	57.0	1.15	106.0	2.70		
30.0	22.5	0.65	50.0	1.40	94.0	4.20
	35.0	1.00	71.0	2.50	110.0	5.40
	41.5	1.15	80.0	3.20	118.0	6.00

B-5.2. Dependence of initial rate on initial allene pressure.
P_{H_2}=50±1 mm

TEMP	C_3H_4	r_o	T	C_3H_4	r_o	T	C_3H_4	r_o
10.0	65.0	0.80	20.0	70.0	1.00	30.0	76.0	1.40
	90.0	0.75		100.0	1.05		100.0	1.40
	121.5	0.75		125.0	1.00		155.0	1.40
	145.5	0.75		150.0	1.00			

B-5.3. Summary of the results.

TEMP °C	$1/Tx10^3$ $°K^{-1}$	m	n	k min^{-1}	$\log_k$	E k cal/mole
0	0.6630	1.0	0.0	1.15	-1.9388	
10	3.5335	1.0	0.0	1.575	-1.8162	7.21
		1.8		2.8	-1.5524	&
20	3.4129	1.0	0.0	2.0	-1.6985	3.4
		1.8		4.6	-1.3368	
30	3.3003	1.0	0.0	2.5	-1.6016	
		1.8		7.4	-1.1304	

B-5.4. Product distribution during the course of reaction.
T=40°C, $P_{C_3H_4}$=50±1 mm

P_{H_2}=50±1 mm H_2=100±1 mm

ΔP mm	C_3H_8 mm	C_3H_6 mm	C_3H_4 mm	S	ΔP mm	C_3H_8 mm	C_3H_6 mm	C_3H_4 mm	S
2.5	0.3	2.2	48.5	0.87	4.0	1.5	2.4	44.5	0.65
7.0	0.6	4.8	44.0	0.88	12.0	2.9	5.6	38.0	0.66
20.0	2.2	13.4	30.7	0.86	20.0	4.8	8.4	34.5	0.64
27.0	3.0	16.8	26.2	0.85	30.0	8.4	12.0	26.0	0.59
35.5	3.7	22.4	19.3	0.86	38.0	11.2	14.5	22.7	0.56
					47.0	14.8	14.5	17.0	0.50
					58.5	20.1	12.0	11.0	0.37

B-5.5. Effect of initial reactant pressure on selectivity.
$P_{C_3H_4}$=50±1 mm, ΔP=20 mm

TEMP °C	H_2 mm	S	H_2 mm	S	H_2 mm	S
40	52.0	0.86	79.0	0.74	121.0	0.57
	68.0	0.79	102.0	0.64	191.0	0.41
30	50.0	0.87	160.0	0.55		
	101.5	0.75	225.0	0.50		
20	54.0	0.88	157.0	0.71		
	104.0	0.79	194.0	0.66		

P_{H_2}=50±1 mm, ΔP=20 mm

TEMP °C	C_3H_4 mm	S	TEMP °C	C_3H_4 mm	S
40	50.0	0.86	20	146.0	0.98
	91.5	0.93		94.0	0.96
	152.0	0.96			

TABLE B-6
Ruthenium-Silica Catalyst

Weight of the catalyst =0.10900gm
Weight of the reduced catalyst = 0.09706gm

B-6.1. Dependence of initial rate on initial hydrogen pressure.
$P_{C_3H_4}$ =50±1 mm

TEMP °C	H_2 mm	r_o mm/min	H_2 mm	r_o mm/min	H_2 mm	r_o mm/min
65.0	49.5	0.60	100.0	1.20	150.5	2.25
	65.5	0.80	120.0	1.50	165.0	2.60
	80.0	0.95	135.5	1.90		
53.0	75.5	0.75	130.5	1.30	160.0	1.60
	100.0	1.00	144.5	1.42		
75.0	40.0	0.60	70.0	1.05	120.5	2.25
	50.0	0.75	85.0	1.25	140.0	2.90
	62.0	0.90	105.0	1.75	160.0	3.55
85.0	35.0	0.60	61.5	1.05	114.5	2.80
	45.0	0.75	85.0	1.65	130.0	3.45
	50.0	0.85	100.0	2.25	150.0	4.15
100.0	21.0	0.40	50.0	1.00	89.5	2.70
	30.0	0.57	60.5	1.25	115.5	3.70
	40.0	0.75	69.5	1.70	125.5	4.45

B-6.2. Dependence of initial rate on allene pressure.
P_{H_2} =50±1 mm

TEMP °C	C_3H_4 mm	r_o mm/min	TEMP °C	C_3H_4 mm	r_o mm/min	TEMP °C	C_3H_4 mm	r_o mm/min
75.0	50.0	0.75	85.0	40.5	0.85	100.0	38.5	1.00
	59.5	0.75		50.5	0.85		50.5	1.00
	88.5	0.75		99.5	0.87		100.5	0.98
	129.5	0.75		160.5	0.85		160.5	0.98
	153.5	0.75					203.5	1.00

B-6.3. Summary of the results.

TEMP °C	$1/Tx10^3$ $°K^{-1}$	m	n	k	$\log_k$	E k cal/mole
53.0	3.0488	1.0	0.0	1.0	-1.9996	
65.0	2.9585	1.0	0.0	1.22	-1.9132	
		1.5		2.44	-1.6125	
75.0	2.8735	1.0	0.0	1.475	-1.8309	
		1.5	0.0	3.136	-1.5033	5.64
85.0	2.7932	1.0	0.0	1.70	-1.7692	&
		1.5		3.84	-1.4153	4.0
100.0	2.6809	1.0	0.0	1.875	-1.7267	
		1.5		5.037	-1.2976	

B-6.4. Product distribution during the course of reaction.
T=100°C, $P_{C_3H_4}$=50±1 mm

H_2	ΔP	C_3H_8	C_3H_6	C_3H_4	S	ΔP	C_3H_8	C_3H_6	C_3H_4	S
50	5.0	0.6	3.0	37.1	0.82	30.0	3.2	15.1	20.1	0.82
±1	14.5	1.9	7.8	30.7	0.80	46.5	5.0	22.6	7.6	0.82
	20.0	2.2	9.9	26.9	0.81					
75	10.0	1.0	5.0	34.9	0.84	30.0	3.7	15.3	20.5	0.81
±1	20.0	2.7	11.2	25.8	0.81	40.0	4.4	19.4	14.4	0.82
100	3.5	0.6	2.8	36.4	0.81	30.0	3.5	15.3	19.7	0.81
±1	10.5	1.3	5.8	33.0	0.82	40.0	4.3	19.4	13.5	0.82
	20.0	1.9	9.5	27.6	0.81	52.0	6.0	25.2	5.7	0.81

B-6.5. Effect of reactant pressure on selectivity.
$P_{C_3H_4}$=50±1 mm, ΔP=20 mm

TEMP °C	H_2 mm	S	H_2 mm	S	H_2 mm	S
100.0	50.0	0.81	100.0	0.82	160.0	0.72
	76.0	0.80	108.0	0.82		
	86.0	0.84	130.0	0.81		
85.0	56.0	0.82	123.5	0.81		
	103.0	0.79	149.0	0.81		
75.0	48.5	0.80	100.5	0.81		
	50.0	0.81	157.0	0.82		

P_{H_2}=50±1 mm, ΔP=20 mm

TEMP °C	C_3H_4	S	C_3H_4	S	C_3H_4	S
100.0	50.0	0.81	100.0	0.81	151.0	0.81
	75.0	0.80	120.0	0.81	156.0	0.82

TABLE B-7
Iridium Catalyst

Weight of the catalyst = 0.03100gm
Weight of the reduced catalyst = 0.02913gm

B-7.1. Dependence of initial rate on initial hydrogen pressure.
$P_{C_3H_4}$ =50±1 mm

TEMP °C	H_2 mm	r_o mm/min	H_2 mm	r_o mm/min	H_2 mm	r_o mm/min
205.0	110.5	0.60	176.0	1.10	248.0	1.50
	153.0	0.95	200.0	1.20		
193.0	74.5	0.30	180.0	0.85	300.0	1.40
	124.5	0.55	232.0	1.10		
220.0	100.0	0.80	180.5	1.45	234.0	2.00
	130.0	1.05	206.0	1.60		
230.0	120.0	1.15	195.5	1.95	272.5	2.70
	160.0	1.60	250.0	2.45		
260.0	100.0	1.55	198.5	3.20	300.0	4.85
	140.0	2.25	250.5	4.00		

B-7.2. Dependence of initial rate on allene pressure.
P_{H_2} =200±2 mm

TEMP °C	C_3H_4 mm	r_o mm/min	TEMP °C	C_3H_4 mm	r_o mm/min	TEMP °C	C_3H_4 mm	r_o mm/min
220.0	200.0	1.70	230.0	50.0	1.95	260.0	49.0	3.10
	105.5	1.65		100.5	1.95		115.0	3.10
	50.5	1.70		150.5	2.00		142.5	3.05
	150.5	1.65		215.0	1.95		199.0	3.10

B-7.3. Summary of the results.

TEMP °C	$1/Tx10^3$ °K-1	m	n	$kx10^2$ min^{-1}/min	$\log_k$	E k cal/mole
193.0	2.1459	1.0	0.0	0.475	-2.3227	
205.0	2.0920	1.0	0.0	0.600	-2.2213	
220.0	2.0283	1.0	0.0	0.787	-2.1035	8.89
230.0	1.9880	1.0	0.0	1.100	-1.9581	
260.0	1.8761	1.0	0.0	1.660	-1.7794	

B-7.4. Product distribution during the course of reaction.
T=260°C, $P_{C_3H_4}$=50±1 mm

H_2	ΔP	C_3H_8	C_3H_6	C_3H_4	S	ΔP	C_3H_8	C_3H_6	C_3H_4	S
200	3.5	0.5	3.0	37.5	0.86	34.5	2.6	17.1	14.0	0.87
±1	11.5	1.1	7.6	26.1	0.87	46.5	3.7	22.7	6.5	0.86
	20.0	1.1	9.0	25.8	0.89					
250	4.0	0.2	1.5	28.8	0.88	30.0	2.2	13.6	16.7	0.86
±1	20.0	1.6	20.0	21.0	0.86	44.0	3.7	19.8	6.5	0.84
300	10.0	2.0	4.5	28.0	0.69	50.0	7.7	15.9	7.6	0.67
±1	20.0	3.0	6.5	22.5	0.68	74.5	20.2	9.5	3.0	0.32
	30.0	3.5	12.0	18.0	0.77	84.5	24.5	4.1	2.6	0.14

B-7.5. Effect of reactant pressures on selectivity.
$P_{C_3H_4}$=50±1 mm, ΔP=20 mm

TEMP °C	H_2 mm	S	TEMP °C	H_2 mm	S	TEMP °C	H_2 mm	S
230.0	154.5	0.88	245.0	156.0	0.88	260.0	100.0	0.90
	199.0	0.86		200.0	0.87		150.0	0.90
	232.0	0.85		244.0	0.84		200.0	0.89
							250.0	0.86
							300.0	0.68

P_{H_2}=200±1 mm, ΔP=20 mm

TEMP °C	C_3H_4 mm	S	C_3H_4 mm	S	C_3H_4 mm	S
260.0	53.0	0.89	105.0	0.90	271.0	0.88
	62.0	0.89	150.0	0.90		
	98.0	0.90	204.5	0.90		

TABLE B-8
Rhodium Catalyst

Weight of the catalyst = 0.02509gm
Weight of the reduced catalyst = 0.02341gm

B-8.1. Dependence of initial rate on initial hydrogen pressure.
$P_{C_3H_4}$ =50±1 mm

TEMP °C	H_2 mm	r_o mm/min	H_2 mm	r_o mm/min	H_2 mm	r_o mm/min
20.0	55.5	0.40	98.5	0.70	143.0	1.02
	65.0	0.50	104.0	0.74		
30.0	49.0	0.54	102.0	1.10	153.0	1.65
	78.0	0.85	128.0	1.35		
40.0	51.0	0.80	92.0	0.96	116.5	1.85
	68.0	1.10	96.0	1.02		
50.0	50.5	1.17	79.5	1.80	100.0	2.27
	60.0	1.38	97.0	2.20	124.5	2.75

B-8.2. Dependence of initial rate on initial allene pressure.
P_{H_2} =50±1 mm

TEMP °C	C_3H_4 mm	r_o mm/min	C_3H_4 mm	r_o mm/min	C_3H_4 mm	r_o mm/min
30.0	50.0	0.54	103.5	0.54	182.5	0.55
	66.5	0.55	149.0	0.54		
40.0	50.5	0.80	127.5	0.80	192.5	0.80
	99.5	0.80	150.5	0.80		
50.0	50.0	1.17	98.0	1.17	205.0	1.17
	79.5	1.16	125.0	1.17		

B-8.3. Summary of the results.

TEMP °C	$1/Tx10^3$ $°K^{-1}$	m	n	$kx10^2$ min^{-1}	$\log_k$	E k cal/mole
20.0	3.4129	1.0	0.0	0.71	-2.1543	7.73
30.0	3.3003	1.0	0.0	1.07	-1.9701	
40.0	3.1948	1.0	0.0	1.58	-1.8008	
50.0	3.0959	1.0	0.0	2.27	-1.6350	

B-8.4. Product distribution during the course of reaction.
T=50°C, $P_{C_3H_4}$=50±1 mm

P_{H_2}=50±1 mm

ΔP mm	C_3H_8 mm	C_3H_6 mm	C_3H_4 mm	S
3.5	0.3	3.3	42.8	0.91
10.0	0.6	7.6	36.4	0.92
20.0	1.3	14.4	29.5	0.92
30.0	1.8	21.6	19.3	0.92
44.0	2.7	30.4	6.8	0.92

P_{H_2}=100±.mm

ΔP	C_3H_8 mm	C_3H_6 mm	C_3H_4 mm	S
2.0	0.2	2.0	43.9	0.93
7.0	0.6	5.6	36.6	0.91
10.0	0.8	9.0	37.5	0.92
20.0	1.3	13.8	28.0	0.91
30.0	2.2	23.3	18.2	0.91
40.0	2.5	27.6	10.2	0.91
51.0	4.3	34.6	3.4	0.89

B-8.5. Effect of initial reactant pressure on selectivity.
$P_{C_3H_4}$=50±1 mm

TEMP °C	H_2	S	TEMP °C	H_2	S	TEMP °C	H_2	S
30.0	50.0	0.92	40.0	52.5	0.92	50.0	47.5	0.94
	63.5	0.88		101.0	0.91		53.0	0.94
	103.5	0.88		148.0	0.91		73.0	0.94
	148.0	0.88					100.0	0.92
							117.0	0.94

P_{H_2}=50±1 mm

TEMP °C	C_3H_4	S	TEMP °C	C_3H_4	S	TEMP °C	C_3H_4	S
30.0	50.0	0.92	40.0	50.0	0.92	50.0	50.0	0.94
	110.0	0.94		101.5	0.94		100.0	0.94
	157.0	0.94		152.0	0.96		166.0	0.94

TABLE B-9
Cobalt Catalyst

Weight of the catalyst = 0.59670gm
Weight of the reduced catalyst = 0.41259gm

B-9.1. Dependence of initial rate on initial hydrogen pressure.
$P_{C_3H_4}$ = 50±1 mm

TEMP °C	H_2 mm	r_o mm/min	H_2 mm	r_o mm/min	H_2 mm	r_o mm/min
50.0	50.5	0.67	60.0	0.75	114.0	1.57
	150.0	2.00	204.5	2.72		
55.0	50.0	1.05	70.0	1.40	90.0	1.90
	105.5	2.10	145.0	2.85		
60.0	50.0	1.30	52.5	1.86	77.5	2.00
	105.0	2.75	153.0	3.95	201.0	5.20
70.0	40.0	1.45	50.5	1.85	53.0	1.95
	67.5	2.45	84.0	3.10		
80.0	37.0	1.50	50.0	2.05	52.5	2.15
	58.5	2.40	105.0	4.30	129.0	5.25

B-9.2. Dependence of initial rate on initial allene pressure.
P_{H_2} =50±1 mm

TEMP °C	C_3H_4 mm	r_o mm/min	C_3H_4 mm	r_o mm/min	C_3H_4 mm	r_o mm/min
50.0	75.0	0.67	115.5	0.67	130.5	0.67
	150.0	0.67				
60.0	68.5	1.35	87.5	1.30	113.5	1.35
	142.5	1.35	171.0	1.35		
80.0	77.0	1.50	99.5	1.50	129.5	1.50
	184.0	1.50				

B-9.3. Summary of the results.

TEMP °C	$1/Tx10^3$ $°K^{-1}$	m	n	$kx10^2$ min^{-1}	$\log_k$	E k cal/mole
50.0	3.0958	1.0	0.0	1.325	-1.8772	8.64
55.0	3.0022	1.0	0.0	2.000	-1.6985	
60.0	2.9410	1.0	0.0	2.600	-1.5846	
70.0	2.8740	1.0	0.0	3.650	-1.4373	
80.0	2.8351	1.0	0.0	4.100	-1.3868	

B-9.4. Product distribution during the course of reaction.
T=80°C, $P_{C_3H_4}$=50±1 mm

P_{H_2}=50±1 mm

ΔP	C_3H_8 mm	C_3H_6 mm	C_3H_4 mm	S
3.0	0.2	5.2	39.2	0.96
9.0	0.3	6.8	35.1	0.95
20.0	0.7	15.7	25.4	0.96
30.0	0.8	20.6	19.0	0.96
39.0	1.0	26.8	12.3	0.96
55.0	1.4	35.0	1.1	0.96

P_{H_2}=100±1 mm

ΔP	C_3H_8 mm	C_3H_6 mm	C_3H_4 mm	S
5.0	0.3	6.4	38.4	0.95
10.0	0.5	9.7	34.0	0.95
20.0	1.0	18.6	24.6	0.95
30.0	1.2	26.2	16.8	0.95
40.0	1.6	34.2	8.2	0.95
49.0	3.9	36.2	3.4	0.90

B-9.5. Effect of initial reactant pressure on selectivity.
$P_{C_3H_4}$=50±1 mm, ΔP=20 mm

TEMP °C	H_2 mm	S	H_2 mm	S	H_2 mm	S
50.0	49.0	0.95	101.0	0.95	151.0	0.96
60.0	50.0	0.96	100.0	0.96	149.0	0.95
70.0	52.0	0.96	100.0	0.96	145.0	0.96
80.0	50.0	0.96	74.0	0.96	102.0	0.95
	155.5	0.94				

P_{H_2}=50±1 mm, ΔP=20 mm

TEMP °C	$P_{C_3H_4}$(A) mm	C_3H_8 mm	C_3H_6 mm	C_3H_4(A) mm	C_3H_4(M) mm	S
80.0	77.5	0.68	13.61	50.40	0.25	0.94
	102.5	0.68	12.78	72.05	0.50	0.92
	146.0	0.68	10.72	110.50	1.00	0.86
	120.0	0.68	10.31	106.00	1.00	0.86

APPENDIX C

RESULTS OF ISOMERIZATION REACTION

TABLE C-1

C-1.1. Isomerization equilibrium on iron catalyst.
Weight of the catalyst = 0.67585gm

P_{allene}=50±2 mm

TEMP °C	t min	A %	M %	TEMP °C	t min	A %	M %
165	1	96.0	4.0	200	0.5	88.4	11.6
	2	94.0	6.0		3	64.7	35.5
	3	92.2	7.8		10	39.0	61.0
	5	86.1	13.9		15	35.5	64.7
	10	76.8	23.2		20	30.2	69.8
	15	70.7	29.3		30	26.2	73.8
	30	57.3	42.7		120	16.5	83.5
	240	17.0	83.0		240	16.4	83.6
	360	16.5	83.5		360	16.2	83.8
	480	16.0	84.0		480	16.1	83.9
	600	15.7	84.3		600	16.1	83.9
	720	15.7	84.3		720	16.1	83.9
175	0.5	91.4	2.6	185	0.5	94.4	5.6
	2	90.7	9.3		3	79.5	20.5
	6	78.0	22.0		10	57.8	42.2
	10	70.8	29.2		15	50.0	50.0
	20	55.5	44.5		20	43.2	56.8
	30	66.4	33.3		30	33.3	66.7
	480	16.0	84.0		360	16.5	83.5
	600	16.0	84.0		480	16.0	84.0
	720	16.0	84.0		600	16.0	84.0
					720	16.0	84.0

A = allene, M = methylacetylene

C-1.2. Distribution of isomers with methylacetylene as the initial substance.
P_M=50±2 mm

TEMP °C	t min	A %	M %	TEMP °C	A %	M %
175	720	15.3	84.7	200	16.0	84.0
	1440	15.8	84.2		16.0	84.0
	2160	15.8	84.2		16.0	84.0

TABLE C-2

C-2.1. Kinetics of isomerization on iron catalyst.
Weight of reduced catalyst = 0.35688gm.

T=115°C

P_A mm	t min	A mm	M mm	A %	M %	r_i	r_{ave}	r_{graph}
50	5	42.4	1.2	97.2	2.8	0.25	0.24	0.25
±2	10	44.7	1.7	95.4	4.6	0.22		
	15	42.5	3.8	91.6	8.4	0.23		
	20	39.4	5.0	88.1	11.9	0.22		

T=135°C

P_A	t	A	M	A+M	%A	%M	r	r_{ave}	r_{graph}
50	0.5	40.9	0.3	41.2	99.2	0.8	0.62		
±2	3	40.1	2.2	42.3	94.9	5.1	0.75	0.69	0.71
	5	42.0	3.4	45.4	92.5	7.5	0.72		
	7.5	38.6	4.7	43.3	89.1	10.9	0.67		
	10	39.5	5.2	45.7	86.4	13.6	0.68		
75	2	62.1	1.6	63.7	97.7	2.3	0.74		
±2	4	60.5	3.0	63.5	95.2	4.8	0.78		
	6	58.3	4.6	62.9	92.6	7.4	0.81	0.77	0.80
	8	58.1	6.0	64.1	90.8	9.2	0.78		
	9	57.2	6.5	63.7	89.8	10.2	0.71		
	15	54.0	10.0	64.0	84.4	15.6	0.74		
100	2	80.4	2.1	82.5	97.5	2.5	1.06		
±2	4	77.2	4.0	81.2	95.0	5.0	1.04		
	6	77.2	5.6	82.8	93.3	6.7	0.97	0.99	0.98
	8	76.5	6.8	83.3	91.8	8.2	0.88		
	10	74.9	7.5	82.4	91.0	9.0	0.79*		
125	15	92.9	11.2	104.1	89.3	10.7	0.80*		
±2	10	95.2	9.3	104.5	91.1	8.9	0.98		
	0.25	105.7	0.6	106.3	99.4	0.6	2.49*	1.13	1.15
	2.5	102.0	3.1	105.1	97.0	3.0	1.28		
	4	97.4	4.7	102.1	95.4	4.6	1.20		
	6	97.4	6.2	103.6			1.07		

T=145°C

50	0.5	42.8	0.3	43.1	99.3	0.7	1.24		
±2	2	40.6	2.2	42.8	44.4	5.6	1.12	1.13	1.20
	4	38.8	3.6	42.4	90.3	9.7	1.09		
	5	38.6	5.0	43.6	88.6	11.4	1.07		

T=155°C

P_A mm	t min	A mm	M mm	A+M mm	%A	%M	r	r_{ave}	r_{graph}
50 ±2	0.25	40.5	0.4	40.9	98.9	1.1	1.73*	1.39	1.45
	2	39.0	3.1	42.1	92.8	7.2	1.57		
	4	36.3	5.2	41.5	87.5	12.5	1.41		
	6.5	34.1	7.4	41.5	82.1	17.9	1.29		
	8	33.1	8.7	41.8	79.2	20.8	1.25		
75 ±2	6.2	59.7	3.3	63.0	94.7	5.3	1.73	1.76	1.80
	6.4	55.7	6.8	62.5	89.1	10.9	1.83		
	6	53.2	9.6	62.8	84.7	15.3	1.77		
	8	50.7	12.2	62.9	80.7	19.2	1.73		
100 ±2	0.75	80.4	1.9	82.3	97.7	2.3	2.51	2.43	2.55
	2	78.0	5.0	83.0	94.0	6.0	2.56		
	4.5	75.4	9.3	84.7	89.0	11.0	2.21		
125 ±2	6	89.9	15.4	105.3	85.4	14.6	2.82	2.76	3.05
	4	94.2	10.3	104.5	90.1	9.9	2.74		
	2	99.0	5.3	104.3	95.0	5.0	2.72		

C-2.2. Summary of the results.

TEMP °C	$1/Tx10^3$ $°K^{-1}$	r*	log r/P	E k cal/mole
115	2.5773	0.24	-2.3177	11.8
135	2.4510	0.69	-1.8626	
145	2.3923	1.13	-1.6460	
155	2.3364	1.39	-1.4590	

Log_k at $1/T=2.5x10^{-3}$ or at 127°C = -2.050

$k = 8.912x10^{-3} min^{-1}$

$= .0250 min^{-1}/gm$

TABLE C-3 .1
Allene isomerization on cobalt catalyst.
Weight of the reduced catalyst = 0.89513.

T=80°C P_A=50±2 mm

P_A mm	t min	A mm	A+M mm	% A	% M	r mm/min	r_{ave} mm/min	r_G mm/min
50.5	2.0	45.17	0.31	99.31	0.69	0.17		
50.5	5.5	44.73	0.75	98.35	1.65	0.15	0.144	1.25
50.0	10.5	44.05	1.26	97.22	2.78	0.13		
52.0	15.0	45.17	1.90	95.96	4.04	0.14		
50.0	34.0	40.37	3.44	92.00	8.00	0.13		

T=90 °C

P_A mm	t min	A mm	A+M mm	% A	% M	r mm/min	r_{ave} mm/min	r_G mm/min
51.0	2.0	45.17	0.63	98.6	1.4	0.36		
49.0	5.0	42.93	1.00	97.7	2.3	0.23		0.20
51.5	10.0	44.07	1.88	95.9	4.1	0.22		
51.0	20.0	42.19	3.57	92.2	7.8	0.21	0.246	
50.0	30.0	38.52	5.00	88.5	11.5	0.21		
100.0	2.0	90.50	1.15	98.75	2.3	0.63 *		
99.0	5.0	88.22	2.30	97.46	2.54	0.51		
99.0	10.0	87.22	3.13	96.54	3.46	0.33	0.375	0.35
99.0	20.0	81.20	5.63	93.51	6.49	0.33		
99.0	30.0	78.20	8.13	90.58	9.42	0.33		
124.5	5.0	103.76	2.19	97.93	2.07	0.52		
124.5	10.0	102.26	3.75	96.56	3.44	0.44	0.453	0.45
124.5	30.0	98.00	6.28	93.93	6.02	0.40		

T=100 °C

P_A mm	t min	A mm	A+M mm	% A	% M	r mm/min	r_{ave} mm/min	r_G mm/min
49.5	1.0	43.8	0.3	43.20	0.7	0.35		
51.0	3.0	44.44	0.94	45.38	2.07	0.36		
49.5	5.0	43.89	1.56	45.45	3.43	0.35	0.343	0.35
49.5	10.0	40.37	2.81	43.18	6.51	0.34		
50.0	20.0	38.15	4.69	42.84	10.95	0.30		
75.0	2.5	65.92	1.25	67.17	1.86	0.56		
75.0	5.0	66.30	2.50	68.80	3.63	0.56		
74.5	10.0	62.20	3.75	65.95	5.69	0.44	0.500	0.43
74.5	21.0	57.0	7.26	64.26	11.30	0.44		
97.0	3.0	86.47	1.75	88.22	1.99	0.65		
98.5	5.0	86.47	2.50	88.97	2.81	0.57	0.590	0.56
100.0	10.0	84.21	4.76	88.97	5.35	0.55		
100.0	20.0	81.20	8.51	90.31	10.51	0.51 *		
126.5	2.0	109.77	1.25	110.02	1.98	0.72		
125.0	5.0	103.00	2.63	105.63	2.50	0.63	0.653	0.65
125.0	10.0	102.25	5.00	107.25	4.70	0.61		
125.0	20.0	98.20	8.76	106.96	8.20	0.54 *		

T=116°C

P_A mm	t min	A mm	M mm	A+M mm	% A	% M	t mm/min	r_{av} mm/min	r_G mm/min
51.5	2.5	42.22	1.50	43.72	96.57	3.42	0.70		
49.0	4.0	40.00	2.19	42.19	94.80	5.20	0.67		
49.0	6.0	38.52	3.25	41.77	92.00	7.78	0.68		
51.0	10.0	38.50	5.26	43.76	97.98	12.02	0.66	0.646	0.700
50.0	12.5	35.90	6.07	42.00	85.55	14.45	0.63		
50.0	25.0	29.63	9.70	39.33	75.33	24.67	0.58		
50.0	15.0	35.56	6.88	42.44	83.79	16.21	0.60		
75.5	2.0	65.55	1.88	67.43	97.76	2.24	0.86		
75.5	4.0	64.81	3.00	67.81	95.57	4.43	0.86		
75.0	6.0	61.11	4.26	65.37	93.48	6.52	0.85	0.830	0.750
75.5	8.0	60.37	5.32	65.69	91.90	8.10	0.81		
76.0	10.0	58.89	6.88	65.77	89.54	10.46	0.85		
75.0	20.0	52.96	11.50	63.46	82.16	17.84	0.75		
102.0	2.0	88.72	2.41	91.13	97.35	2.65	1.35		
102.0	4.0	85.71	4.07	89.78	95.47	4.53	1.19		
98.0	6.0	81.20	5.27	86.45	93.92	6.08	1.05		
99.0	8.0	78.95	6.88	85.83	91.98	8.02	1.05	1.090	0.950
100.0	10.0	78.94	8.13	87.07	90.66	9.34	1.00		
100.5	20.0	69.93	13.45	83.38	83.87	16.13	0.90		
125.5	2.0	106.01	2.88	108.89	97.35	2.65	1.68		
125.0	4.0	105.26	4.88	109.15	95.57	4.43	1.42		
126.5	6.0	103.00	6.26	109.26	94.27	5.73	1.25	1.267	1.200
125.5	8.0	95.25	7.76	107.01	92.75	7.25	1.18		
125.5	10.0	96.99	9.01	106.00	91.50	8.50	1.11		
124.5	20.0	90.22	15.01	105.23	85.73	14.27	0.96		
125.5	30.0	85.71	20.26	105.97	80.88	19.12	0.88		

C-3.2. Summary of the results.

T °C	$1/Tx10^3$ $°K^{-1}$	r_G mm/min	r/P min^{-1}	log r/P	E k cal/mole
80	2.8329	0.125	.0025	-2.60206	
90	2.7548	0.20	.004	-2.39794	11.8
100	2.6810	0.35	.007	-2.15490	
116	2.5707	0.70	.014	-1.85387	

log k at $1/T=2.5x10^3$ or at 127 = -1.645

$k = 0.023 min^{-1}$

$k=0.0253\ min^{-1}/gm$

APPENDIX D

RESULTS OF ADSORPTION STUDIES

TABLE D-1

10% Nickel-Silica Catalyst

Weight of the reduced catalyst = 0.05483gm.

FRESHLY REDUCED CATSLYST (FR)		HYDROGEN EXPOSED CAT (HE)		REREDUCED CAT		HYDROGEN EXPOSED CAT	
P mm	V cc(STP)/gm	P mm	V cc(STP)/gm	P mm	V cc(STP)/gm	P mm	V cc(STP)/gm
0.0514	2.367	0.2035	1.108	0.0025	1.172	0.0818	1.066
0.0913	3.614	0.6683	1.380	0.0339	2.369	0.4588	1.439
1.0636	3.906	1.5385	1.641	0.1920	3.279	0.9426	1.603
1.8068	4.277	2.8712	1.903	0.5615	3.780	2.3031	1.908
2.2510	4.534	4.2543	2.122	0.9902	4.106	3.6446	2.139
2.7132	4.754	7.4148	2.600	1.7255	4.450	5.3885	2.398
3.9057	5.068	10.6407	3.017	3.8357	4.905	9.3332	2.907
5.2099	5.408	13.3041	3.358	5.0806	5.323	13.2036	3.367
10.0085	6.140	17.0242	3.817	7.7313	5.767	17.4106	3.801
12.5357	6.178	18.5710	5.642	10.3190	6.179		
14.6428	6.952			14.1620	6.721		
				18.3047	7.288		

TABLE D-2
Nickel-Silica Catalyst

Weight of the reduced catalyst = 0.04328gm

HYDROGEN ADSORPTION				ALLENE		PROPYLENE	
FRESHLY REDUCED		HYDROGEN EXPOSED					
P mm	V cc(STP)/gm	P mm	V cc(STP)/gm	P mm	V cc(STP)/gm	P mm	V cc(STP)/gm
0.0035	0.398	0.0509	0.750	0.0050	1.652	0.2474	0.662
0.0505	0.999	0.2100	0.975	0.0449	5.481	2.2158	2.563
0.1009	1.753	0.6752	1.355	0.0509	6.317	4.8745	3.834
0.2139	1.849	0.9995	1.500	0.0798	9.267	10.0201	5.139
0.4162	2.045	1.4995	1.655	0.0958	15.415	13.9576	6.924
0.6979	2.176	4.1225	1.834	0.1740	22.739	18.0832	7.610
1.4239	2.365	6.5529	2.065	0.1895	28.936		
3.7980	2.670	9.2255	2.305	1.2163	36.667		
5.9571	2.901	11.0096	2.453	2.4351	44.493		
8.4133	3.151	13.9956	2.721				
11.5333	3.501						
14.7125	3.853						

TABLE D-3
Nickel-Copper Catalyst

Weight of the reduced catalyst = 0.03914gm

HYDROGEN				ALLEN		PROPYLENE	
FRESHLY REDUCED		HYDROGEN EXPLOSED					
P mm	V cc(STP)/gm	P mm	V cc(STP)/gm	P mm	V cc(STP)/gm	P mm	V cc(STP)/gm
0.0000	0.451	0.0075	0.465	0.0000	0.947	0.1496	0.483
0.0060	0.897	0.0648	0.793	0.0389	5.762	0.3257	0.876
0.0429	1.310	0.2808	1.054	0.0559	10.171	4.1552	2.565
0.1591	1.825	0.5226	1.216	0.0723	14.663	9.7922	3.800
0.8340	2.530	1.3476	1.536	0.0908	21.423	14.4992	4.805
3.1939	3.878	3.9057	2.170	0.1142	25.979		
7.3696	5.250	6.5032	2.700	0.1396	33.130		
12.8857	6.187	10.4773	3.406	0.2224	47.511		
16.5810	7.012			0.2793	60.139		
20.1238	7.584			0.5566	81.466		

TABLE D-4
Copper Catalyst

Weight of the reduced catalyst = 0.06209gm

HYDROGEN				ALLENE		PROPYLENE	
FRESHLY REDUCED		HYDROGEN EXPOSED					
P mm	V cc(STP)/gm	P mm	V cc(STP)/gm	P mm	cc(STP)/gm	P mm	V cc(STP)/gm
0.0020	0.125	0.0035	0.150	0.0070	0.272	0.4007	0.285
0.0785	0.500	0.0512	0.251	0.0479	0.592	2.9513	0.998
0.2019	0.575	0.0998	0.322	0.2728	1.306	3.9125	1.607
1.2017	0.849	0.5127	0.451	0.7780	2.382	6.1229	2.313
3.8007	1.503	2.2178	0.873	3.5395	4.535	8.0000	2.899
5.5892	1.962	5.9761	1.754	8.8611	7.790	10.9556	3.825
7.7000	2.511	8.235	2.301	13.2213	10.614	13.9730	4.246
10.1556	3.150	11.1005	3.007				
13.5217	4.015	14.6000	3.850				
15.3910	4.507						
18.1003	5.200						

TABLE D-5
Cobalt Catalyst

Weight of the reduced catalyst = 0.09965gm.

HYDROGEN FRESHLY REDUCED		HYDROGEN EXPOSED		ALLENE		PROPYLENE	
P mm	V cc(STP)/gm	P mm	V cc(STP)/gm	P mm	V cc(STP)/gm	P mm	V cc(STP)/gm
0.0050	0.475	0.0559	0.200	0.0050	0.450	0.0531	0.425
0.0375	1.105	0.2136	0.252	0.0521	1.654	0.6871	0.785
0.1397	1.500	0.7338	0.349	0.7213	4.855	3.3995	1.974
0.3061	1.625	1.3589	0.444	2.0017	6.799	5.9007	2.800
0.5687	1.750	3.7900	0.799	4.4213	9.603	8.8997	3.699
0.9991	1.849	5.9936	1.128	5.0000	10.652	11.6000	4.605
2.5479	2.045	8.0135	1.435	7.3561	16.039		
5.2137	2.355	11.3956	1.951	10.0035	21.354		
9.0871	2.752	15.0039	2.356				
12.3341	3.099						
14.9980	3.367						

TABLE D-6
Iron Catalyst

Weight of the reduçed catalyst = 0.10640gm

HYDROGEN				ALLENE		PROPYLENE	
FRESHLY REDUCED		HYDROGEN EXPOSED					
P mm	V cc(STP)/gm	P mm	V cc(STP)/gm	P mm	V cc(STP)/gm	P mm	V cc(STP)/gm
0.1332	0.016	0.1347	0.018	0.0035	0.164	0.0020	0.179
0.5486	0.086	0.7326	0.106	0.0279	0.470	0.0199	0.487
1.4384	0.233	1.5480	0.212	0.1227	1.020	0.2653	0.998
4.4759	0.549	4.3659	0.550	0.8895	2.115	1.0013	2.789
7.0370	0.800	7.2882	1.016	2.9253	3.180	3.4555	4.320
9.8408	1.076	10.0701	1.190	6.4964	4.547	6.5396	6.314
13.8321	1.460	14.8631	1.525	10.2123	5.822	11.3918	7.499
17.3209	1.841			14.5815	6.858	15.6173	8.386

TABLE D-7
Palladium Catalyst

Weight of the reduced catalyst = 0.09486gm.

HYDROGEN				ALLENE		PROPYLENE	
FRESHLY REDUCED		HYDROGEN EXPOSED					
P mm	V cc(STP)/gm	P mm	V cc(STP)/gm	P mm	V cc(STP)/gm	P mm	V cc(STP)/gm
0.0030	0.601	0.0050	0.711	0.0100	0.222	0.1082	0.064
0.0758	1.631	0.0956	1.301	0.0464	0.605	0.3436	0.177
0.5456	1.916	0.5985	1.758	0.4887	1.672	1.1250	0.460
1.0045	1.957	0.9588	1.907	2.2069	3.337	4.1458	1.451
1.8544	2.053	2.1255	2.075	4.1193	6.448	6.5417	2.373
4.3959	2.295	4.3347	2.298	6.0122	9.058	11.3783	3.827
7.0872	2.556	7.4957	2.599	8.5002	12.8512	15.7036	5.006
11.8778	3.026	10.6891	2.920	12.2237	16.9514	18.5754	6.821
14.1053	3.101	13.1135	3.162				
15.5154	4.122	14.9101	3.799				
16.3168	5.811						

TABLE D-8
Iridium Catalyst

Weight of the reduced catalyst = 0.08992gm.

HYDROGEN				ALLENE		PROPYLENE	
FRESHLY REDUCED		HYDROGEN EXPOSED					
P mm	V cc(STP)/gm	P mm	V cc(STP)/gm	P mm	V cc(STP)/gm	P mm	V cc(STP)/gm
0.0511	0.105	0.0658	0.158	0.0439	0.096	0.0873	0.106
0.1567	0.152	0.2195	0.249	0.3466	0.361	0.2992	0.207
0.5133	0.360	1.1056	0.380	1.2153	0.999	0.9500	0.496
1.0357	0.549	4.7996	0.921	3.0623	1.617	2.7242	1.093
2.2579	0.722	8.3179	1.418	5.1151	2.445	7.0792	2.445
5.3160	1.050	11.9900	1.924	9.1752	3.474	11.5000	3.408
9.7532	1.523	14.8003	2.463	13.1185	4.417	15.5189	4.245
12.9979	1.875			15.4263	4.984	19.2110	5.051
16.7558	2.310			16.7085	5.391		

TABLE D-9
Osmium Catalyst

Weight of the reduced catalyst = 0.08890gm.

HYDROGEN FRESHLY REDUCED		HYDROGEN EXPOSED		ALLENE		PROPYLENE	
P mm	V cc(STP)/gm	P mm	V cc(STP)/gm	P mm	V cc(STP)/gm	P mm	V cc(STP)/gm
0.0000	0.207	0.2194	0.137	0.5985	0.846	0.2194	0.269
0.1885	0.334	1.4076	0.399	1.2807	1.384	0.6114	0.608
0.7062	0.449	3.7856	0.899	3.2654	2.671	1.3630	0.983
1.5242	0.635	6.1221	1.347	5.4205	3.632	2.4351	1.476
4.2318	1.155	10.1727	2.108	8.8561	4.981	4.6295	2.357
6.3337	1.555	14.0745	2.833	12.2917	6.217	7.9674	3.781
11.2896	2.378			14.6820	7.523	12.0482	5.200
15.8191	3.222						
19.2440	3.855						

TABLE D-10
Platinum Catalyst

Weight of the reduced catalyst = 0.09837gm.

HYDROGEN FRESHLY REDUCED		HYDROGEN EXPOSED		ALLENE		PROPYLENE	
P mm	V cc(STP)/gm	P mm	V cc(STP)/gm	P mm	V cc(STP)/gm	P mm	V cc(STP)/gm
0.0005	0.403	0.1920	0.135	0.0000	0.374	0.0050	0.350
0.0010	0.527	1.0358	0.215	0.0025	0.760	0.1568	0.565
0.0185	0.736	2.8227	0.298	0.0818	1.047	1.4065	1.000
0.1177	0.841	5.1081	0.405	0.2878	1.167	4.0039	1.643
0.3526	0.915	3.7876	0.550	1.0358	1.404	9.9507	2.557
0.8672	0.997	9.6522	0.698	2.9598	2.131	15.2895	3.389
1.5405	1.079	12.5447	0.889	9.5022	3.043		
2.9893	1.250	15.4565	1.126	14.6720	3.696		
6.2623	1.470			18.5102	4.123		
12.5497	2.278						

TABLE D-11
Rhodium Catalyst

Weight of the reduced catalyst = 0.09816gm.

HYDROGEN				ALLENE		PROPYLENE	
FRESHLY REDUCED		HYDROGEN EXPOSED					
P mm	V cc(STP)/gm	P mm	V cc(STP)/gm	P mm	V cc(STP)/gm	P mm	V cc(STP)/gm
0.0020	0.359	0.0019	0.295	0.0025	0.226	0.0259	0.172
0.0825	1.200	0.0556	0.401	0.0050	0.505	0.3177	0.588
0.2126	1.395	0.2007	0.906	0.0065	0.984	1.3293	1.240
0.3975	1.550	0.4172	1.056	0.1416	1.755	2.6531	1.827
0.5003	1.599	0.6029	1.111	2.0869	3.622	5.2872	2.890
1.1056	1.652	1.4551	1.203	5.9864	6.202	8.0819	3.909
3.9789	1.960	4.0009	1.500	10.2163	8.151	12.5013	5.500
6.3502	2.211	8.0998	1.999	14.1309	9.639		
10.7928	2.650	11.3752	2.375				
14.1000	2.951	14.5000	2.755				
17.3120	3.311						

TABLE D-12
Ruthenium Catalyst

Weight of the reduced catalyst = 0.09707gm.

HYDROGEN				ALLENE		PROPYLENE	
FRESHLY REDUCED		HYDROGEN EXPOSED					
P mm	V cc(STP)/gm	P mm	V cc(STP)/gm	P mm	V cc(STP)/gm	P mm	V cc(STP)/gm
0.0743	0.102	0.0997	0.241	0.0040	0.187	0.0723	0.118
0.4468	0.445	0.4608	0.399	0.0773	0.459	0.4842	0.353
1.2242	0.698	1.2490	0.600	0.4548	0.805	1.3234	0.712
2.6406	0.875	3.3765	0.875	1.5673	1.442	4.0392	1.760
5.1490	1.287	5.9515	1.259	3.5725	2.542	6.2965	2.414
9.6512	1.998	9.4071	1.781	7.7559	3.876	10.8221	3.615
14.1389	2.752	14.1258	2.480	11.9430	5.105	14.8229	4.650
17.7945	3.286	18.0076	3.039	15.8201	6.307	17.9172	5.756
				18.9379	7.172		

SETTING OF THE SPECTROPHOTOMETER

Slit program	program (1000)
Gain	4
Attenuator speed	1100
Scan time	10 x 32
Suppression	6
Scale	linear
Source current	0.8 Amps.

Spectral slit width

The approximate spectral slit width may be determined from the following equations.

1. $\text{Sin } \theta = \frac{mn}{2V}$

2. $\Delta\nu = F(s) \frac{\nu \cos\theta}{na} + \frac{\nu^2 s}{mnf} \text{ Cos } \theta$

θ = the angle of diffraction

n = grating lines per centimeter

$\Delta\nu$ = spectral slit width in cm^{-1}

F = monochromator focal length

m = grating order

ν = frequency, cm^{-1} at which $\Delta\nu$ is determined

a = effective aperture of the collimated beam

ρ = mechanical slit width in centimeters

F(s) = A function of slit width which has a value of approximately 0.9 at extremely narrow slits. For a slit opening such that the first term of Eqn. (a) approaches the Rayleight term $\left(\frac{\lambda}{2b(dn/d\lambda} \right)$, the value of F(s) approaches 0.5 For simplicity, with reasonable accuracy, F(s) shall be considered as a constant equal to 0.5.

APPENDIX E

SAMPLE CALCULATIONS

Ni-Silica Catalyst

E-1. Weight of reduced catalyst

Weight of silica = W_S

Weight of compound used = W_{com}

Total weight = $W_S + W_{com} = W_C$

M = molecular weight of compound

A = atomic weight of metal

M gm of compound contains = A gm of metal

W_{com} will contain = $\frac{A}{M} \times W_{com}$

After reduction, total weight should be:

$$(W_S + \frac{A}{M} W_{com})$$

$$W_C \equiv (W_S + \frac{A}{M} W_{com})$$

W gm catalyst is reduced:

$$W \equiv \frac{W}{W_C} (W_S + \frac{A}{M} W_{com})$$

For Ni

$$= \frac{.02585}{1.45112+0.37874} (1.45112+ \frac{58.71}{290.81} \times 0.37874)$$

$$= .02158.$$

II. Catalyst = 5% metal by weight

Weight of (silica+metal) $\equiv$ (weight of silica + $\frac{5}{95}$ x wt. of silica)

$$= \text{wt. of silica} \times \frac{20}{19}$$

Reduced wt. = $\frac{\text{wt. of silica}}{\text{total wt.}} \times \frac{20}{19} \times$ wt. of catalyst used

$$= \frac{1.45112}{1.82988} \times \frac{20}{19} \times .02585 = .02158\text{gm.}$$

E-2. Calculation of Energy of Activation (E)

Using Eqn. 4.5 and Fig. 7

$$\text{Slope} = -\frac{E}{2.303xR} = \frac{.52}{.22} \times 10^3 = 2.36x10^3$$

$$E = 2.363 \times 2.0 \times 2.303 \times 10^3 = 10.8 \text{ k cal/mole.}$$

E-3. Calculation of overall rate constant (k_{100}) and frequency factor.

From Fig. 7 at 100°C or ($1/T=2.6801x10^{-3}$)

the value of $\log_{10}k=-1.7565 = \bar{2}.2435$

$$k_{100} = .01752$$

$$k_{100}/gm = \frac{.01752}{.02158} = 0.8119 min^{-1}/gm$$

$$\log_{10}k = \log_{10}A - \frac{E}{RT}$$

$$\log_{10}A = \log_{10}k + \frac{E}{RT}$$

$$= 0.8119 + \frac{10.81x10^3}{1.9865x(100+273)}$$

$$\log_{10}A = 6.242$$

$$A = 1.75x10^6 \text{ min}^{-1}/gm$$

E-4. Calculation of selectivity data given in Table B-1.3.

$P_{H_2}=100\pm1$ mm, $P_{C_3H_4}=50\pm.5$ mm, $\Delta P=60$ mm

$$S = \frac{23.3}{7.9+23.3} = 0.75$$

E-5. Adsorption Studies

E-5.1. Volume of the doser (V_d)

Volume of Hg calibrated loop = V_1 = 15.6600 cc.

Pressure of He in the Hg calibrated loop = P_1

Pressure after expansion in the doser = P_2

$$P_1V_1 = P_2V_2 = P_2 \ (V_1 + \text{volume of the doser})$$

$$= P_2(V_1+V_d)$$

$$V_d = \frac{P_1V_1}{P_2} - V_1 = V_1 \ \frac{P_1-P_2}{P_2}$$

Several runs were taken and the average volume of the doser was calculated to be 25.2103 cc.

E-5.2. Volume of the cell

Nitrogen or helium gases at known pressures were introduced in the doser and the gas was expanded in the cell. Following the same procedure (to calculate the volume of the doser), the volume of the cell was calculated to be 65.2053 cc.

E-5.3. Using the following program, the amount of the gas adsorbed at a particular pressure was calculated using Eqns. 4.8 to 4.20.

E-5.4. From Fig. 35, the volume of hydrogen adsorbed at zero pressure equals 2.25 cc (STP)/gm.

Surface metal per gm. of catalyst = $\frac{2VM}{2.24\times10^4}$

$$= \frac{2\times2.25\times58.71}{2.24\times10^4} = 117.94\times10^{-4} \text{ gm}.$$

PROGRAM TO CALCULATE AMOUNT OF GAS ADSORBED

Nomenclature

WET = Weight of the catalyst

P(J) = Pressure before expansion

PR(J) = Pressure at equilibrium (after adsorption)

INE PRES = P(N) = Initial pressure

PRE INCR = Pressure increase

PRE EXPD = Expanded pressure

PRE CAL = Calculated pressure after expansion

PRE DIF = Difference of calculated pressure and actual pressure

V ADIO+3 = Volume adsorbed x 10^3 cc(STP)

ACTU PRE = Actual pressure

TOT V AD = Total volume adsorbed at actual pressure

V/G,M = Volume adsorbed per gm of the catalyst x 10^3

```
      $JOB   ACCT-NUM,C,KHULBE,TIME=30,PAGES=20
             DIMENSION P(25),PR(25),HEAD(20),SUBH(18),AVOL(25),BVOL(25)
1            INTEGER*2 BL(120)/120*' '/,BLK/' '/,AST/'*'/,LINE/'|'/,DASH/'-'/
2            REAL CORR(17)/+0.0,+0.002,+0.015,+0.014,+0.017,+0.006,-0.004,
3           1-0.009,-0.027,-0.033,-0.045,-0.053,-0.041,-0.037,-0.012,+0.0,
            2+0.011/,PRES(17)/0.0,0.776,2.327,4.654,6.206,8.533,10.084,12.412,
            315.514,17.066,19.393,21.720,23.272,25.599,27.926,30.253,31.029/
             DO 154 J4=1,10
4            READ(5,7) (HEAD(N),N=1,20),(SUBH(L),L=1,18),WET
5          7 FORMAT (20A4,/,18A4,/,F10.5)
6            WRITE(6,14) (HEAD(N),N=1,20),(SUBH(L),L=1,18)
7         14 FORMAT ('1',3X,20A4,////,2X,8(2A4,5X),2A4)
8            J=1
9          4 J=J+1
10           READ(5,5) P(J),PR(J)
11         5 FORMAT (2F10.5)
12           IF(P(J).NE.0.0) GO TO 4
13           AVOL(1)=0.0
14           P(1)=0.0
15           PR(1)=0.0
16           J=J-1
17           DO 17 N=2,J
18           K2=2
19         6 IF (P(N).LE.PRES(K2)) GO TO 8
20           K2=K2+1
21           GO TO 6
22         8 P(N) = P(N)-CORR(K2-1)-(CORR(K2)-CORR(K2-1))*(P(N)-PRES(K2-1))/
23          1(PRES(K2)-PRES(K2-1))
             K2=2
24         9 IF (PR(N).LE.PRES(K2))GO TO11
25           K2 =K2+1
26           GO TO 9
27        11 PR(N)=PR(N)-CORR(K2-1)-(CORR(K2)-CORR(K2-1))*(PR(N)-PRES(K2-1))/
28          2(PRES(K2)-PRES(K2-1))
29        17 CONTINUE
30           DO 10 N=2,J
31           PINC = P(N)-PR(N-1)
32           PEXP = 0.27883*PINC
33           PCAL = PR(N-1)+PEXP
34           DIFF = PCAL-PR(N)
35           VOL = 118.967*DIFF
36           AVOL(N) = AVOL(N-1)+VOL
37           BVOL(N) = AVOL(N)/WET
38           WRITE(6,16) P(N),PINC,PEXP,PCAL,DIFF,VOL,PR(N),AVOL(N),BVOL(N)
39        16 FORMAT (//,8(F10.4,3X),F12.5)
40        10 CONTINUE
41       154 CONTINUE
42           STOP
43           END

      $ENTRY
```

ADSORPTION OF H2 ON HEATED AND EVACUATED .. 10% NI 16/1/73

INE PRES	PRE INCR	PRE EXPD	PRE CAL	PRE DIFF	V AD10+3	ACTU PRE	TOT V AD	V/GM
1.9461	1.9461	0.5426	0.5426	0 5401	64.2583	0.0025	64.2583	1171.95400
2.0943	2.0918	0.5833	0.5858	0.5519	65.6519	0.0339	129.9102	2369.32600
2.1043	2.0703	0.5773	0.6112	0.4192	49.8688	0.1920	179.7790	3278.84300
2.3450	2.1530	0.6003	0.7923	0.2308	27.4550	0.5615	207.2340	3779.57200
2.6391	2.0776	0.5793	1.1408	0.1507	17.9248	0.9902	225.1588	4106.48800
4.1958	3.2056	0.8938	1.8840	0.1585	18.8613	1.7255	244.0201	4450.48400
10.1166	8.3911	2.3397	4.0651	0.2305	27.4213	3.8347	271.4414	4950.59700
8.9195	5.0849	1.4178	5.2525	0.1718	20.4408	5.0806	291.8821	5323.39800
15.3197	10.2391	2.8550	7.9356	0 2044	24.3111	7.7313	316.1931	5763.78900
17.6940	9.9628	2.7779	10.5092	0.1902	22.6258	10.3190	338.8188	6179.44100
24.9971	14.6781	4.0927	14.4117	0.2496	29.6992	14.1620	368.5178	6721.09700
29.9565	15.7945	4.4040	18.5660	0.2613	31.0905	18.3047	399.6082	7288.12800

$$\text{Metal surface area} = \frac{2VN\sigma}{(2.24\times10^4)\times10^4}$$

$$= \frac{2\times2.25\times(6.202\times10^{23})\times6\times10^{-16}}{(2.24\times10^4)\times10^4}\ m^2/gm$$

$$= 7.262 m^2/gm$$

$$D = \frac{H}{M} = \frac{2VM}{2.24\times10^4 \times \text{wt. of metal present in the catalyst}}$$

$$= \frac{2\times2.25\times58.71}{2.24\times10^4\times.05}$$

$$= 0.24.$$